

UNIVERSITY OF SOUTHERN QUEENSLAND



**Real Time Depth of Anaesthesia Monitoring Through
Electroencephalogram (EEG) Signal Analysis Based On
Bayesian Method and Analytical Technique**

A dissertation submitted by

Mario Elvis Palendeng

MENR (Electrical and Electronics Engineering)

BEng (Electrical and Electronics Engineering)

For the award of

Doctor of Philosophy

School of Mechanical and Electrical Engineering

Faculty of Health, Engineering and Sciences

University of Southern Queensland

Australia

2015

ABSTRACT

The electroencephalogram (EEG) signal from the brain is used for analysing brain abnormality, diseases, and monitoring patient conditions during surgery. One of the applications of the EEG signals analysis is real-time anaesthesia monitoring, as the anaesthetic drugs normally targeted the central nervous system.

Depth of anaesthesia has been clinically assessed through breathing pattern, heart rate, arterial blood pressure, pupil dilation, sweating and the presence of movement. Those assessments are useful but are an indirect-measurement of anaesthetic drug effects. A direct method of assessment is through EEG signals because most anaesthetic drugs affect neuronal activity and cause a changed pattern in EEG signals.

The aim of this research is to improve real-time anaesthesia assessment through EEG signal analysis which includes the filtering process, EEG features extraction and signal analysis for depth of anaesthesia assessment. The first phase of the research is EEG signal acquisition. When EEG signal is recorded, noises are also recorded along with the brain waves. Therefore, the filtering is necessary for EEG signal analysis.

The filtering method introduced in this dissertation is Bayesian adaptive least mean square (LMS) filter which applies the Bayesian based method to find the best filter weight step for filter adaptation. The results show that the filtering technique is able to remove the unwanted signals from the EEG signals.

This dissertation proposed three methods for EEG signal features extraction and analysing. The first is the strong analytical signal analysis which is based on the Hilbert transform for EEG signal features' extraction and analysis. The second is to extract EEG signal features using the Bayesian spike accumulation technique. The third is to apply the robust Bayesian Student-t distribution for real-time anaesthesia assessment.

Computational results from the three methods are analysed and compared with the recorded BIS index which is the most popular and widely accepted depth of anaesthesia monitor. The outcomes show that computation times from the three methods are leading the BIS index approximately 18-120 seconds. Furthermore, the responses to anaesthetic drugs are verified with the anaesthetist's documentation and then compared with the BIS index to evaluate the performance. The results indicate that the three methods are able to extract EEG signal features efficiently, improve computation time, and respond faster to anaesthetic drugs compared to the existing BIS index.

CERTIFICATION OF DISSERTATION

I certify that the ideas, experimental works, results, analyses, software and conclusions reported in this dissertation are entirely my own effort, except where otherwise acknowledged. I also certify that the work is original and has not been previously submitted for any other award, except where otherwise acknowledged.

MARIO ELVIS PALENDENG

Signature of Candidate

Date

ENDORSEMENT

Signature of Principal Supervisor

Date

Signature of Associate Supervisor

Date

PUBLICATIONS

1. Palendeng, M, Wen, P & Li, Y 2014, 'Real-time depth of anaesthesia assessment using strong analytical signal transform technique', *Australasian Physical & Engineering Sciences in Medicine*, vol. 37, no. 4, pp. 723-30.
2. Palendeng, M, Zhang, Q, Pang, C & Li, Y 2012, 'EEG data compression to monitor DoA in telemedicine', *Studies in Health Technology and Informatics*, vol. 178, pp. 163-8.
3. Palendeng, M, Wen, P & Li, Y 2015, 'Depth of anaesthesia assessment using Bayesian spikes accumulation technique', *IET Journal of Signal Processing* (under review)
4. Palendeng, M, Wen, P & Li, Y 2015, 'Electroencephalogram signal analysis for depth of anaesthesia monitoring using Bayesian approximation with Student-t distribution', (finalising for submission in *IEEE Transactions on Biomedical Engineering*)
5. Palendeng, M, Wen, P & Li, Y 2015, 'Electroencephalogram signal filtering using Bayesian adaptive LMS filter', (In preparation for submission)

ACKNOWLEDGEMENT

This research has been a challenging journey. There are ups and downs during the research period. My study has become a meaningful journey with the support from many people.

I would like to express my sincere gratitude to my supervisor, Associate Professor Peng (Paul) Wen and associate supervisor, Associate Professor Yan Li, for their guidance, consistent support, inspiration and the discussion throughout the PhD journey.

I am thankful for the USQ Postgraduate Award. I would like to thank the Indonesian Government for its financial support. My special thanks to Dean Beliveau and Juanita Ryan for their kind assistance throughout my study.

For the inspirational motivation from Dr. Qing Zhang, I am truly inspired. My special thanks to Dr Richard Landers for generous advice and discussions. I also acknowledge my colleague Dr. Tai Nguyen-Ky, Tianning Li, Marilia Menezes De Oliveira, Bo Song, Dr. Genkung (Eric) Wang, Rebeca, and Dr. Guohun Zhu for the valuable discussions.

I would like to acknowledge and thank the assistance in proof-reading of the dissertation manuscript provided by Ms. Sandra Cochrane.

For the abundant love, support and cheering from my families and relatives in Tomohon, Indonesia, I am feeling really blessed.

I would like to express my deepest gratitude to my wife, Adriana and our daughter, Kearney for love, support and encouragement throughout my study.

For the love, prayers and support from the Twedells and the Thursday night home-group and Rangeville Community Church (RCC) Toowoomba, I am forever

thankful. My gratitude is also offered for the love and friendship from Brian and Linda Hensel. For the lovely friendship and sincere encouragement from Handy, Lia and Mitchell, I feel really blessed.

My gratefulness also goes to everyone who has supported me in various ways during my study but I have failed to mention here.

LIST OF CONTENTS

Abstract	ii
Certification of dissertation	iv
Publications.....	v
Acknowledgement.....	vi
List of contents	viii
List of figures.....	xii
List of tables.....	xvi
List of abbreviations	xvii
Chapter 1	1
1 Introduction	1
1.1 Background.....	1
1.2 Research problems	3
1.3 Objectives	5
1.4 Research workflow.....	6
1.5 Dissertation outline.....	7
Chapter 2.....	9
2 Literature Review	9
2.1 General anaesthesia practice	9
2.1.1 The history of general anaesthesia.....	9
2.1.2 Anaesthesia effects	13

2.1.3 Anaesthesia on the cellular levels	17
2.2 Electroencephalogram signal	20
2.3 Typical anaesthesia drug effects on EEG signals.....	23
2.4 Measuring depth of anaesthesia	24
2.4.1 Time domain analysis.....	28
2.4.2 Frequency domain analysis	29
Chapter 3.....	34
3 Electroencephalogram data acquisition	34
3.1 Equipment and settings	34
3.2 EEG signal conversion.....	37
3.3 EEG signal acquisition	39
3.4 Summary.....	49
Chapter 4.....	50
4 Stationary Wavelet transform and Bayesian adaptive LMS filtering.....	50
4.1 Stationary wavelet transform	51
4.2 EEG signal denoising using SWT method	54
4.3 EEG filtering using adaptive Student-t distribution	57
4.4 Experimental results and analysis.....	62
4.4.1 Result of the SWT filtering technique	63
4.4.2 Results of the Bayesian adaptive LMS filter	67
4.4.3 Comparison of the filtering techniques.....	71
4.5 Summary.....	73

Chapter 5.....	74
5 Depth of anaesthesia assessment using strong analytical signal analysis	74
5.1 EEG feature extraction using the strong analytical signal technique ...	74
5.2 Features extraction and DoA index development	76
5.3 Results.....	79
5.4 Summary.....	87
Chapter 6.....	89
6 Bayesian spikes accumulation technique to analyse electroencephalogram signal for depth of anaesthesia assessment.....	89
6.1 Bayesian Method.....	89
6.2 Bayesian spike accumulation	93
6.3 DoA with Bayesian Gaussian distribution.....	95
6.4 Results and analysis.....	98
6.4.1 Spike accumulation technique	98
6.4.2 Depth of anaesthesia using Bayesian technique	102
6.5 Summary.....	108
Chapter 7	109
7 Electroencephalogram signal analysis using Bayesian approximation with Student-t distribution for depth of anaesthesia monitoring	109
7.1 Student-t distribution.....	109
7.2 Depth of anaesthesia assessment using the student-t distribution.....	112
7.3 Experimental results and analysis	114

7.4	Summary.....	125
	Chapter 8.....	127
8	Conclusion and future work.....	127
8.1	Primary work and contributions.....	127
8.2	Outcomes and conclusions.....	128
8.3	Future work.....	132
	References.....	134

LIST OF FIGURES

Figure 1-1. Three main phases of this research.	6
Figure 2-1. The PET scan of the brain in different anaesthesia states shows the neuronal activity using %BMR and the result compared with BIS index (Alkire 1998; Kelly 2003).	13
Figure 2-2. The effect of anaesthetic drugs in cerebral metabolism which reflects on the EEG signal (Brown, Lydic & Schiff 2010).	14
Figure 2-3. Typical neuron structure and synaptic terminal (Wikipedia 2015).	18
Figure 2-4. Different target of anaesthetic drugs (Alkire, Hudetz & Tononi 2008).	19
Figure 2-5. Inhibitory in the receptor as the neurotransmitter releases chemicals through the synapse (Steyn-Ross, 2002).	20
Figure 2-6. EEG signal patterns in different anaesthesia stages.	21
Figure 2-7. EEG burst suppression during deep anaesthesia.	23
Figure 2-8. Guedel introduced four stages of ether anaesthesia (Guedel 1920; Oshima 2008).	25
Figure 2-9 EEG burst suppression in deep anaesthesia (Rampil 1998).	29
Figure 3-1. BIS Index – Vista Monitor includes monitor, sensor, BISx and patient interface cable (Aspect Medical System 2009)	35
Figure 3-2. Percentage of the patients according to age group.	37
Figure 3-3. Raw EEG data in binary format.	38
Figure 3-4. The diagram of 16 bit data stored in 2 bytes locations left byte and right byte.	39
Figure 3-5. EEG signal snapshot from the BIS monitor.	40
Figure 3-6. Converted EEG signal from the obtained data.	40
Figure 3-7. Verification of the converted EEG raw signal.	41

Figure 3-8. The EEG signal.....	42
Figure 3-9. Data from patient number 21 where the BIS index could not provide the index (a) The EEG signal; (b) BIS index; (c) EMG value.	43
Figure 3-10. Patient number 3 shows the BIS index increase as the EMG value increases.	44
Figure 3-11. BIS index from patient number 12 showing that the BIS index was affected by noise.....	45
Figure 3-12. EEG signal is corrupted with noises. There are many high amplitude spikes in the signal.....	46
Figure 3-13. Frequency content in the EEG signal from patient number 12.	48
Figure 4-1. SWT decomposition and filter at the level j with a low pass filter (g_j) and a high pass filter (h_j)	51
Figure 4-2. SWT decomposition in three levels	52
Figure 4-3. EEG signals before decomposition, the approximation and detail after decomposition.	53
Figure 4-4. Details of the SWT and the frequency component on associate with the detail.....	55
Figure 4-5. SWT approximation and the frequency component related to the approximation level.	56
Figure 4-6. Overlapping noises in EEG signal.	58
Figure 4-7. (a) Bayesian adaptive LMS filter diagram. (b) The FIR filter structure.....	59
Figure 4-8. EEG raw signal was recorded for over one hour.....	62
Figure 4-9. The result of signal filtering using SWT.	63
Figure 4-10 EEG signal spectrum before and after filtering process.....	64
Figure 4-11. Cross correlation between the signal before and after filtering.	65
Figure 4-12. Coherence estimate and the cross spectrum phase.....	66
Figure 4-13. EEG signal filtering using Bayesian adaptive LMS filter.....	67

Figure 4-14. EEG signal spectrum before and after the Bayesian adaptive LMS filtering process.	68
Figure 4-15. Signal coherence between two signals.....	69
Figure 4-16. Comparison of the EEG signal power before and after filtering.....	70
Figure 4-17. Comparison of the EEG signal filtered with the SWT and Bayesian adaptive filters.....	71
Figure 4-18. EEG signal power between the raw signal, Bayesian adaptive LMS filter, and the SWT filtering technique	72
Figure 5-1. Comparisons between the new DoA and the Wavelet entropy method.....	79
Figure 5-2. Comparisons between the new DoA index and the BIS index.	81
Figure 5-3. Time delay in BIS.....	83
Figure 5-4. The comparison between new DoA and the BIS.	84
Figure 5-5. Time delay of the BIS index.	85
Figure 6-1. Histogram of the EEG signal in different frequency bands.	92
Figure 6-2. Posterior estimation for one epoch of observed data.	96
Figure 6-3. Probability response of patients in different level of anaesthesia.	97
Figure 6-4. Four stages of anaesthesia which are awake, light anaesthesia, general anaesthesia and deep anaesthesia	97
Figure 6-5. Different levels of anaesthesia (a) awake patient correlate with BIS 97, (b) moderate anaesthesia correlates with BIS 50, (c) deep anaesthesia correlates with BIS 30 and (d) very deep anaesthesia correlates with BIS 15.	99
Figure 6-6. Comparison of the spike accumulation and the BIS index	100
Figure 6-7. Comparison of spike accumulation and BIS index in patient number 6	102
Figure 6-8. Comparison between BIS index and the DoA index based on Bayesian Gaussian distribution	103
Figure 6-9. BIS index and the EMG signal	104

Figure 6-10 BIS index is unable to provide the DoA level. (a) Comparison between BIS and the DoA Bayes; (b) The section where BIS index is unable to produce the DoA level	105
Figure 6-11. Patient's blood pressure and the comparison between the DoA Bayes and the BIS Index	107
Figure 7-1. Data histogram shows the presence of outlier that can minimise the estimation. It is shows that the Student-t distribution can maximise the estimation	110
Figure 7-2. Posterior distribution value	114
Figure 7-3. Comparison between BIS index, anaesthesia assessment using Student-t distribution and Gaussian distribution.....	115
Figure 7-4. Comparison between new depths of anaesthesia based on student-t distribution and BIS index.....	116
Figure 7-5. Scatter Plot with marginal histogram.....	117
Figure 7-6. (a) BIS index is unable to provide the DoA level and the DoA based on the student-t distribution is able to give the DoA level. (b) Zoomed image of BIS index.....	118
Figure 7-7. The Comparison between BIS and the nDoA	119
Figure 7-8. Comparison between nDoA student and the DoA Bayes based on BSA technique	120
Figure 7-9. Transition period to calculate the time delay.....	121
Figure 7-10. Time delay data from the patients.....	122
Figure 7-11. Correlation graph and Blant-Alman. (a) Correlation graph between BIS index and Bayesian Student-t. (b) Blant-Alman graph shows the mean standard deviation differences between the two methods	125

LIST OF TABLES

Table 2-1 Places that pioneering ether was used in general anaesthesia	12
Table 2-2. Review of incidents of awareness (Bruhn et al. 2006; Shepherd et al. 2013).....	16
Table 2-3 Neurotoxicity of anaesthesia drugs (Soriano & Vutskits 2015).....	17
Table 2-4. EEG frequency band.....	22
Table 2-5 MOAA/S score to assess unconscious patient (Gelb et al. 2009)	26
Table 2-6. A comparison of DoA monitor in the market	31
Table 3-1. Patient demography	36
Table 5-1. Signal decomposition levels and their corresponding frequency bands.....	75
Table 5-2. Correlation between the BIS index and the new DoA index for 20 patients	86
Table 5-3. The mean, standard deviation and correlation in each anaesthesia stage	87
Table 6-1. Spike accumulation in different anaesthesia stage	101
Table 7-1. Five stage depth of anaesthesia value	113
Table 7-2. Descriptive statistics of BIS index time delay	123
Table 7-3. One-Sample statistics test for BIS time delay.....	124
Table 8-1. Comparisons of DoA assessment methods and performance	132

LIST OF ABBREVIATIONS

AD	:	Anno Domini
AEP	:	Auditory evoked potential
AIC	:	Akaike information criterion
AMPA	:	α -amino-3-hydroxy-5-methyl-4-isoxazolepropionic acid
AR	:	Autoregressive method
BC	:	Before Christ
BIC	:	Bayesian Information Criterion
BIS	:	Bispectral Index
BMR	:	Brain glucose metabolism rate
BSA	:	Bayesian spike accumulation
CNS	:	Central Nervous System
dB	:	Decibel
DoA	:	Depth of Anaesthesia
DWT	:	Discrete Wavelet Transform
ECG	:	Electrocardiography
EEG	:	Electroencephalograph
EMG	:	Electromyography
EOG	:	Electro-oculography
FFT	:	Fast Fourier transforms
GABAA	:	γ -aminobutyric acid type A
Hz	:	Hertz
LMA	:	Laryngeal mask airway
LMS	:	Least mean square

MAD	:	Mean absolute deviation
MLAEP	:	Mid-latency auditory-evoked potential
MLE	:	Maximum Likelihood Estimation
MOAA/S	:	Modified observer assessment of alertness/sedation
N2O	:	Nitrous Oxide
NMDA	:	N-methyl-D-aspartate
PermEn	:	Permutation entropy
PET	:	Positron Emission Tomography
RE	:	Response entropy
RMS	:	Root mean square
SampEn	:	Sample entropy
SE	:	State entropy
SFS	:	Sync Fast Slow
STFT	:	Short Time Fourier transforms
SWT	:	Stationary Wavelet Transform
UCH	:	University college hospital in London
UK	:	United Kingdom
USA	:	United States of America
USB	:	Universal serial bus
WHO	:	World Health Organisation

1 INTRODUCTION

1.1 Background

The word anaesthesia was first introduced in 19th Century. It was suggested by Oliver Wendell Holmes to Morton on the 21st November 1846. Holmes sent a private letter to Morton suggesting the word anaesthesia. The word anaesthesia itself comes from the Greek "esthesia", which means sensation. By adding a prefix "a" in *esthesia* becomes "aesthesia", which means no sensation or a state of being unable to feel anything.

In practice, there are three different types of anaesthesia, local anaesthesia, regional anaesthesia, and general anaesthesia. Local anaesthesia is normally used for minor operations in a specific area. In local anaesthesia, the patient is normally awake and aware all activities during the medical procedures. Regional anaesthesia is used to eliminate sensation in a larger area for procedures such as limb operation or during child birth. General anaesthesia is a term where patients are fully unconscious. The ideal target in general anaesthesia is to prevent the patient from feeling any pain

and from having any memories of the operation. All chapters in this dissertation refer to general anaesthesia.

Depth of anaesthesia (DoA) monitors have been used to monitor patients' conditions under general anaesthesia. Data from the Australian and New Zealand College of Anaesthetists shows that factors such as patient assessment, anaesthesia management and inadequate monitoring are related to mortality in anaesthesia (ANZCA 2009). For this reason, it is important to provide reliable monitoring for anaesthetist to assess and maintain the patient's condition.

Development in DoA assessment brings a lot of benefits to the medical professions and the general community. One of the advantages of improvement in DoA assessment in term of the patients' safety is to reduce post-operative side effects. A post-operative side effect includes drowsiness, nausea and vomiting, pain and discomfort (Myles 2007). Other post-operative side effects caused by incident of awareness do not harm but psychological affect patients throughout their life (Goddard & Smith 2013; Lennmarken et al. 2002; Sebel et al. 2004). The DoA monitor would help control delivering the right amount of anaesthetic drugs and as, a result of the accurate monitoring, prevent awareness and overdose (Goddard & Smith 2013; Marchant et al. 2014; Myles 2007). In addition, accurate monitoring could reduce the cost of spending money for hospital stays and anaesthetics drugs.

Before the discovery of neurophysiological DoA monitor, DoA was estimated through the physiological assessment of the patient. A physiological evaluation includes heart rate, pupil response, temperature, breathing pattern, increased blood pressure, and absence of movement (Avidan et al. 2008; Gelb et al. 2009; Kelly 2003; Marchant et al. 2014; Myles 2007; Shepherd et al. 2013). However, due to numerous variables between patients such as weight, ages, and disease history, DoA monitoring through physiological assessment is not reliable. In addition, physiological assessment does not give an accurate representation of the central

nervous system. Therefore, it is necessary to monitor the depth of anaesthesia with a reliable monitor.

Neurophysiological assessment is considered to be able to give a direct measurement of the central nervous system. Neurophysiological monitoring of the central nervous system can be done through electroencephalogram (EEG) signal. Current DoA monitoring is based on observations of the central nervous system through the EEG signal. The main reasons the EEG signal is used to measure the depth of anaesthesia are:

- a) It represents the cortical activity of the brain (Gelb et al. 2009)
- b) The effect of anaesthetics is connected to cerebral blood flow and cerebral metabolism which is related to different states of the brain activity (Freye 2005; Ionescu et al. 2013; Kuramoto et al. 1979)
- c) The EEG patterns, metabolism, and cerebral blood flow are affected by anaesthetic agents and surgical stimulus. As the result of administering anaesthetic agents, the EEG pattern characteristics change (Freye 2005; Gelb et al. 2009; Kelly 2003).

1.2 Research problems

The studies mentioned above highlight some of the problems which can arise during or after the anaesthesia procedures. Anaesthesia awareness and post-operative side effects could arise during and after the operation. These problems can arise if the patient receives too much or inadequate anaesthetic drugs. Incorrect or inadequate DoA monitoring can also cause overdose or under dose in administering anaesthetic drugs (ANZCA 2009; Ireland 2007). Existing monitors

used in hospitals normally assist the anaesthetist in administering the anaesthetic drugs. However, there are limitations and drawbacks that have been identified from the current monitors. Based on the review of current DoA monitors, the following research gaps in the field were identified:

- BIS does not respond properly to all anaesthetic agents such as nitrous oxide, ketamine and opioids (Bowdle 2006)
- The existing filtering technique is not able to remove noise such as Electromyography (EMG), Electrocardiography (ECG) and Electro-oculography (EOG) (Johansen 2006) which result in the increasing value of BIS index caused by the EMG signals (Bowdle 2006; Wei et al. 2013)
- There is a time delay in computations which results in longer time to produce the DoA index (Zanner et al. 2009)
- The uncertainties of the BIS value make it difficult to compare the result with other versions of the BIS monitor. In addition, the BIS index does not give a consistent value for different types of anaesthetic agent (Frey, 2011)
- The BIS monitor failed to produce DoA index in some patients (Nguyen-Ky, Wen & Li 2013).

Based on the research problems listed above, this research focuses on developing new DoA algorithms to improve current DoA monitoring by providing better EEG signal analysis methods and better DoA assessment algorithms. To develop accurate DoA monitor, this research firstly address the filtering problems by

proposing new techniques to filter the EEG signal. Secondly, reduce the time delay by improving the EEG signal analysis technique in DoA assessment.

1.3 Objectives

The aim of this research is to develop novel and robust algorithms for real time DoA monitoring.

The specific objectives are:

1. Develop a digital signal filtering technique to remove noise in the EEG signal
2. Develop new DoA algorithms using a strong analytical signal and amplitude detection
3. Investigate the Bayesian based method for DoA assessment
4. Introduce a novel Bayesian spike accumulation technique to extract the EEG signal information and to analyse the EEG signal for monitoring DoA. Then, the Bayesian spike accumulation technique combined with Gaussian Bayesian method for robust DoA assessment
5. Investigate the Bayesian Student-t distribution for EEG signal analysis
6. Improve the Gaussian EEG signal analysis by using the Bayesian Student-t distribution for DoA monitoring.

1.4 Research workflow

This research is divided into three main phases as illustrated in Figure 1-1. It begins with the signal precondition which includes EEG data acquisition, EEG signal conversion and filtering. The EEG data is recorded from the patients under general anaesthesia and the data is collected and stored in the BIS index Vista monitor. Converting the data from a binary number to a decimal number must be done before the filtering process. A novel technique in the filtering process is introduced. Adaptive Bayesian filtering is applied for the EEG signal filtering process.

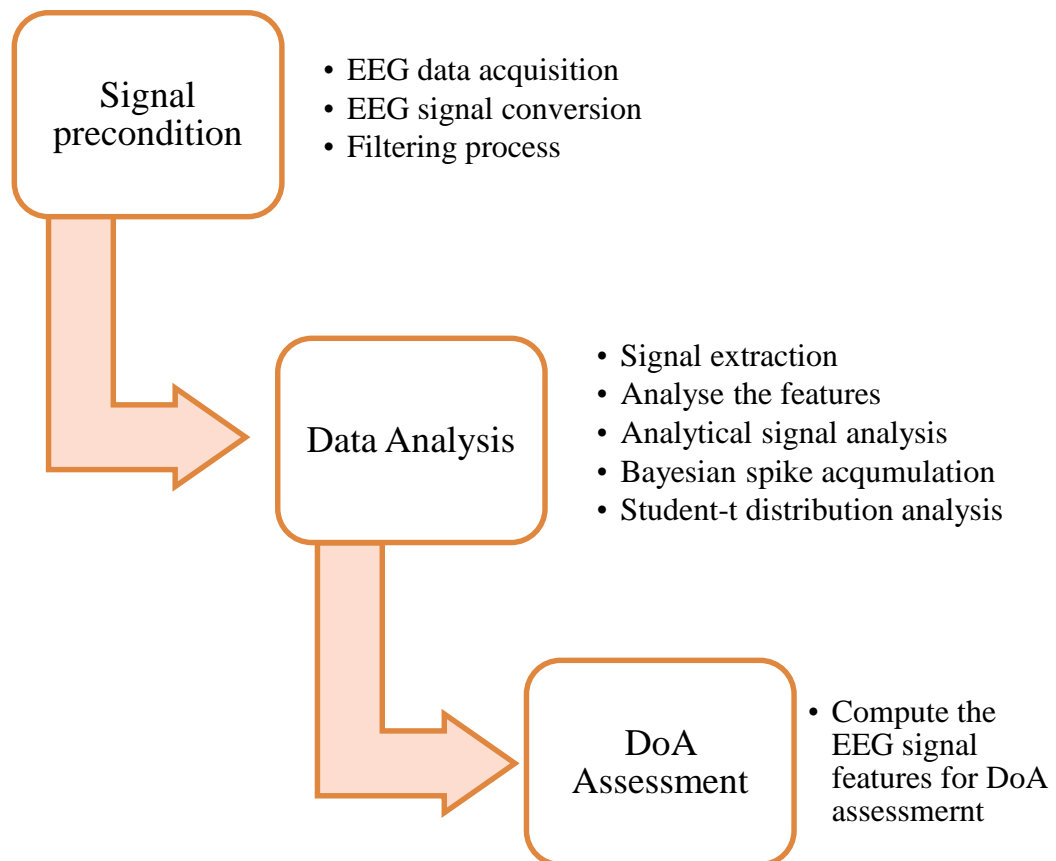


Figure 1-1. Three main phases of this research.

The next phase of the research is data analysis. In data analysis, the EEG signal after filtering, is analysed to extract its time and frequency features. Three methods are introduced to extract EEG signal features: strong analytical signal analysis, the Bayesian spike accumulation technique and the Student-t distribution technique.

The final phase is the DoA assessment. The extracted EEG signal features are analysed to determine the DoA level. The results are evaluated and compared with the most acceptable DoA monitor on the market, which is BIS index monitor.

1.5 Dissertation outline

This dissertation is presented in eight chapters. The dissertation is structured as follows:

Chapter Two is the literature review which introduces the general anaesthesia practice. The sub-section of general anaesthesia practice talks about the history of general anaesthesia; the effect of anaesthesia and how anaesthesia affects the central nervous system. In addition, Chapter two also discusses EEG signals, the effect of anaesthetic drugs on EEG signals and the current method for analysing EEG signals.

Chapter Three presents the EEG data used in this research. It covers EEG data acquisition, patient demography, and the frequency features of EEG signals. The EEG signal pre-process is also described in this chapter.

Chapter Four introduces the filtering process of EEG signals. This chapter investigates the novel technique in adaptive filtering based on Bayesian student-t distribution.

Chapter Five presents a method for feature extraction from EEG signals based on strong analytical signals. The new DoA index is also developed using the strong analytical signal analysis.

Chapter Six presents a novel technique for EEG signal processing using the Bayesian spike accumulation method. Furthermore, a new DoA index is also developed.

Chapter Seven presents an improved method for analysing the EEG signal for DoA monitoring using the Bayesian Student-t distribution. The Student-t distribution is introduced to extract information from the EEG signals and to analyse the EEG signal parameters for DoA monitoring.

Chapter Eight is the conclusion of this dissertation and suggestions for further work in EEG signal analysis and DoA monitoring.

2 LITERATURE REVIEW

2.1 General anaesthesia practice

Anaesthesia procedures have been used in surgery for more than a century. The anaesthesia technique, chemical compounds in the anaesthetic agent and monitoring technique, have improved since first introduced in 19th Century. The first anaesthesia demonstration used ether to make the patient unconscious during the operation (Alkire, Hudetz & Tononi 2008; Hall 1847; Landes 2002; Lundy 1940; Plomley 1847; Traill 2003). The definition of anaesthesia also evolved with discovery of new anaesthetic drugs. This chapter presents the definition of anaesthesia, anaesthesia effects in central nervous system, the technique used to measure the depth of anaesthesia and the EEG signal generation and its analysis.

2.1.1 The history of general anaesthesia

Anaesthesia compounds have been used in some ancient medicine and traditional ceremonies. The Greek historian Herodotus in 4th century BC wrote, in one of his

books, about the Scythians tribal customs in Southern Russia. The Scythians tribe used hemp to induced insensibility. The inhalation of hemp vapour was described as making people intoxicated and unconscious (Lundy 1940; Rawlinson). One of Nero's physician in 77 AD, Pedanius Dioscorides wrote in *Materia Medica*, about mandragora and wine producing an anaesthetic effect. Pedanius also described the effect of mandragora and wine in the incision. In addition, the ancient Chinese used opium to mitigate the horror in punishment and makes people unconscious during their punishment (Lundy 1940).

Before the ether anaesthesia technique discovered in the 19th Century, there is another inhaled technique used in 9th Century. The technique came from a Benedictine monastery at Monte Cassino, Italy. The technique is described as a mixture of several ingredients making the patient asleep and so feel no pain during surgery. The ingredients used to create the liquid hypnotic were opium, mandragora, fresh hemlock juice, hyposcyanus and water. These ingredients form a liquid which was absorbed with sponge. After the operation, the sponge was dried for further use. To make the patients sleep, the dried sponge was placed in hot water and then the vapour inhaled by the patient (Larson 2005).

In the late 18th Century and early 19th Century, many scientists attempted to find another compound of anaesthesia to deliver pain free in surgery. Nitrous oxide was discovered by Priestly and Joseph Black before the 19th Century. Humphry Davy, young chemist from Bristol UK, described the properties of Nitrous oxide (Larson 2005; West 2014). Davy conducted experiments using the Nitrous oxide. He wrote that Nirous oxide is capable of destroying physical pain. At that time, Nitrous oxide was used as a drug to gain euphoria and high imagination (West 2014). During the period of 1863 to 1881 Colton performed dental surgery 121709 times using Nitrous oxide without any fatality (Landes 2002). Nitrous oxide is still widely used in the operating theatre.

Scientists believe that the first modern anaesthesia practice was performed in 19th Century. The pioneering successful general anaesthesia demonstration was conducted on 16 October 1846 by William TG Morton. Morton gave a demonstration of ether anaesthesia in Boston, Massachusetts (Beecher 1947; Marjot 2009). However, four years before Morton publicly demonstrated the operation, Crawford Long performed the anaesthetics on 30 March 1842 in Jefferson, Georgia (Traill 2003). Unfortunately, Crawford Long did not publish his works in that year. Instead he published his result later in 1849. In anaesthesia history, Crawford Long was not the first person to give the anaesthetics but the credit of anaesthetic discovery goes to him (Traill 2003).

Once ether anaesthesia was introduced to the public, many surgical operations were performed successfully in the United States and in Europe. News of the discovery of ether anaesthetics in the United States travelled a long journey to Europe. A number of European hospitals pioneered the use of ether anaesthesia during operation (Marjot 2009). Table 2-1 shows the places in Europe and America that pioneered the use of ether in general anaesthesia. It tells us that the anaesthesia compound demonstrated by Morton was long awaited by physicians.

The discovery of ether anaesthesia was a revolution in medical history that stimulated the development of a new anaesthesia compound and anaesthetic delivery. The improvement in anaesthesia techniques began in the early 20th Century. The discovery of these compounds led to the replacements of the hazardous anaesthetic drugs used in the previous century. Most of the anaesthetics drugs introduced in 19th Century were flammable, had unpleasant smells or were explosive (Larson 2005; Lundy 1940). Some examples of hazardous anaesthetics are Divinyl ether, Cyclopropane and trichloroethylene. Divinyl ether is flammable, Cyclopropane is highly explosive and trichloroethylene is toxic. The anaesthetics introduced in the 20th Century were fluroxene, enflurane, isoflurane, desflurane, ketamine, propofol, etc (Bard 2001; Gelb et al. 2009; Larson 2005; Purdon et al.

2013). New anaesthetic delivery techniques also were developed during that period.

Table 2-1 Places that pioneering ether was used in general anaesthesia

Place	Date
Boston, USA	16 October 1846
London, Gower St.	19 December 1846
Dumfries	19 December 1846
London, UCH	21 December 1846
Paris,	22 December 1846
Bristol	31 December 1846
Cambridge	2 January 1847
Glasgow	4 January 1847
Bath	5 January 1847
London, Kings College	January 1847
London, Guys	January 1847
Edinburg	9 January 1847
Liverpool	12 January 1847
Manchester	12 January 1847
London, St. George	14 January 1847
Middlesex Hospital	25 January 1847

The first anaesthetics delivery method widely used was the inhalation of gases or vapours. The inhaled anaesthetics are still used in the operating theatre and dental surgery (Landes 2002; Migeon et al. 2013; West 2014). The other anaesthetic delivery method used is intravenous. The intravenous anaesthetic technique was first used successfully in the late 19th Century. The discovery of this technique was drawn from intravenous fluid therapy. Intravenous fluid therapy was discovered in the late 19th Century and early 20th Century when a number of physicians realised that maintenance of the fluid balance in human body during the operation was

important (Larson 2005). Then, they discovered a way to deliver fluid into the body using gravity. The technique was named "intravenous". Both of these anaesthetics delivery techniques are still used it was today and there has been much improvement in anaesthetic delivery since it was first introduced. Over the next section, the effects of inhaled anaesthetic and intravenous anaesthetic will be discussed.

2.1.2 Anaesthesia Effects

Modern general anaesthesia techniques use a combination of anaesthetic drugs. In most operations, the patient is induced with anaesthetic drug which contains sedatives or narcotics to bring on sleep and unconsciousness, and analgesics delivered for pain relief and muscle relaxation. Common anaesthetic drugs are intravenous drugs and inhaled anaesthetics (also known as volatile anaesthetics drug). Intravenous drugs are normally used to induce anaesthesia. Both the anaesthetic delivery method (inhaled and intravenous anaesthetics) affects different part of the brain (Leung et al. 2014; Parker 2006). The two anaesthetic methods affect different parts of the brain because the anaesthetic compounds are different. Therefore, a combination of anaesthetics drugs makes difficult to assess patient condition.

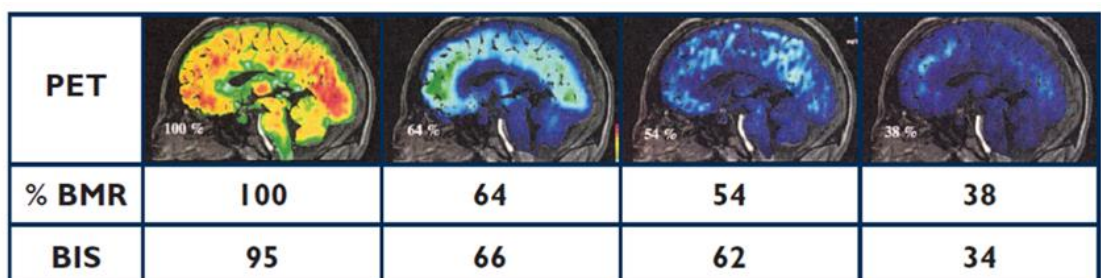


Figure 2-1. The PET scan of the brain in different anaesthesia states shows the neuronal activity using %BMR and the result compared with BIS index (Alkire 1998; Kelly 2003).

Anaesthetic drugs can depress brain function. This relationship can be observed from a Positron Emission Tomography (PET) scan as shown in Figure 2-1, where the percentage of brain glucose metabolism (%BMR) is a measurement for the activity of the brain based on the glucose metabolism in the brain. The 100 %BMR is indicated as awake where cerebral metabolism is active. Activities in the brain depend on the oxygen supply from the blood to process glucose for neuronal activity (Alkire 1998). The %BMR and Bispectral Index are reduced as the amount of anaesthetic drugs in the brain increases (Kelly 2003). Figure 2-2 shows the effect of anaesthetic drugs in cerebral metabolism which reflects on the EEG signal. The increasing effect of anaesthetic drugs causes the decreasing neuronal metabolism in central nervous system which results in the decreasing level of awareness. The PET scan also shows the correlation between the brain metabolism and the effect of the anaesthetic drugs in the central nervous system. Both Figure 2-1 and Figure 2-2 show the different stages of brain metabolism. Figure 2-1 shows these stages of brain metabolism based on the relationship of %BMR and the BIS index. Meanwhile, Figure 2-2 shows the correlation between cerebral metabolism and the EEG signals in different stages of consciousness. A higher percentage of BMR indicates brain activities or awake conditions.

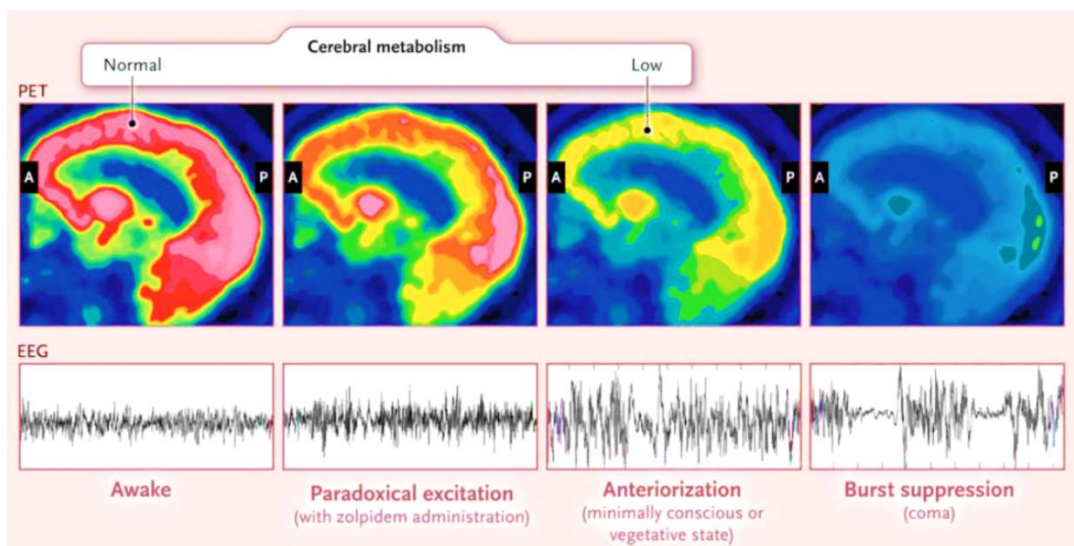


Figure 2-2. The effect of anaesthetic drugs in cerebral metabolism which reflects on the EEG signal (Brown, Lydic & Schiff 2010).

The general target of the administered anaesthetic compound is to make the patient unconscious and unresponsive to any pain during surgery. The amount of anaesthetic drugs administered to the patients determines the patient's response during the surgery. If the anaesthetic drugs administered to the patient was overdose, the recovery time would be prolonged, which might affect the nervous system and may cause brain damage (Bowdle 2006). On the other hand, if the anaesthetic drug administered to the patient was too little or not enough to maintain patient's unconscious level, the patient would awake during surgery (Musizza & Ribaric 2010; Myles 2007). Insufficient anaesthetic drugs administered to the patient is known as "awareness during the surgery". Awareness during surgery can affect patients' mental anxiety and potentially have long term psychological effects (Avidan et al. 2008; Lennmarken et al. 2002).

In the last two decades there has been a significant improvement in patient safety issues during surgery. For instance, the incident of awareness under general anaesthesia has been reduced from 1-2 % in 1980s to about 0.1% (Musizza & Ribaric 2010; Myles 2007; Shepherd et al. 2013). Similarly, Bruhn et al. (2006) presented the decreasing incidence of awareness since 1960, as shown in Table 2-2. Across the world, the mortality rate related to general anaesthesia has been reduced significantly during the period of 1990 to 2006 (Braz et al. 2009). Incidents of awareness are declining due to the improvement of general anaesthesia delivery techniques. For further reductions in incidence awareness during surgery, depth of anaesthesia (DoA) monitoring technique needs to be improved.

A new report has suggested that there is a long term neurological effect of anaesthesia. The sedative compounds of anaesthesia have potential neurotoxic effects. Soriano and Vutskits (2015) reported that some anaesthesia compounds potentially have neurotoxic effects and it is only Dexmedetomidine which does not have a neurotoxicity effect (Soriano & Vutskits 2015). Table 2-3 shows the number of anaesthesia drugs which have a neurotoxic effect. The high dose of the anaesthetic drugs and long term exposure of these sedatives leads to neurocognitive

deficits (Brambrink et al. 2012; Paule et al. 2011; Soriano & Vutskits 2015). The study of the neurocognitive deficits was done with primates where the results showed that there was a significant decrease of cognitive function (Paule et al. 2011). The severe effect of ketamine impacted the foetuses of the Macaque compared with the effect in neonates (Brambrink et al. 2012).

Table 2-2. Review of incidents of awareness (Bruhn et al. 2006; Shepherd et al. 2013)

Author	Year	Sample size	Awareness
Hutchinson (Hutchinson 1961)	1960	656	1.2
Harris (Harris, Lubarsky & Candiotti 2009)	1971	120	1.6
McKenna (McKenna & Wilton 1973)	1973	200	1.5
Wilson (Wilson, Vaughan & Stephen 1975)	1975	490	0.8
Liu et al. (Liu et al. 1991)	1990	1000	0.2
Sandin (Sandin et al. 2000)	1997-1998	11785	0.15
Myles (Myles 2007)	1993-2000	10811	0.11
Sebel (Sebel et al. 2004)	2001-2002	19575	0.13
Ekman et al. (Ekman et al. 2004)	2003	7826	0.18
Lenmarken & Sandin(Lenmarken et al. 2002)	2004	1238	0.9
Pollard et al.(Pollard et al. 2007)	2007	87361	0.07
Xu (in China) (Xu, WU & Yue 2009)	2009	11101	4.1

Table 2-3 Neurotoxicity of anaesthesia drugs (Soriano & Vutskits 2015)

Anaesthesia drug	Neurotoxicity
Propofol	Yes
Midazolam	Yes
Pentobarbital	Yes
Chloral hydrate	Yes
Ketamine	Yes
Dexmetomidine	No

Anaesthesia drugs could cause short term side effects or a long term side effects to the patients. In order to prevent the drug side effects, anaesthesia technique and anaesthesia assessment need to be improved. Accurate monitoring provides support in the administration of correct anaesthetic drugs, better assessment, reduction of intra operative awareness and reduction of mortality rates (Gelb et al. 2009; Zanner et al. 2009).

Anaesthesia drugs have different effects on the brain, as different components of anaesthesia drugs impact differently in the central nervous system. But, in general, all anaesthesia drugs produce loss of consciousness.

2.1.3 Anaesthesia on the Cellular Levels

EEG's are generated by the central nervous system. The central nervous system consists of nerve and glia cells. Nerve cells consist primarily of axon, dendrite and cell bodies. Axon transmits electrical impulse in the nerve while dendrite acts as a link or signal transmitter between other cells, other dendrites and other nerves. Electrical current in central nervous system is generated during the synaptic excitation (Sanei & Chambers 2007). Figure 2-3 shows the structure of the neuron

which consists of three main parts cell body, axon and dendrite. The inset picture in Figure 2-3 shows the synaptic terminal where the electrical impulses from the cell body are transmitted through the axon to the dendrites. These electrical impulses are called action potential. Generated signals are in the form of a chemical ion which is called neurotransmitter. The neurotransmitters (chemical ions) from the cell body allow the signals to transmit between the neuron and other cells by releasing the neurotransmitter and bind to the receptor.

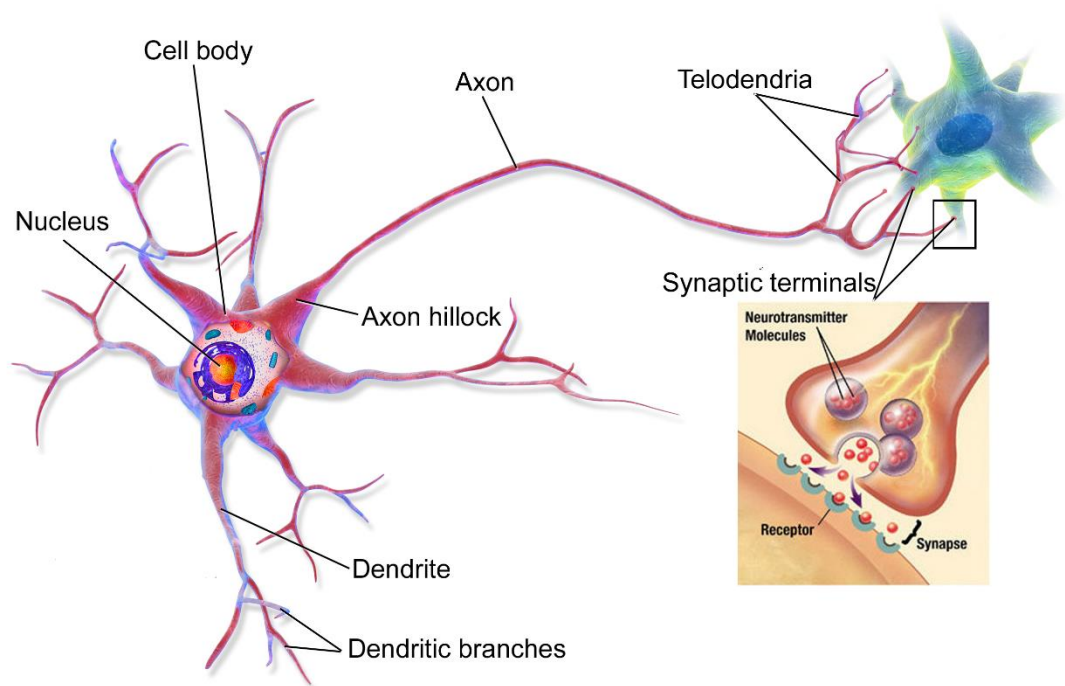


Figure 2-3. Typical neuron structure and synaptic terminal (Wikipedia 2015)

There are two types of anaesthetics the intravenous and inhaled. The intravenous are mainly used to induce the patients. The inhaled drugs target the ion channel. The inhaled anaesthetic is used for anaesthesia maintenance (Alkire, Hudetz & Tononi 2008). Once the anaesthetics bind with the ion channels, they can control the synapse and the postsynaptic membrane potential (Alkire, Hudetz & Tononi 2008; Pauling 1961; Steyn-Ross 2002). Different components of anaesthetic drugs can affect different neurotransmitters and target different receptors. Figure 2-4

shows the anaesthetic drugs and their different targets (Alkire, Hudetz & Tononi 2008). Some anaesthetic drugs target NMDA (*N-methyl-D-aspartate*), potassium channels, Glycine, Nicotinic Ach (*acetylcholine*), Muscarinic Ach (*acetylcholine*), Serotonin, and AMPA (*α -amino-3-hydroxy-5-methyl-4-isoxazolepropionic acid*) (Leung et al. 2014). However, most anaesthetic drugs (intravenous and inhaled drugs) bind with the GABA_A (*γ -aminobutyric acid type A*).

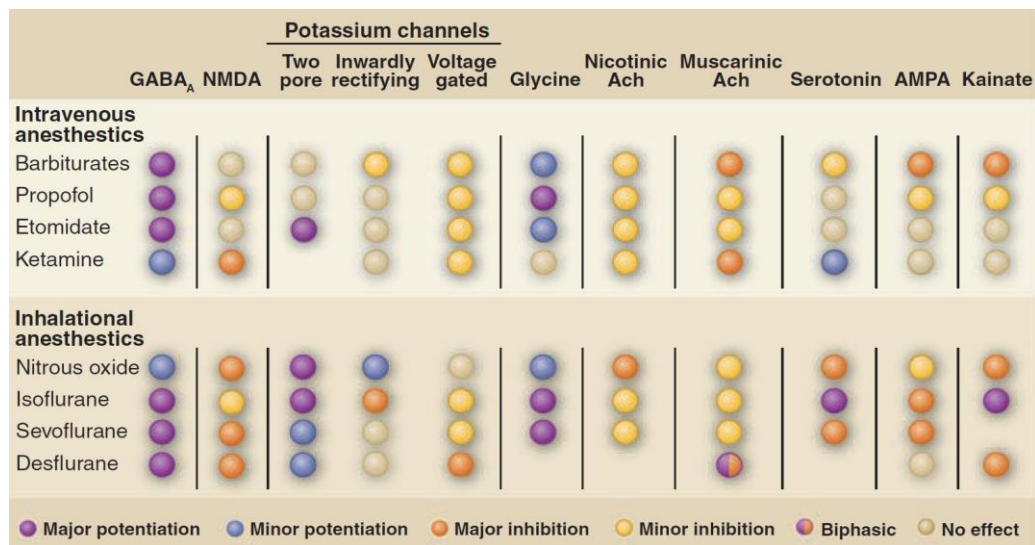


Figure 2-4. Different target of anaesthetic drugs (Alkire, Hudetz & Tononi 2008).

General anaesthetic drugs affect the central nervous system. Most of the general anaesthetics drugs are apolar, meaning they are able to cross the blood brain barrier and collaborate with receptor (Alkire, Hudetz & Tononi 2008; Franks 2008; Franks & Zecharia 2011; Musizza & Ribaric 2010). The receptor can be increasing in firing rate (excitatory) or decreasing in firing rate (inhibitory). Many anaesthetics drugs bind the GABA_A (*γ -aminobutyric acid type A*) to the postsynaptic membrane (Brown, Lydic & Schiff 2010). Figure 2-5 shows the neurotransmitter releasing the chemical through the synapse (gap) causing the Chloride ion (Cl⁻) channel to remain open. The more Cl⁻ ion enter the postsynaptic membrane, the more it will become negatives (hyperpolarised) and less action potential for firing (Franks 2008; Steyn-

Ross 2002). Anaesthetic drugs increase the duration of inhibitory and decrease the excitatory (Alkire, Hudetz & Tononi 2008; Steyn-Ross 2002). Alterations at the molecular level are reflected in the brain's electrical activity. The increasing duration of inhibitory causes slow EEG (low frequency and high amplitude). The increasing excitatory from slow EEG to fast EEG (high frequency and low amplitude) is reflected in arousal (wakefulness).

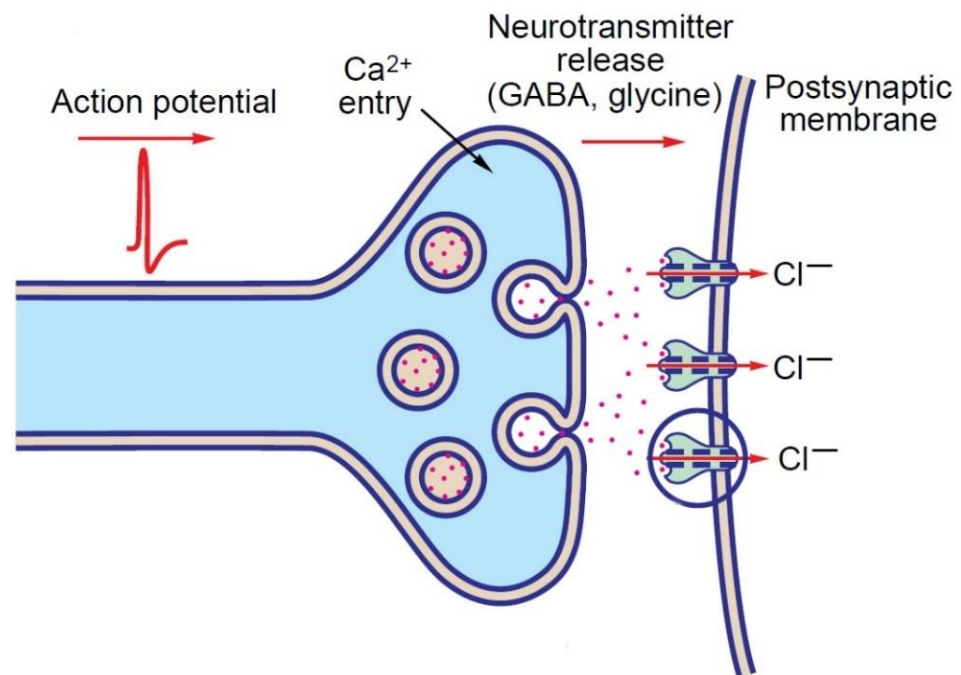


Figure 2-5. Inhibitory in the receptor as the neurotransmitter releases chemicals through the synapse (Steyn-Ross, 2002).

2.2 Electroencephalogram signal

Hans Berger was the first person to measure the effect of chloroform in the EEG signals. Berger was able to differentiate the physiological state from potential changes in the galvanometer (Freye 2005). This early research in EEG signals became a foundation of EEG signal analysis. Most EEG signal analysis has been based on the evaluation of EEG signal patterns. The EEG signal patterns such as

frequency, amplitude, frequency power, and asymmetry of the signals are used in current EEG signals analysis (Rampil 1998).

The increasing inhibitory caused by the anaesthetic drugs reflects less action potential firing from the central nervous system. The increasing inhibitory causes the loss of consciousness or vice versa (increasing excitatory in the synapses leads to arousal). The first study to describe anaesthetic's biphasic effect on the EEG signal was Martin and his colleagues (Dubois et al. 1978; Gelb et al. 2009; Kuizenga, Wierda & Kalkman 2001). Biphasic EEG effects are defined as the increasing effect of the anaesthetic drugs to the patients followed by the changing in amplitude and frequency in the EEG signals (Kuizenga, Wierda & Kalkman 2001). The changing pattern in the EEG signals can be seen in Figure 2-6.

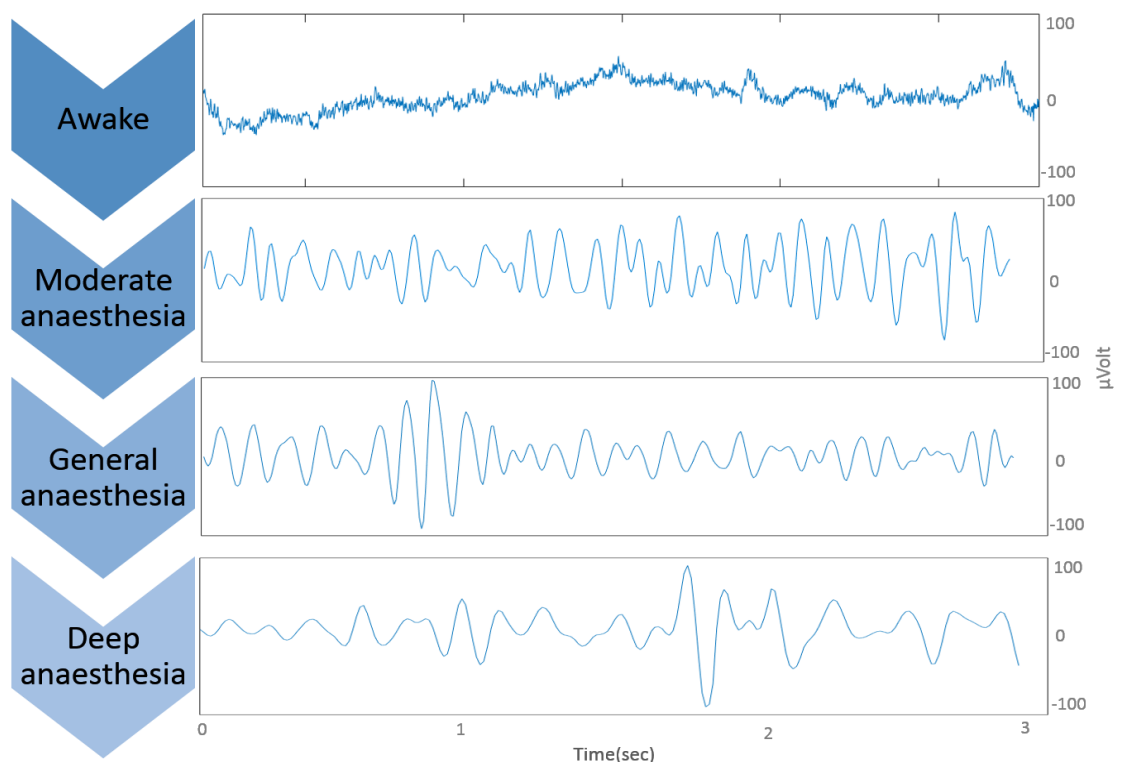


Figure 2-6. EEG signal patterns in different anaesthesia stages.

The EEG signal patterns in awake patients are high frequency and low amplitude. The interference of muscle signal and eye blinking create a slightly high amplitude deflection from the baseline signals (Bennett et al. 2009). As the dose of anaesthesia drugs increases, the patient begins to lose consciousness and this is reflected in the EEG signal patterns. The EEG signal becomes slow in frequency and high in amplitude (Brown, Lydic & Schiff 2010; Kelly 2003; Kortelainen & Seppänen 2013).

Typical EEG signal frequency are recorded in the scalp from δ (delta) waves 0– 4 Hz to more than 100 Hz. Characteristics of the amplitude signal fluctuates from 20 micro volts to 200 microvolts depending on the anaesthesia levels (Kelly 2003). Table 2-4 shows that the EEG signal frequency is divided into different frequency bands (Freye 2005; Jagadeesan et al. 2013; Rampil 1998). A moderate stage of general anaesthesia is indicated by the decreasing in the EEG beta band (13 - 30 Hz) and the increasing in the EEG alpha band (8 – 13Hz) and EEG delta band (0 – 4 Hz) (Brown, Lydic & Schiff 2010; Kelz et al. 2009; Otto 2008). As the anaesthesia goes deeper, the beta and alpha bands disappear (Bennett et al. 2009). Burst suppression normally appears during the deep anaesthesia stage. The EEG burst suppression is identified by the EEG signal being suppress for a period of time and interposed with an alternating period of high voltage (beta and alpha) activity (Brandon Westover et al. 2013). Figure 2-7 shows the EEG burst suppression during deep anaesthesia stage.

Table 2-4. EEG frequency band

EEG band	Frequency
Delta (δ) band	0.3 – 4 Hz
Theta (θ) band	4 - 8 Hz
Alpha (α) band	8 - 13 Hz
Beta (β) band	13 – 30 Hz
Gamma (γ) band	30 - >100 Hz

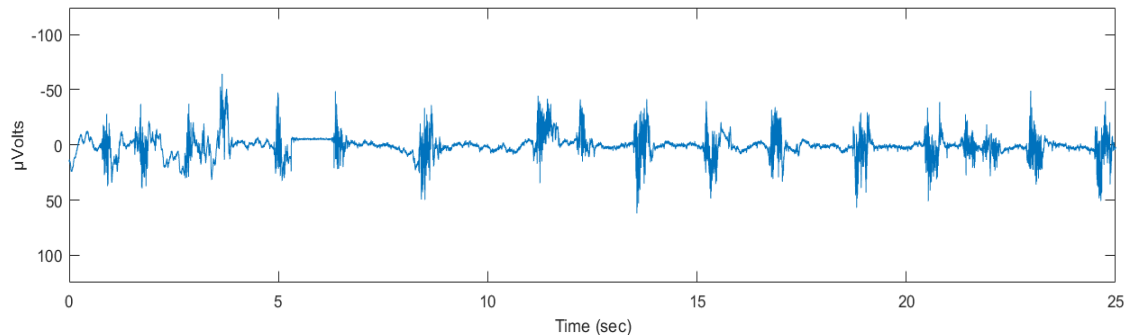


Figure 2-7. EEG burst suppression during deep anaesthesia.

2.3 Typical anaesthesia drug effects on EEG signals

Not all anaesthetic drugs can give the same response in the EEG signal patterns. Following is the anaesthetic drugs and its effects on the EEG signals.

- *Ketamin*

Some anaesthetic drugs such as Ketamine do not correlate well with the EEG signal pattern (Bowdle 2006; Jagadeesan et al. 2013; Myles 2007; Shepherd et al. 2013). Even though Ketamine reduces the alpha band activity and induced high amplitude theta activity, and looks similar to other anaesthetic drugs, but it creates different effects on the EEG signals.

- Isoflurane

Isoflurane is normally used for anaesthesia maintenance. Isoflurane can take patients into deep anaesthesia. A high dose Isoflurane can produce isoelectric EEG signals. Deep anaesthesia can be reached by using a high dose of isoflurane (1.2%) (Bischoff,

Kochs & Schulte am Esch 1994). The effect of this drugs in the EEG signal is increasing the delta band activity and decreasing alpha band activity (Freye 2005).

- *Propofol and Benzodiazepine*

Propofol and benzodiazepines have similar effects on the EEG signals. Both drugs are usually administered to the patients for induction or preoperative purposes. The effects on EEG signals is increasing the EEG beta and alpha bands followed by the delta activity, but the patient is unresponsive (Fontanet et al. 2014; Jeong et al. 2006; Kuizenga, Wierda & Kalkman 2001; Lapébie et al. 2014; Purdon et al. 2013; Yin, Wang & Liu 2014).

- *Nitrous Oxide*

A low dose of nitrous oxide has less effect on EEG signals. A study revealed that a stable GABA_A with up to 30% of nitrous oxide in the oxygen has minimal effect on EEG signals (Bennett et al. 2009; Bischoff et al. 1996; Kochs et al. 1994; West 2014). An increasing dose up to 50% of nitrous oxide in oxygen is reflected in the disappearance of the alpha band and an increase in the theta band. At this stage patients develops unconsciousness (Freye 2005).

2.4 Measuring depth of anaesthesia

Depth of anaesthesia has been assessed and monitored since the introduction of ether anaesthesia in the 19th Century. Long before the neurophysiological signal was discovered, monitoring DoA was based on clinical signs such as breathing pattern, muscle tone, eye movement, and blood pressure. Guedel (1920) introduced the four stages of ether anaesthesia and its diagram (Guedel 1920). Figure 2-8 shows the diagram introduced by Guedel for DoA monitoring. The first stage is

analgesia where the patient is conscious but insensible to pain. The second stage is excitement or delirium where the patient has a transition from consciousness to unconsciousness with excessive motor activity (Oshima 2008). The third stage is a surgical anaesthesia and this divided into four planes. The breathing pattern from the first plane to the fourth plane becomes weaker. The fourth stage is a very deep anaesthesia where the respiratory system is paralysed. The Guedel assessment diagram and clinical signs could not be applicable to all anaesthetic drugs (Bowdle 2006; Oshima 2008). Today, even though clinical sign assessment is not the primary method in determining the DoA stage, it is still being used to assess patients' state along with the neurological monitor.

Stage	Muscle tone	Breathing	Eye movement
1	Normal		Slight
2	Normal to markedly increased		Moderate
3 Surgical anaesthesia ↓	Slightly relaxed		Slight
	Moderately relaxed		None
	Markedly relaxed		None
	Markedly relaxed		None
4 Respiratory paralysis	Flaccid		None

Figure 2-8. Guedel introduced four stages of ether anaesthesia (Guedel 1920; Oshima 2008).

The modified observer assessment of alertness/sedation (MOAA/S) method has been used to assess patients under general anaesthesia. This method can be used along-side the EEG signal assessment to validate the patient's conditions (Freye 2005). The MOAA/S method is required to stimulate the patients with verbal or physical stimulation to find out the patient response score. Table 2-5 shows the MOAA/S score used to assess the unconscious patient. There are a number of studies showing that the MOAA/S score has a good correlation with common hypnotic drugs (Gelb et al. 2009; Miller 2005).

Table 2-5 MOAA/S score to assess unconscious patient (Gelb et al. 2009)

Score	Responsiveness
5	Responds readily to name spoken in normal tone
4	Lethargic response to name spoken in a normal tone
3	Responds only after name is called loudly repeatedly
2	Responds only after mild prodding or shaking
1	Responds only after painful trapezius squeeze
0	No response after painful trapezius squeeze

The modern DoA monitor uses the neurophysiological signals to monitor patients' conditions. Some of the benefits of the neurophysiological monitor using EEG signal is its ability to monitor the patients continuously and the ease of application to the patients. In addition, general anaesthetic drugs effects on the central nervous system are reflected in the EEG signal patterns (Bischoff, Schmidt & Schulte am Esch 2000; Kelly 2003; Kortelainen & Seppänen 2013; Krieger et al. 2014). In order to estimate a patient's condition under general anaesthesia, the EEG signals need to be interpreted.

There are numerous studies recommending that the EEG signal be used to monitor the DoA (Bischoff, Kochs & Schulte am Esch 1994; Gelb et al. 2009; Ishizawa 2007; Johansen 2006; Marchant et al. 2014; Nguyen-Ky et al. 2011; Otto 2008; Purdon et al. 2013; Rampil 1998; Zikov et al. 2006). However, the improvement in anaesthetic delivery with combination anaesthetic drugs techniques, the EEG signal analyses become complicated (Kortelainen & Seppänen 2013; Kortelainen, Vayrynen & Seppanen 2011). A combination of anaesthetic drugs administered to the patients creates challenges in analysing the EEG signals (Freye 2005; Kortelainen & Seppänen 2013). Extracting the EEG signals pattern to further analyse the DoA is not as simple as taking clinical signs from the patient. The complexity of the EEG signals makes it difficult to interpret the underlying information in the signals. Therefore, it is important to apply a proper filtering technique and to extract information from the EEG signals with the right method.

There are a number of approaches to analyse EEG signals such as spectral analysis, bispectral analysis, Fourier transform, burst suppression, spectral edge frequency analyses, Wavelet transform, entropy, and statistical analysis (Gelb et al. 2009; Musizza & Ribaric 2010; Nguyen-Ky, Wen & Li 2013; Nguyen-Ky et al. 2012; Shalhaf et al. 2013; Taheri et al. 2009). Spectral analysis, bispectral analysis, Fourier transform and spectral edge frequency are used to analyse EEG signals in frequency domain. Frequency domain analysis examines the EEG signals based on the frequency interval for a certain period of time (Otto 2008). Wavelet transform is capable of extracting frequency content of the signal in different scales without losing the EEG signal time information (Juan et al. 2014; Li et al. 2003; Park, Eckley & Ombao 2014; Suyi & Jun 2009; Taruttis et al. 2014). Burst suppression and statistical analysis are normally used to analyse signals in time domain (Rampil 1998). One of the advantages of time domain signal analysis is that the signal can be directly analysed without converting.

2.4.1 Time domain analysis

EEG signals in time domain is analysed based on variation of the voltage over time (Rampil 1998). Most of the approaches are based on the statistical signal analysis such as mean, variance and standard deviation of the signals (Musizza & Ribaric 2010; Rampil 1998). In addition, morphology of the signal is also used to analyse the signal in time domain.

The autoregressive method (AR) is computed based on EEG signals in time domain. The AR method is a method for the prediction of a next value by using the linear combination of the previous values (Bender, Schultz & Grouven 1993). Before administering the anaesthetic drugs, the AR coefficient is fixed and should not change. As the anaesthetist administers the anaesthetic drugs, the AR coefficient will change (Bender, Schultz & Grouven 1993). The outcome of AR value has been used as an input to neural networks for predicting the DoA (Muthuswamy & Roy 1999). This AR method is also used for classifying the basic pattern of the EEG signal (Broek 2003).

Burst suppression occurs in the case of deep anaesthesia as mentioned previously. It happens when the anaesthetics concentration in the patient is high (Musiza, 2010; Rampil, 1998). In burst suppression the EEG signal drops from high amplitude to low amplitude and stays in low amplitude for a period of time. Figure 2-9 shows the event of burst suppression. The burst suppression ratio is defined as a ratio of summation of the suppression in an epoch (a defined time slot to analyse a signal) and the total number of epochs (Broek, 2003; Rampil, 1998).

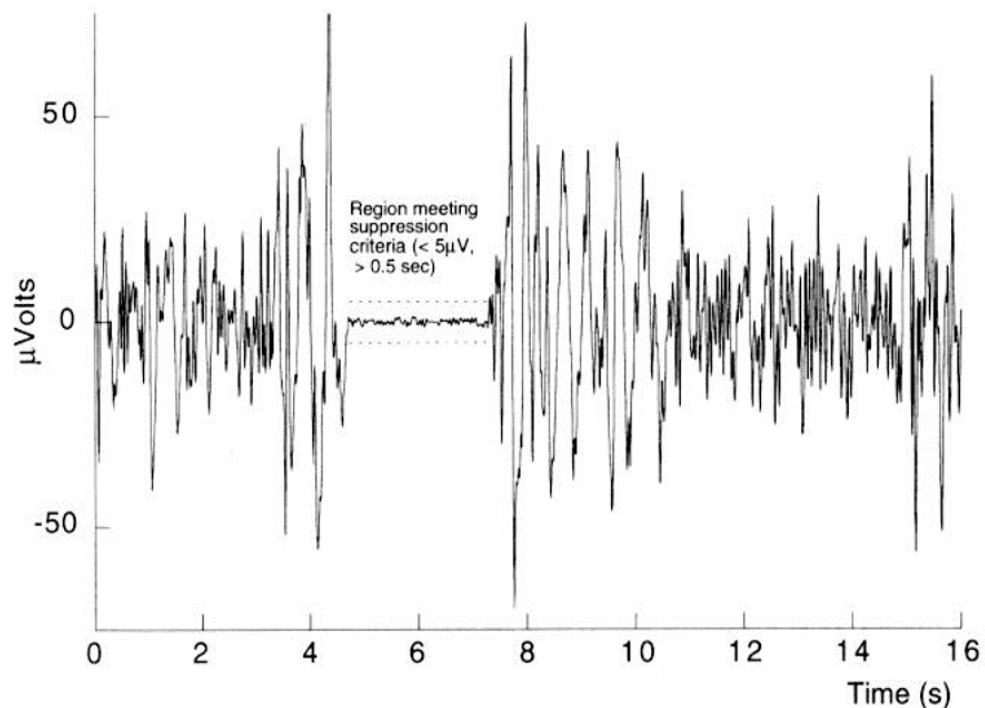


Figure 2-9 EEG burst suppression in deep anaesthesia (Rampil 1998).

2.4.2 Frequency domain analysis

Frequency domain analysis is another popular method for analysing the EEG signal. Fourier transform is widely used to extract the EEG signal information in frequency domain. The features extracted from the signal are amplitude, frequency, power spectrum, phase, and angle of the signal.

Most of the DoA monitors on the market use frequency domain analysis (Bischoff, Schmidt & Schulte am Esch 2000; Musizza & Ribaric 2010). Power spectrum analysis, spectral entropy, spectral edge frequency and the phase coupling of the signals have been used to obtain the DoA index (Bowdle 2006; Kortelainen & Seppänen 2013; Li & Li 2014). These monitors use different signal processing method to produce an index of DoA. The following are several DoA monitors currently available on the market (Bowdle 2006; Musizza & Ribaric 2010):

- Bispectral Index (BIS)
- Narcotrend
- Cerebral State Index
- M-Entropy
- AEP or AAI (Mid-latency auditory-evoked potential=MLAEP)

Although all of these monitors are available on the market, the BIS monitor is the most widely used in hospitals around the world (Bowdle 2006; Kortelainen & Seppänen 2013). Even though the actual algorithm of BIS has not been published, the computation method and the formula in BIS are widely used in many DoA research studies (Otto 2008; Rampil 1998). The BIS index is a dimensionless number between 0 and 100. The BIS monitor indicates the level of consciousness using an index from 100 (awake) to zero (isoelectric) (Aspect Medical Systems 2009; Kelly 2003; System 2009). Table 2-6 shows the comparison between the DoA monitor with the computed parameters from the EEG signals.

Despite the popularity and benefits of the BIS monitor in the operating theatre, it has several limitations. Limitations of BIS monitor that have been identified in several studies are:

- it does not respond properly to some anaesthetic drugs such as nitrous oxide, ketamine and opioids
- BIS index can be influenced by EMG and EOG (Bowdle 2006; Johansen 2006; Li & Li 2014; Palendeng, Wen & Li 2014)
- the BIS index does not provide a consistent value for different types of anaesthetic drugs
- the computation takes approximately 30 to 120 seconds to produce the index (Freye 2005; Frey 2007-2011; Marchant et al. 2014; Zanner et al. 2009).

Table 2-6. A comparison of DoA monitor in the market

DoA Monitor	Computed Parameters	Range of Value	Time Delay (Seconds)
BIS Index	• Relatif β ratio	0 – 100	$\pm 30 - 60$
	• SyncFastSlow (SFS)		
	• Quasi-flat activity		
	• Burst suppression		
	• Bispectrum		
Narcotrend	• Spectral	0 – 100	± 20
	• Entropy		
	• Autoregressive		
Cerebral state index	• α and β ratio	0 - 100	± 15
	• $\alpha - \beta$ difference		
	• Burst suppression		
M-Entropy	• Power spectrum	0 -100	$\pm 2 - 60$
	• Shannon entropy		
	• Response entropy		
	• State entropy		
AEP	Mid-latency auditory evoked potential (MLAEP) and amplitude	0 - 99	± 0.144

In the last two decades, a number of methods have been introduced to analyse the EEG signals for DoA, such as nonlinear analysis and statistical Bayesian analysis. The nonlinear analysis methods include the entropy algorithm, detrended technique, and wavelet transform technique (Bennett et al. 2009; Castro et al. 2009; Ellerkmann et al. 2006; Jospin et al. 2007; Li et al. 2008; Nguyen-Ky et al. 2014;

Nguyen-Ky et al. 2012; Shalhaf et al. 2013; Shepherd et al. 2013; Soghomonyan et al. 2014; Valencia et al. 2014; Zhiqian et al. 2005; Zoughi et al. 2012).

The entropy method is normally employed to analyse the EEG signals using Shannon entropy functions. The Shannon entropy function has been improved by combining the power spectral density function to derive the spectral entropy function for EEG signal analysis (Marchant et al. 2014; Shalhaf et al. 2013; Valencia et al. 2014). The response entropy (RE) and state entropy (SE) are derived from the Shannon entropy function and power spectrum analysis (Kortelainen & Seppänen 2013). Other entropy techniques such as sample entropy (SampEn) and permutation entropy (PermEn) have also been introduced to analyse EEG signals. Shalhaf et al. (2013) reported that both SampEn and PermEn are able to detect brain activity in anaesthesia. However, the entropy shows an inconsistent number for the patient with a neurological disorder (Liu et al. 2012; Schmidt et al. 2003; Wei et al. 2013). In addition, the interference from noises affects the entropy parameters (Wei et al. 2013).

Anaesthesia assessment based on Wavelet transform introduced by Nguyen-Ky (Nguyen-Ky et al., 2012), utilised the Discrete Wavelet Transform (DWT) technique and the eigenvector to derive the DoA index. Zikov et al. (2006) used the Stationary Wavelet Transform (SWT) technique for signal decomposition and claimed that the technique can be used as an alternative to the BIS monitor (Zikov et al., 2006). In Zikov et al. (2006), parameters such as average value, root mean square (RMS), probability density function, maximum or minimum value and standard deviation were also extracted.

A method introduced by Nicolaou and Georgiou (2013b) to assess the anaesthesia awareness used the autoregressive model estimation which applied the Bayesian information criterion (BIC) and the Akaike information criterion (AIC) (Nicolaou & Georgiou 2013a). Nguyen-Ky, Wen and Li (2013), introduced the EEG signal analysis using the Bayesian based method. The EEG signal is analysed by taking

the maximum posterior of the data using the probability density function. Then, the value is used as a parameter to derive the DoA index. The research also reported that the normal distribution gives the best value for the posterior compared to other distributions such as gamma distribution, Rayleigh distribution, extreme fit distribution, inverse Gaussian distribution, and exponential distribution (Nguyen-Ky, Wen & Li 2013).

This chapter has discussed the history of general anaesthesia, the side effects of anaesthetic drugs to the patients, and the typical response of central nervous system and EEG signal to the anaesthetic drugs. It has also provided information about DoA monitors available on the market and technique used in each of these DoA monitors. Furthermore, this chapter has also discussed common method and most popular methods for DoA assessment. It is argued that those methods are able to analyse the EEG signal and provide reliable DoA assessment. However, there are a number of limitations with these techniques for DoA assessment such as: longer computation time, there are noises in the signal which interfere the DoA assessment, and in some cases the DoA index did not respond properly to some anaesthetics drugs. This research highlights the development of new algorithms for filtering and extracting the EEG signals, and analysing EEG signal for DoA assessment to improve current DoA monitor.

The following Chapter Three provides a brief introduction about data acquisition, EEG signal conversion and frequency separation.

3 ELECTROENCEPHALOGRAM DATA ACQUISITION

As anaesthetic drugs and the technique to deliver anaesthesia improve, the anaesthetic monitoring also improves. Modern anaesthesia monitors use neuronal activity as a parameter to identify the patient's condition. Recorded neuronal activity in the central nervous system is known as the electroencephalogram (EEG) signal. The recorded EEG signals are the sum of all brain activity. The EEG signal is recorded from the scalp or from the forehead of the patients. In this particular research, the EEG signals are recorded from the forehead of the patients.

3.1 Equipment and settings

The EEG signals used for this research are recorded from patients under general anaesthesia using the BIS monitor. Figure 3-1 shows the BIS index Vista monitor. The monitor includes the BIS vista monitor screen, BISx, patient interface cable and sensors. The BISx is used for collecting signals from the sensors. The sensor used in BIS index Vista is a QUADRO sensor. The QUADRO sensor is an improved sensor compared to earlier BIS sensors. It consists of four electrodes which need to be placed on the forehead. Covidien Company (Previously Aspect

Medical Company) claims that the sensors are able to minimise interference from noises (Aspect Medical Systems 2009; Kelly 2003).



Figure 3-1. BIS Index – Vista Monitor includes monitor, sensor, BISx and patient interface cable (Aspect Medical System 2009)

EEG signals were collected using a BIS Vista monitor version 3 with algorithm revision BIS 4.1 from Aspect Medical Systems. These raw EEG signals were often contaminated with noises (artifacts) such as EMG, EOG and ECG (electrocardiogram) (Krishnaveni et al. 2006). EMG noise is caused by electrical activity produced by skeletal muscles. The EMG signals are characterised by high amplitude and high frequency. According to Jensen et al. (2004) the frequency range of EMG noise is approximately 0 - 200 Hz. The frequency range of 0 – 70 Hz from the EMG signal overlaps with the EEG signals. In this study, frequencies higher than 120 Hz were filtered out. The EOG is caused by eye movement and eye blinking. The EOG signal appears in the frequency range 0 - 16 Hz with high

amplitude (Krishnaveni et al. 2006). These noises affect the EEG signals and may result in an incorrect DoA assessment.

The anaesthetic drugs administered to the patients are a combination of volatile and intravenous drugs. The patients received a combination of midazolam, alfentanil or fentanyl, and propofol. Midazolam is used as an anaesthetic induction drug. All patients were administered with propofol before intubation (insertion a tube for airway) or inserted with a LMA (laryngeal mask airway). Desflurane or sevoflurane with oxygen were used as the anaesthesia maintenance drugs. Data collection in this study was approved by the Ethics Committee of the University of Southern Queensland, and the Ethics Committee of the Toowoomba and Darling Down Health Service District.

Thirty eight EEG samples are used in this research. Table 3-1 shows the demography of the patients. Around 34% of the patients were in the age group 50 to 59. 10.2% of patients were over 70 years old. Figure 3-2 shows the percentage of the patients based on their age group. Patients are grouped into their age group because the study showed that patients older than 40 years of age are categorised as high risk cardiac complication during surgery. In addition, there are alterations in vascular reactivity due to ageing such as changes in blood pressure and diminished baroreceptor responsiveness (Miller 2005).

Table 3-1. Patient demography

Range age	Number of Patients	Age (year) mean \pm SD	Weight (kg) mean \pm SD	Heights mean \pm SD
20 – 29	2	24 \pm 2	93.5 \pm 7.5	178.5 \pm 5.5
30 – 39	2	38.5 \pm 0.5	145 \pm 21.5	174 \pm 9
40 – 49	8	43.7 \pm 2.3	81.4 \pm 20.5	174.6 \pm 14.2
50 – 59	13	54.7 \pm 2.4	89.8 \pm 20.2	170.7 \pm 9
60 – 69	9	63.7 \pm 2.5	82.8 \pm 13.5	166.4 \pm 10.3
70 – 79	3	73 \pm 2.2	90.7 \pm 7.4	172.7 \pm 2.1
80 - 89	1	88 \pm 0	70 \pm 0	172 \pm 0

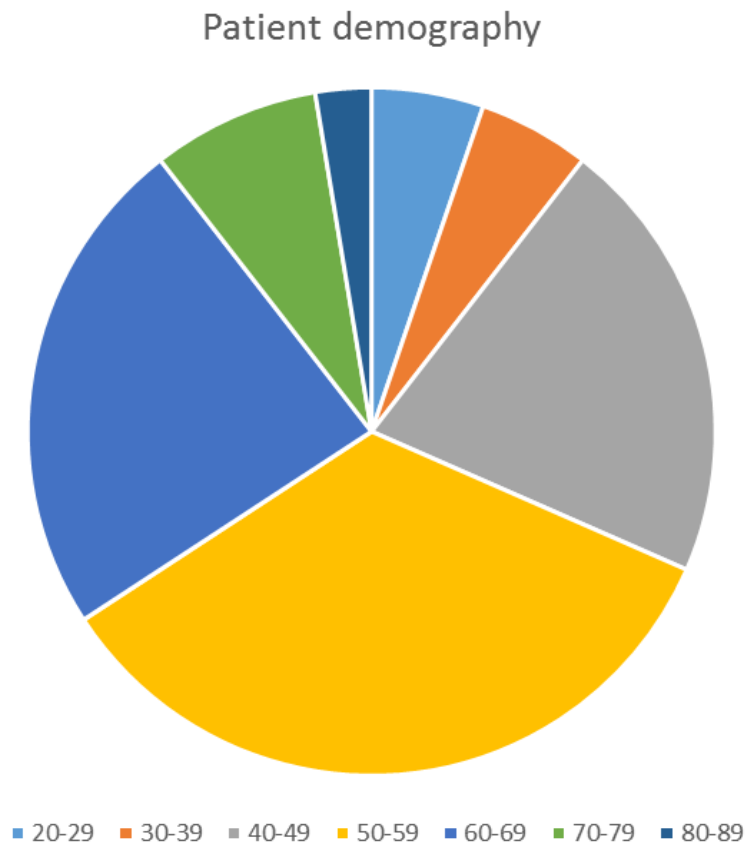


Figure 3-2. Percentage of the patients according to age group.

3.2 EEG signal conversion

The raw EEG data and BIS values were obtained from the BIS monitor and exported to a USB flash drive for off line analysis. In the BIS monitor, there are two channels of EEG signal collection. Both are in binary format. The signal from channel 1 and 2 are sampled at 128 Hz and saved as 16-bit signed integers. The data are stored consecutively in one line until it reaches 128 bits. Once the EEG raw data reaches 128 bits, it starts a new row underneath the previous one. Figure 3-3 shows the format of raw EEG data downloaded from the BIS monitor. The format uses a Little Endian

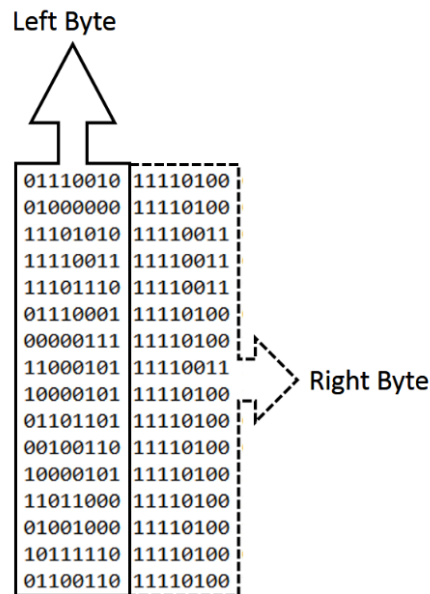


Figure 3-4. The diagram of 16 bit data stored in 2 bytes locations left byte and right byte.

3.3 EEG signal acquisition

The BIS index snapshots were taken from the monitor to verify the EEG raw data conversion. The EEG snapshots are taken as pdf file. The verification was done by comparing the converted EEG data with the EEG snapshot from the BIS monitor. The visual observation has been done by lining up the two data sets side by side. Figure 3-5 shows the EEG signal snapshot from the BIS index monitor. In order to verify the converted data, the example of the EEG signal snapshot in Figure 3-5 is compared with the converted EEG data in Figure 3-6. By lining-up the time between two figures, we can see that the two data sets have the same pattern. The data, provided in this example, shows that the conversion method from raw EEG data gives the same value as the BIS index monitor.

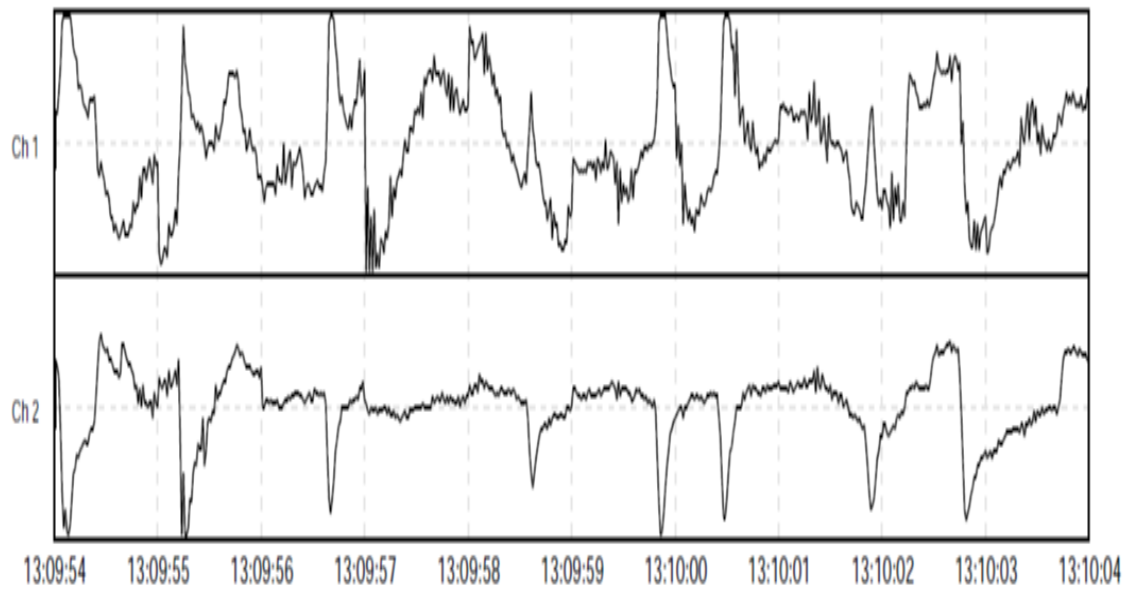


Figure 3-5. EEG signal snapshot from the BIS monitor.

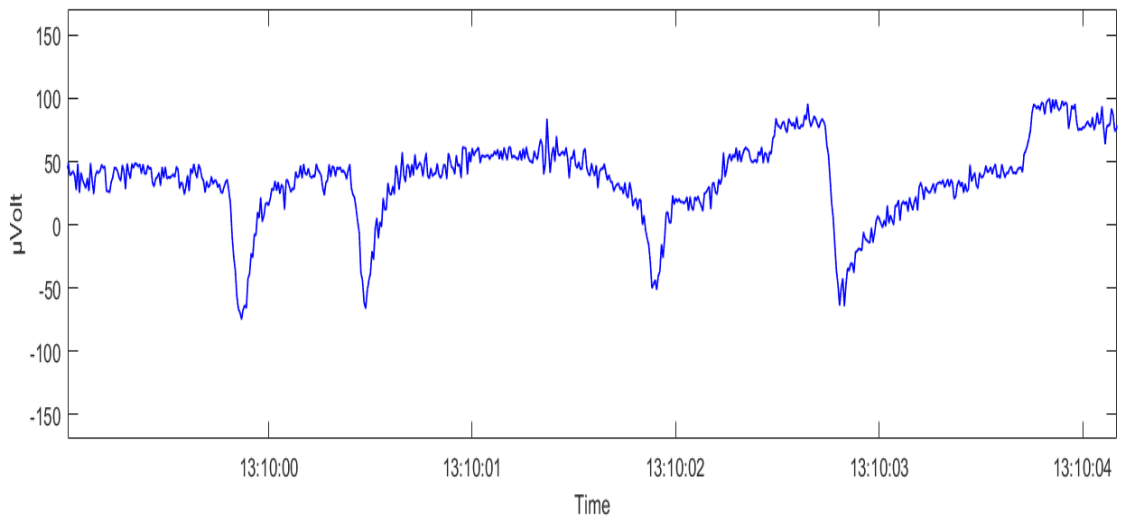


Figure 3-6. Converted EEG signal from the obtained data.

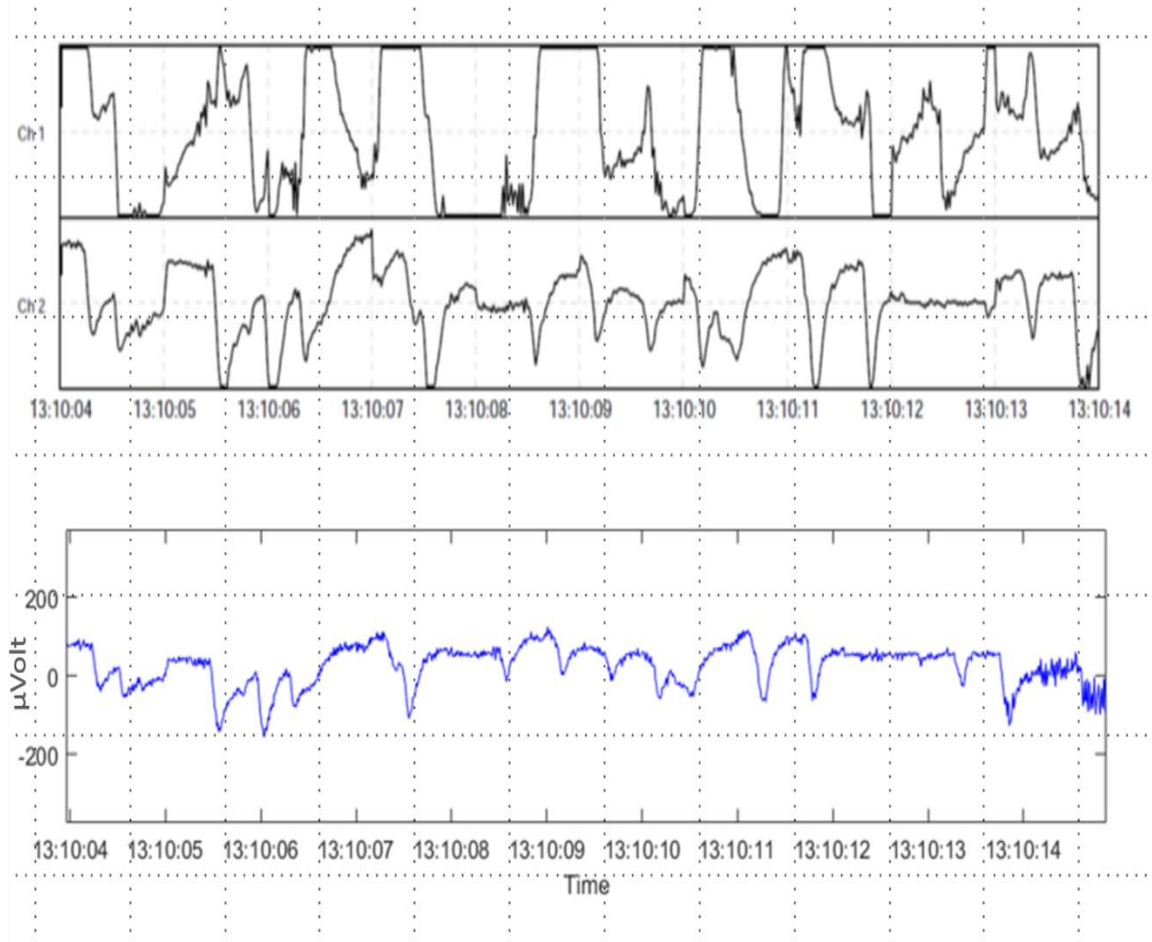


Figure 3-7. Verification of the converted EEG raw signal.

Figure 3-7 displays the verification of the converted EEG raw data and the snapshot from the BIS index.

Figure 3-7b in blue line is the converted EEG raw data, it is indicated that the converted signal had a similar pattern with the channel 2 in the snapshot. Figure 3-8 shows the EEG signal after conversion. The signal contains many spikes which are considered as noises in the signals. It is difficult to analyse these noisy signals because information in the signal is corrupted and interpreting the data becomes extremely challenging.

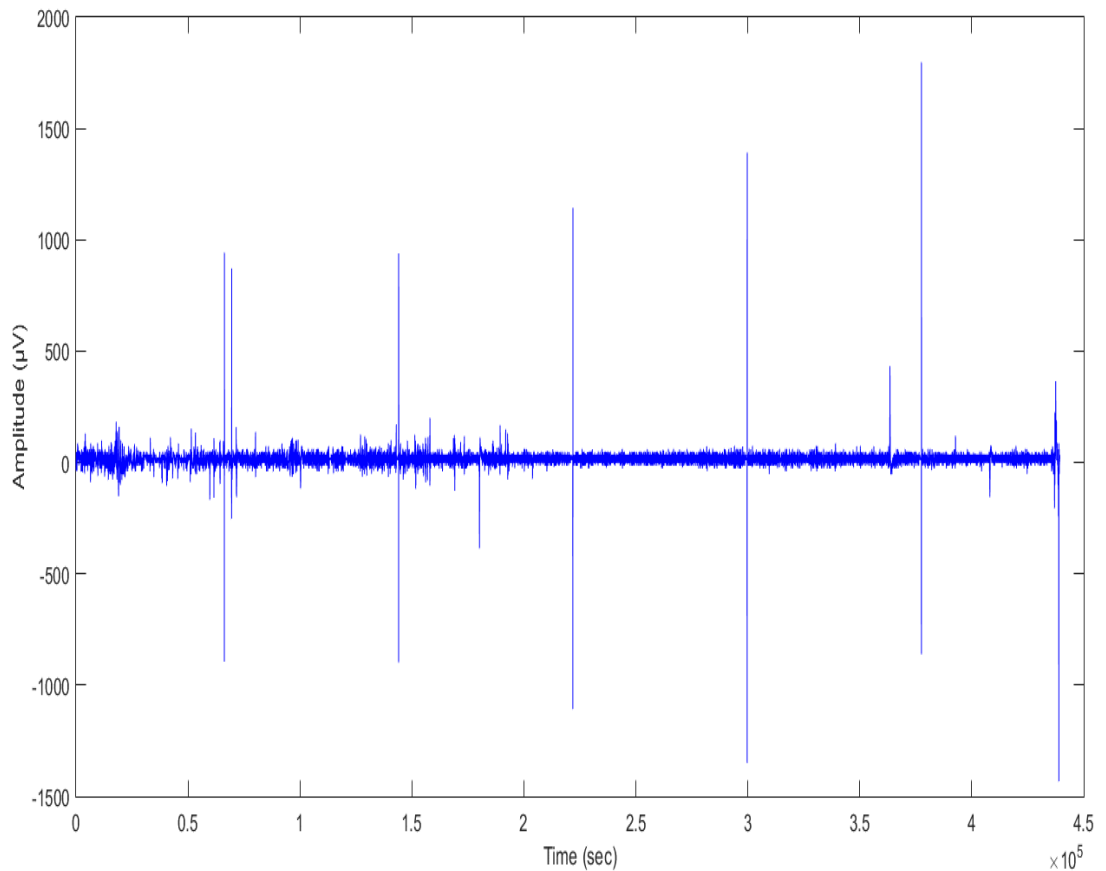


Figure 3-8. The EEG signal.

In some cases, the BIS index does not give a valid DoA value. This is one of the drawbacks for BIS. Nguyen-Ky, Wen and Li (2013) pointed out that the BIS index did not response to anaesthetic drugs and could not provide the DoA value. The same cases also rise in this research where the BIS index does not give any value for a period of time. Figure 3-9(b) shows the case where the BIS index does not give an index for a period of time. In the operating theatre, if the monitor did not give any indication of the patient's condition during the operation, the anaesthetist has to physically check patient condition and response promptly. Figure 3-9(c) shows the EMG signal recorded in company with the EEG signals.

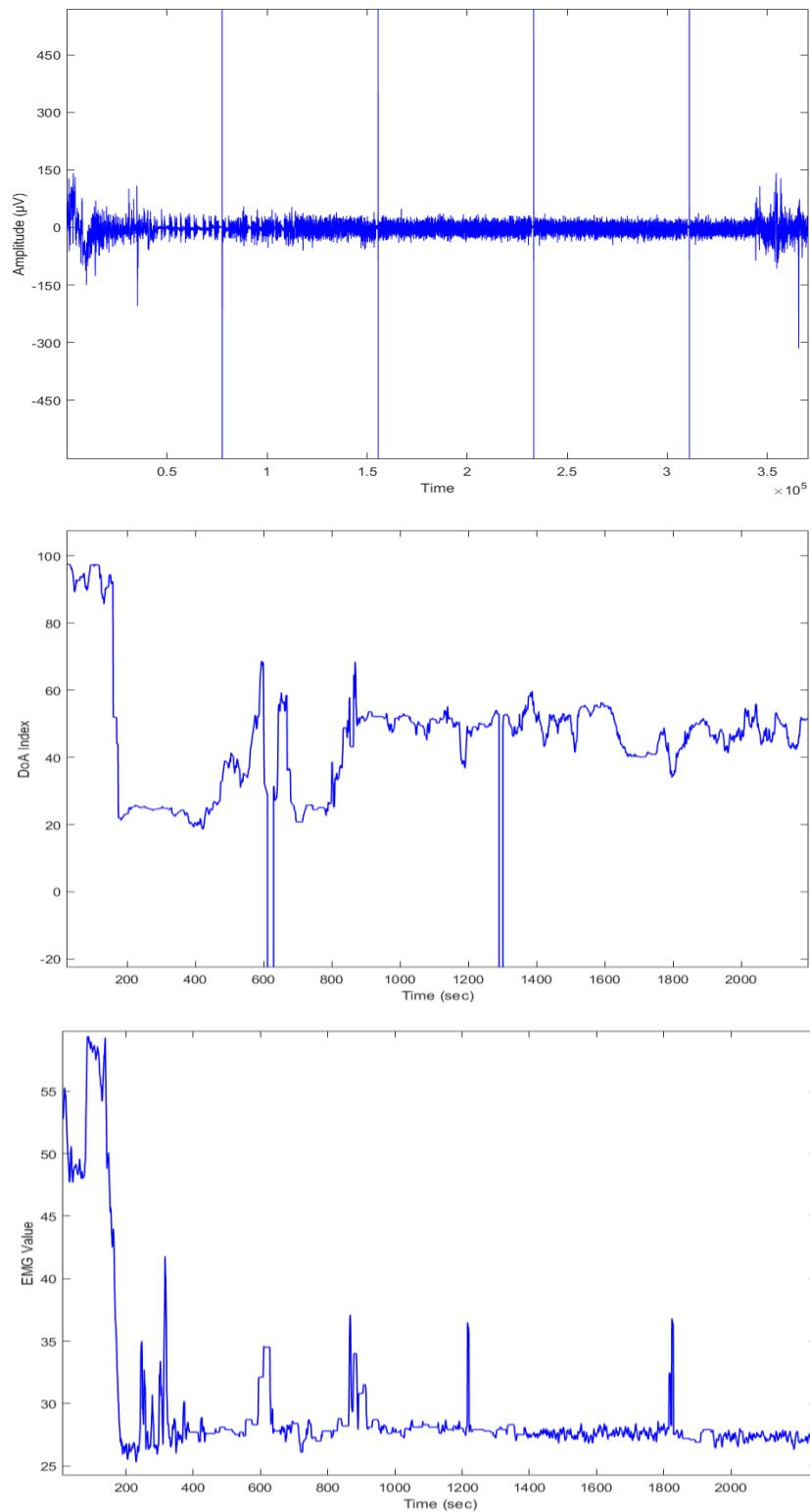


Figure 3-9. Data from patient number 21 where the BIS index could not provide the index (a) The EEG signal; (b) BIS index; (c) EMG value.

The BIS index value can rise when EMG noise is present. There were a number of patients for whom the BIS index level increased as the EMG signal rose. Figure 3-10 shows that the BIS index value increases when the EMG signal rises. The BIS index value is affected by the high frequency of the EMG signal. Data from patient number 12 shows that the BIS index does not give any index for a period of time. Figure 3-11 also shows that the BIS index does not give any index for a period of several seconds in multiple time. Data from patient number 12 was recorded for an operation of more than one hour (4416 seconds). The blue line in Figure 3-11 is the BIS index and the red line is the EMG signal.

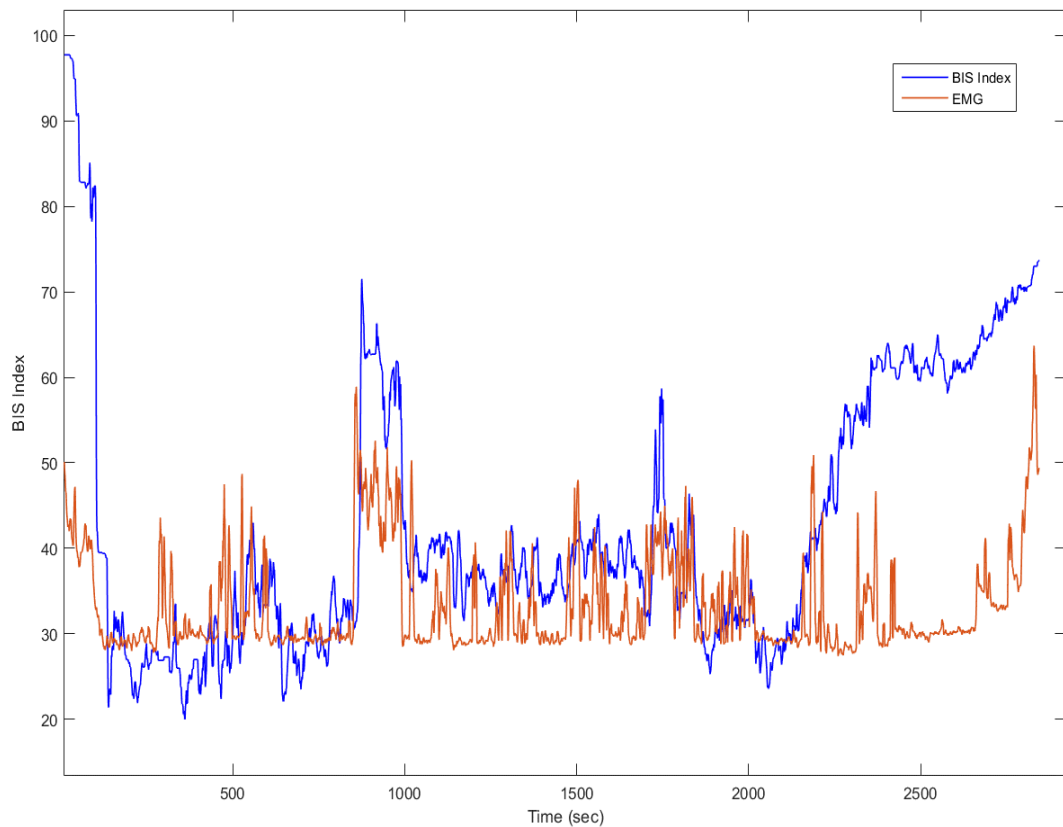


Figure 3-10. Patient number 3 shows the BIS index increase as the EMG value increases.

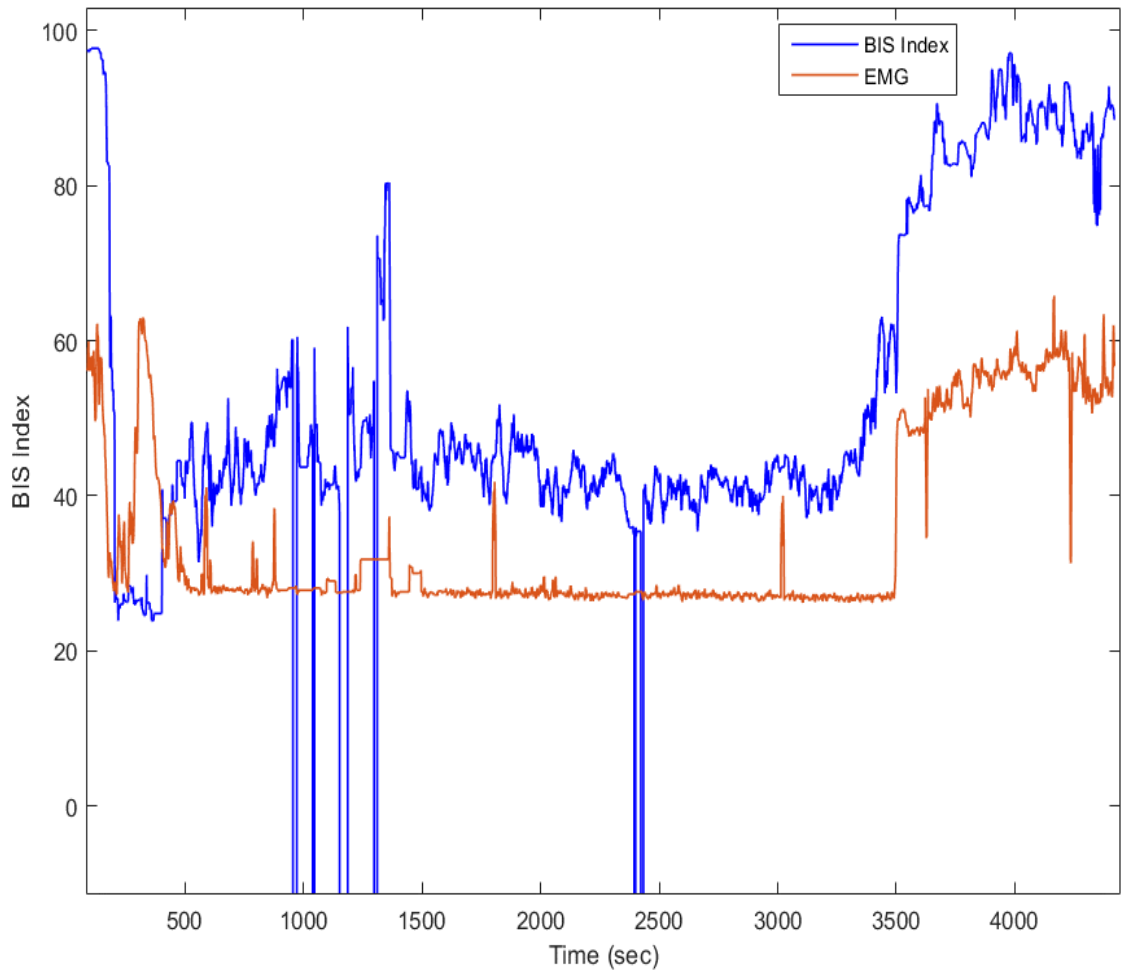


Figure 3-11. BIS index from patient number 12 showing that the BIS index was affected by noise.

During the data acquisition, there were a number of noises recorded together with the EEG signal. Figure 3-12 shows the EEG signal from patient number 12. The BIS index value from patient 12 shows indication that the noises has interfered the BIS index during the operation. It also shows many high amplitude spikes in the signal. It indicates that the BIS index filtering is unable to compensate the high amplitudes spikes from the EEG signal.

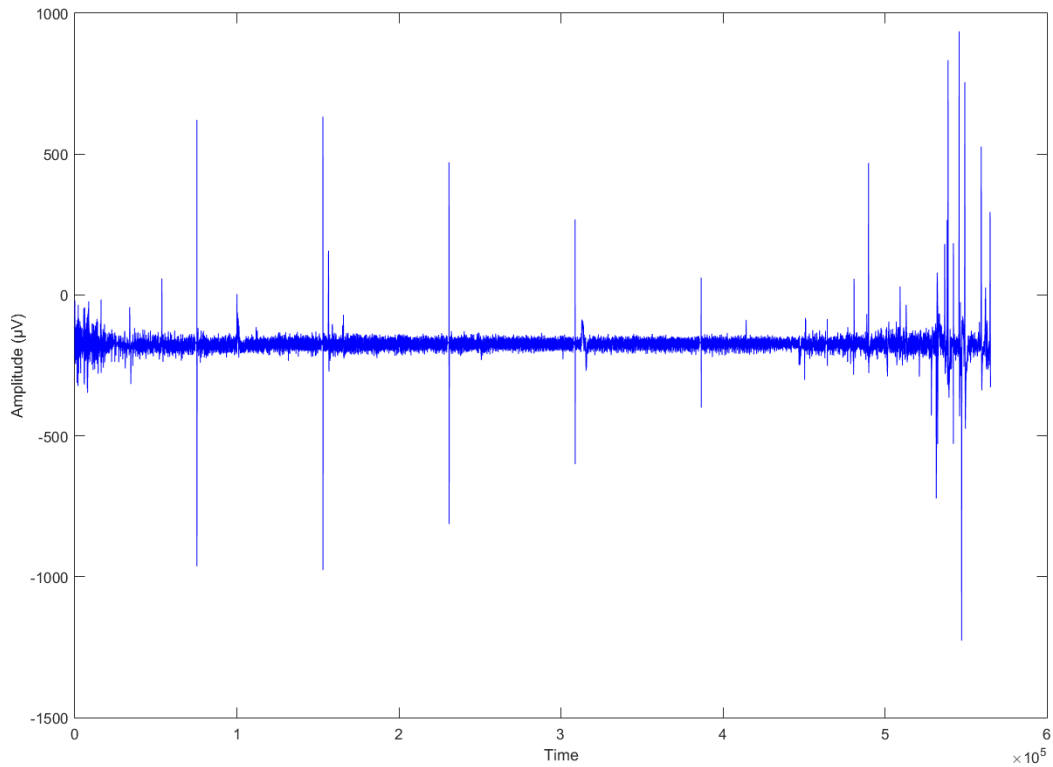


Figure 3-12. EEG signal is corrupted with noises. There are many high amplitude spikes in the signal.

Frequency content of the signal can be seen clearly by taking the 2D plot of the signal. The frequency content of the signal is computed using the short time Fourier transforms (STFT) of the EEG signals. The STFT $X(n, \omega)$ of the EEG data sequence $x[n]$ is defined:

$$X(n, \omega) = \sum_{m=-\infty}^{\infty} x[n]w[n-m]e^{-j\omega n} \quad 3-1$$

$$f_n[m] = x[n]w[n-m] \quad 3-2$$

where the sequence of $f_n[m]$ is known as a short time section of $x[n]$ at time n ; $\omega = \frac{2\pi}{N}$; and $w[m]$ is the window size. The EEG frequency spectrum $X(n, \omega)$ can be determined from the raw EEG signal $x[n]$. The STFT is computed by multiply the window $w[m]$ with $x[n]$ and take the FFT value of $(x[n]w[n - m])$.

The STFT analyses the signal by windowing the signal and then taking the FFT on every segment. The STFT result is a frequency spectrum on each $[m]$ that move along the windows segment (Sethares 2007). The window used in this spectrogram is a Hamming window. The resolution in digital frequency for Hamming windows is $\Delta\omega = 8\pi/N$; where N is the resolution in time given by window m . The spectrogram colour of each signal is the magnitude of the discrete STFT.

The spectrogram is the relative energy of the EEG signal frequency at different time. Figure 3-13 shows the frequency content of the signal which was recorded with the EEG signal from patient number 12. Figure 3-13 contains the EEG signal frequency estimated using Fourier transform, time localised frequency and the signal power (dB). It is showed that the low frequency noises and the high frequency noises overpower the EEG signal. Low frequency approximately less than 10 Hz is associated with EOG noise. On the other hand, high frequency approximately more than 80 Hz is associated with EMG signal. Power line frequency (50 Hz) is also recorded in the signal. The second figure has the same data but it presented in different angle in order to observe the frequency component of the signals. Therefore, it is important to do filtering before analysing the EEG signals.

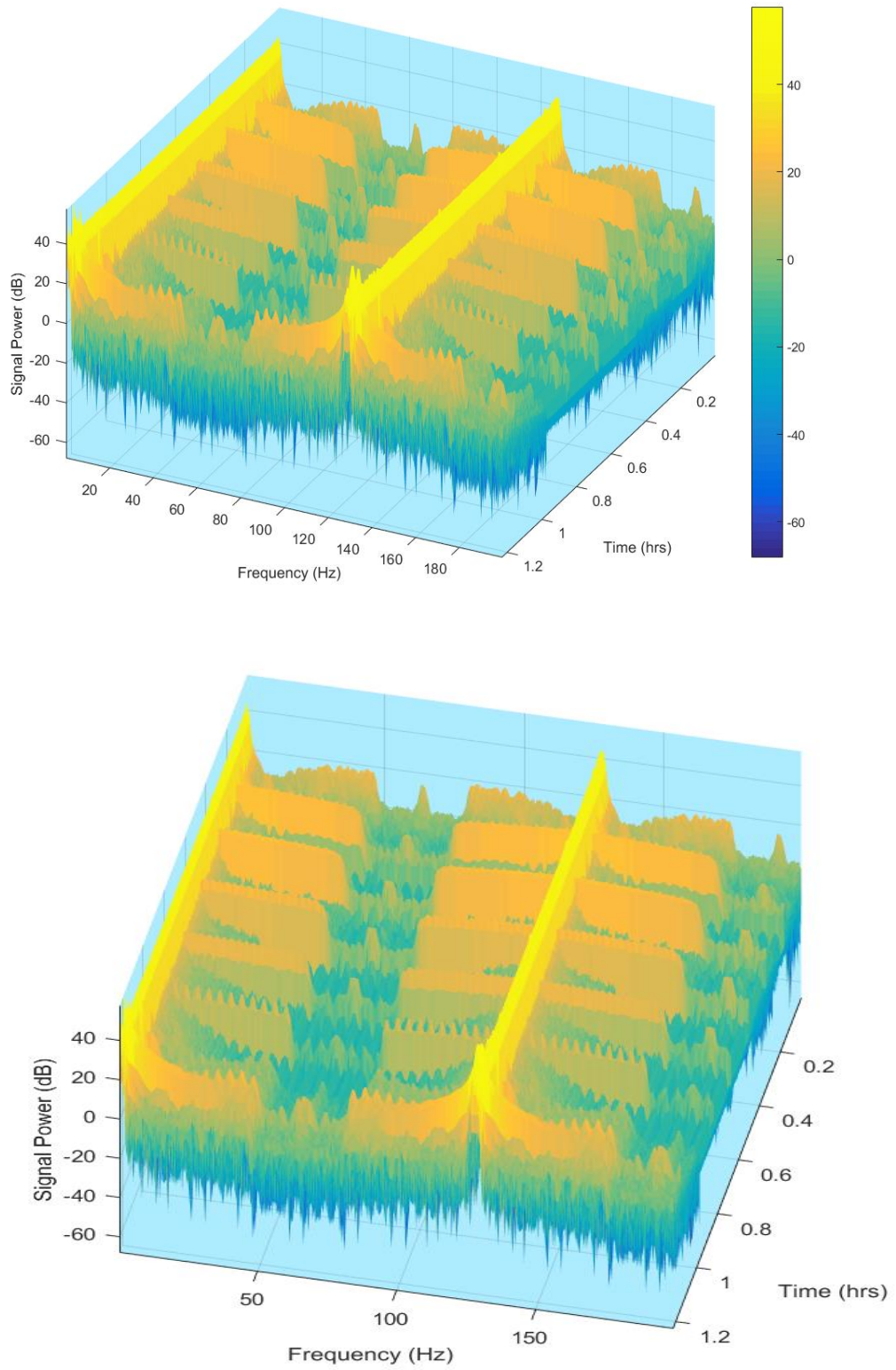


Figure 3-13. Frequency content in the EEG signal from patient number 12.

3.4 Summary

This chapter has discussed the equipment used for data acquisition, EEG signal acquisition, and conversion of raw EEG data from binary to decimal numbers. It demonstrates that the EEG signal data from the monitor is contaminated with noises such as EMG, EOG, ECG and power line frequency. This chapter also highlights some of the drawbacks of the BIS monitor. There are a number of recorded data from patients showing that the BIS index monitor was unable to output a valid BIS index value because of the interference from the noises. Therefore, it is important to remove the noise in the signal before further analysing.

4 STATIONARY WAVELET TRANSFORM AND BAYESIAN ADAPTIVE LMS FILTERING

Filtering the EEG signals prior to analysis is essential because the recorded EEG signal is contaminated with noises. Such noises can affect the analysis and may result in inaccurate DoA assessment. The EEG signal contains a lot of information from the central nervous system and, during data acquisition, various information from the head is recorded along with the EEG signals. Apart from the EEG, EMG, EOG, and ECG signals, power line frequency also can be captured within the EEG signal acquisition. The EEG signal is recorded through forehead. The signal in the forehead is the sum of all the information from the brain activity.

The first part of this chapter is discusses the Stationary wavelet transform (SWT). The filtering process introduced in this chapter is a novel technique using combination of the adaptive filter and the Bayesian based method. The result of Bayesian adaptive filter is compared with the filtering process using Stationary Wavelet Transform.

4.1 Stationary wavelet transform

The stationary wavelet transform is an improved method from discrete wavelet transform (DWT). In the DWT method, the down sampling method is applied to decomposing a signal. The down sampling method in DWT reduces half of the length of signal coefficients after decomposition. It could also eliminate the time invariant property in the signal (Morsi & El-Hawary 2008). The time invariant property is very important in signal processing because it helps to identify and detect the changes in, or transient characteristics of, a signal. Unlike the DWT, the SWT uses the up sampling method to decompose a signal. The SWT method is a robust method compare with the DWT because the decomposition method in SWT retains the time invariance property of the signal (Juan et al. 2014; Li et al. 2003; Park, Eckley & Ombao 2014; Suyi & Jun 2009; Taruttis et al. 2014). In the SWT method, the original signal is convolved with an up sample low pass filter or high pass filter at each level of decomposition (Suyi & Jun 2009). Figure 4-1 shows the SWT decomposition and filter computations at level j . The approximation cA_j is obtained by convolving the original signal with an up sample low pass filter (g_j). On the other hand, the detail cD_j is derived by convolving the original signal with an up sample high pass filter (h_j) (Misiti et al. 2009).

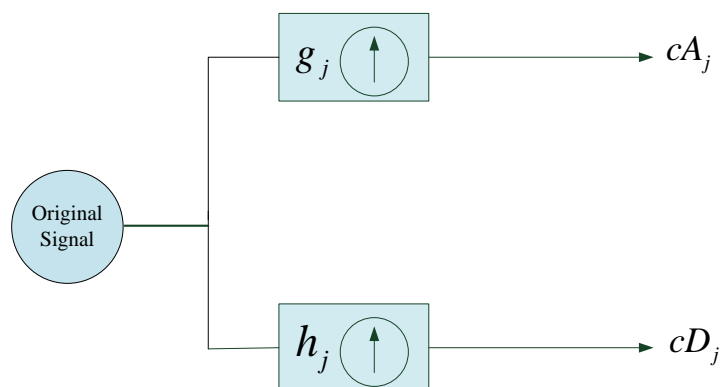


Figure 4-1. SWT decomposition and filter at the level j with a low pass filter (g_j) and a high pass filter (h_j)

Figure 4-1 shows the SWT decomposition in one level. The decomposition signal in more than one level is based on the approximation on level 1. Figure 4-2 shows the SWT decomposition in three levels.

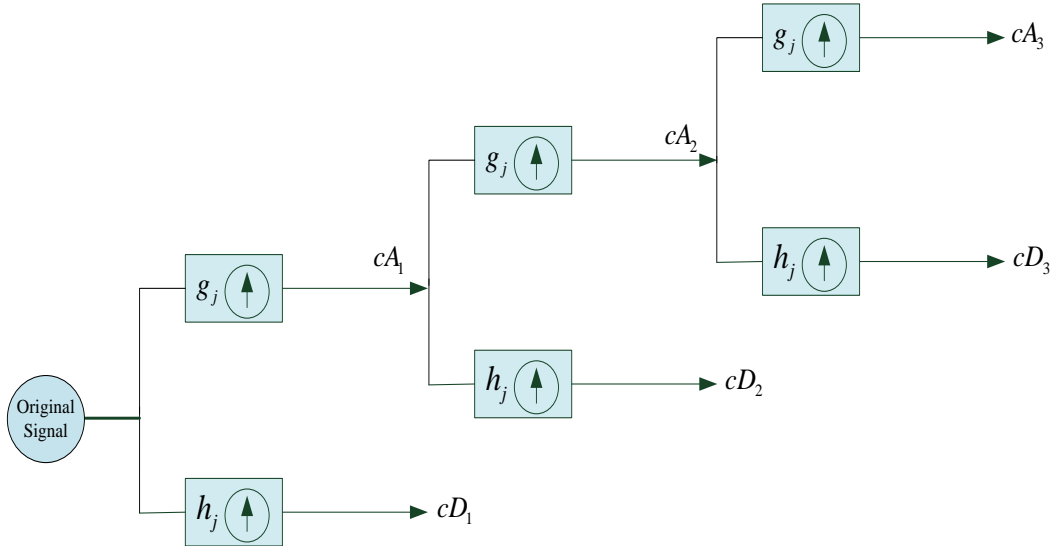


Figure 4-2. SWT decomposition in three levels

Both the approximation and the details after decomposition have the same length as the original signal. Figure 4-3 shows EEG signals before decomposition, the approximation and detail after decomposition. Note that the original signal length and the decomposition signal length are the same, demonstrating one advantage of SWT. The decomposition of SWT is computed as follows (Morsi & El-Hawary 2008; Nason & Silverman 1995):

$$cA_{j,k}^{SWT} = \sum_n cA_{j-1,k+2^j n}^{SWT} g_{j,k}(n) \quad 4-1$$

$$cD_{j,k}^{SWT} = \sum_n cD_{j-1,k+2^j n}^{SWT} h_{j,k}(n) \quad 4-2$$

where $cA_{j,k}^{SWT}$ is the approximation coefficient, $cD_{j,k}^{SWT}$ is the detail coefficient of the signals. The notation j and k are the indices of the decomposition level and position. The parameters $g_{j,k}(n)$ in Equation 4-1 and $h_{j,k}(n)$ in Equation 4-2 provide the characteristics of the low pass filter and high pass filter respectively for approximation and details decomposition.

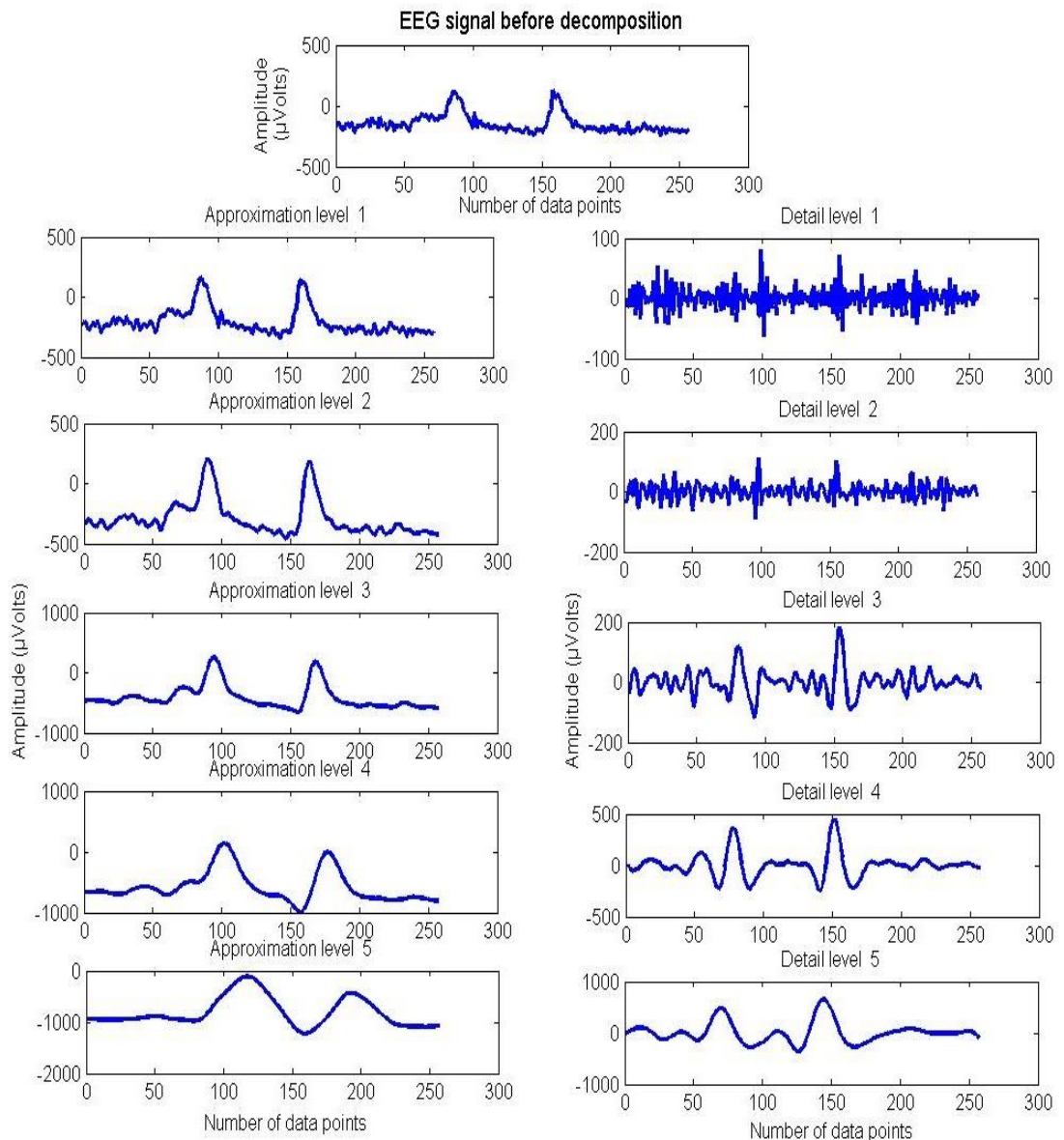


Figure 4-3. EEG signals before decomposition, the approximation and detail after decomposition.

4.2 EEG signal denoising using SWT method

There are three steps in EEG signal denoising using SWT. First, the signal is decomposed into five levels. Second, a threshold is applied in order to select the coefficients to remove the unwanted signal. Third, the decomposed signal is reconstructed by using the inverse SWT method.

The first step for the EEG signal denoising is decomposing the signal. The decomposed signal is in two parts: the approximation and the details. In the approximation and the details, the original signals are broken down into different frequency resolution components. Figure 4-4 shows the SWT detail and its frequency component associated with the details signals. Figure 4-5 shows the approximation and the frequency component of the approximation.

By looking at the frequency component on the details and approximation, we can easily choose the signal that corresponds with the EEG signal band. The unwanted signal can be eliminated before reconstruction of the decomposed signals. The SWT decomposition technique is also used to find the EEG frequency band. The extraction EEG signal into different frequency bands can be achieved by taking the decomposed signal from the SWT. The decomposed signal needs to be specified with the EEG band such as beta, alpha, theta and delta.

The second step applies a soft threshold to remove the EOG noise. The EOG is a low frequency signal that appears in the EEG signal. The third step is to reconstruct the signal after decomposition. The reconstructed signal is a clean EEG signal. The signal with noise is described as:

$$Y(t) = f(t) + \varepsilon(t), \quad t = 1, \dots, n - 1$$

4-3

where $f(t)$ is the signal, $\varepsilon(t)$ is the noise, and $Y(t)$ is the sum of the signal and the noise. The denoising method used in this study applies a soft threshold.

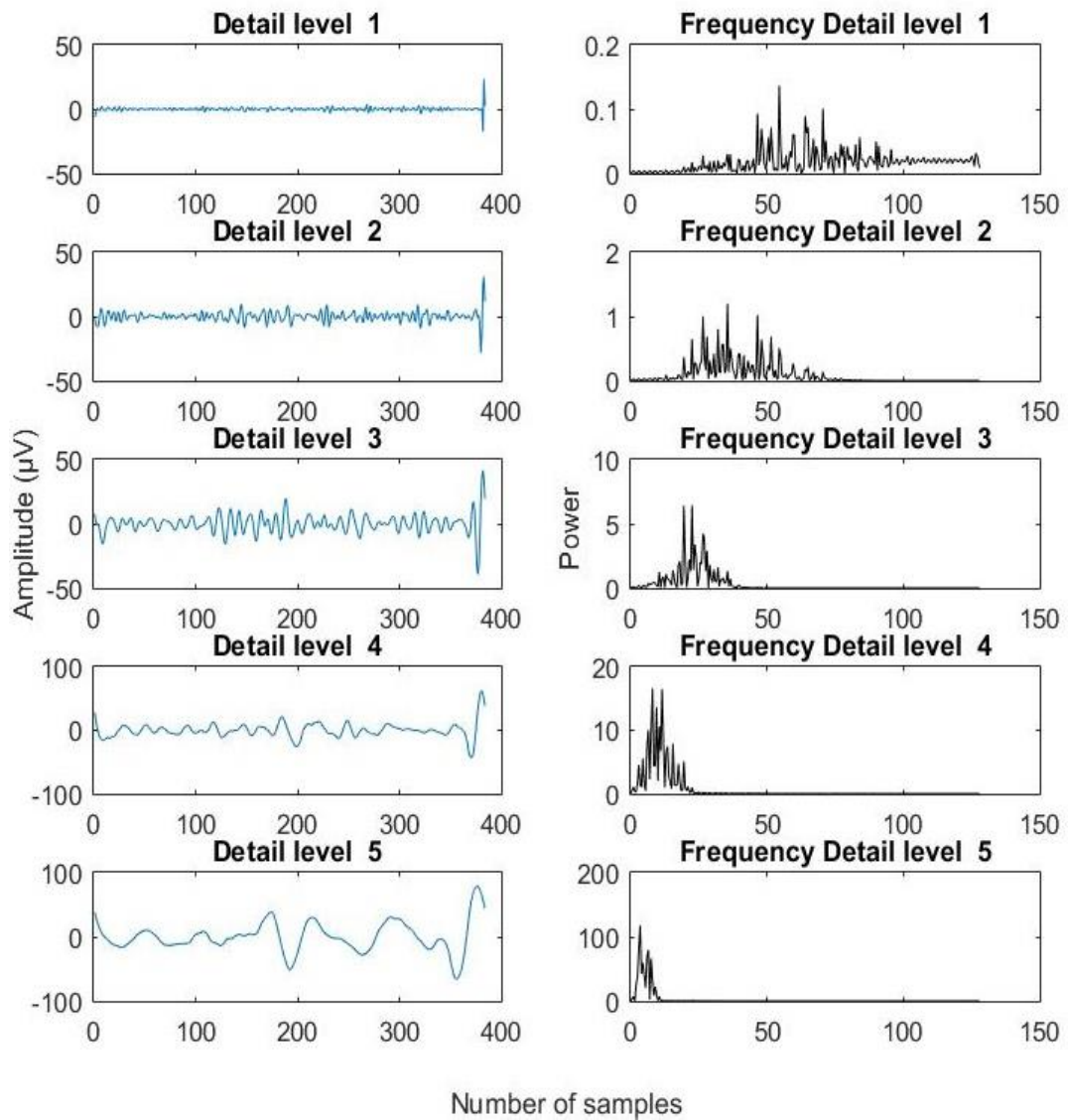


Figure 4-4. Details of the SWT and the frequency component on associate with the detail.

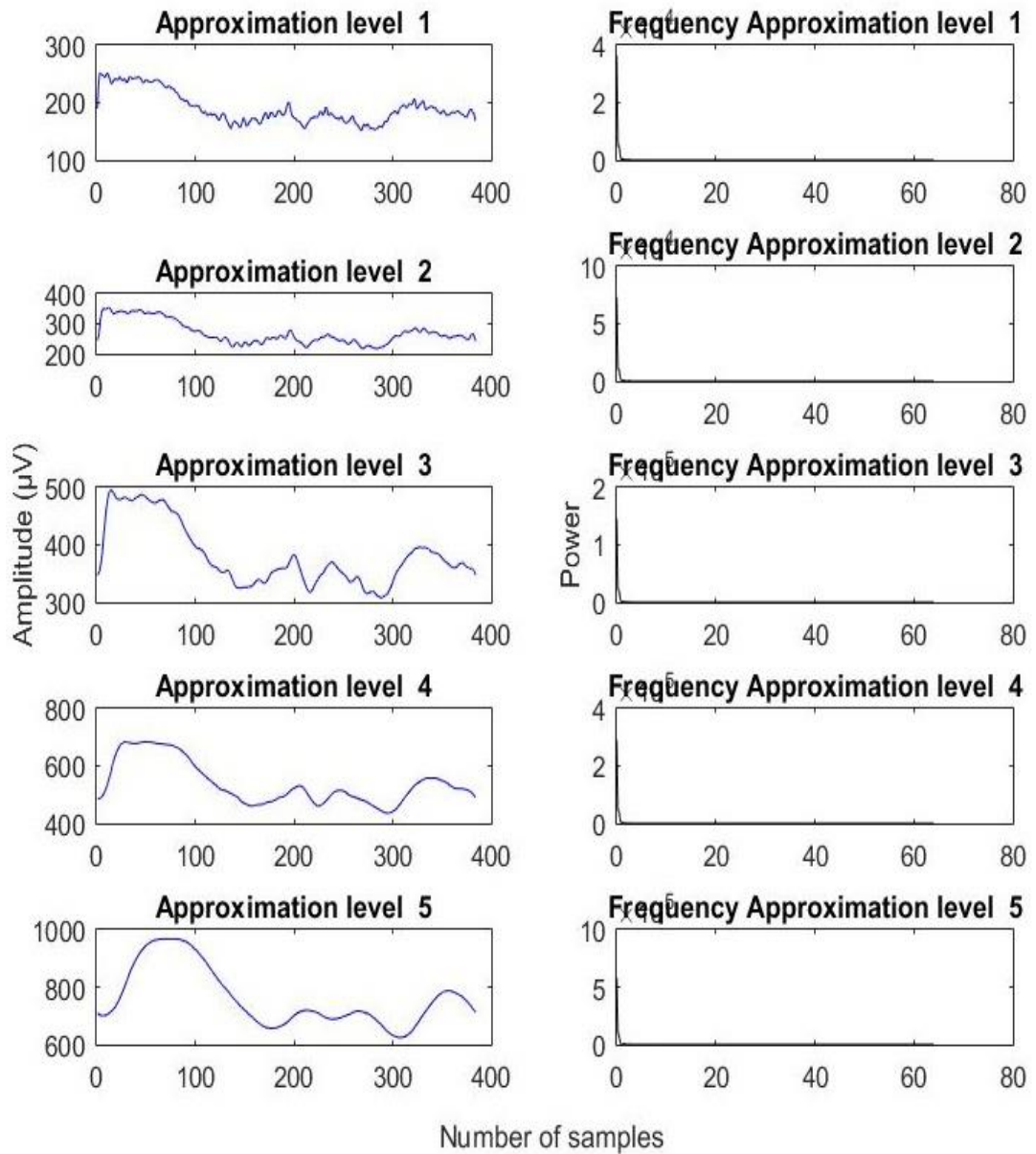


Figure 4-5. SWT approximation and the frequency component related to the approximation level.

The soft threshold function is given by (Donoho 1995):

$$T_s = \varepsilon_1 \sqrt{2 \log(n)} \quad 4-4$$

where T_s is the threshold and ε_1 is defined as $\varepsilon_1 = \gamma \cdot \sigma / \sqrt{n}$. If $\gamma = 0.67$ is selected as a constant, which is 75% of the standard normal distribution, then $\sigma = \text{MAD}/0.67$; MAD represents the median absolute value of the normalized fine scale wavelet coefficient.

The simplified threshold function from Equation 4-4 can be rewritten as:

$$T_s = \sigma \sqrt{2 \log(n) / n} \quad 4-5$$

The SWT denoising technique is able to eliminate signals ≥ 100 Hz and reduces the amplitude of the noise signal. The SWT denoising method is able to retain the EEG signal's component after filtering.

4.3 EEG filtering using adaptive Student-t distribution

During data acquisition period, there are a number of signals that might be recorded along with the EEG signal. The most common signals are electromyography, eye ball movement and eye blinking or electrooculogram signals. These signals overlap with EEG signals in frequency and power. Figure 4-6 shows the noises recorded besides the EEG signal. The noises overlap with the EEG signal. As shown in Figure 4-6, usually EMG noise contaminates EEG signal frequency range and EOG noises contaminate low frequency of EEG signals. The EOG signal frequency from

0 - 0.1 rad/sample overpowers the low frequency range of the EEG signal. The EMG signal noise from 0 - 0.6 rad/sample also overpowers the EEG signal. Therefore, it is necessary to filter and to separate these signals before the EEG signal analysis.

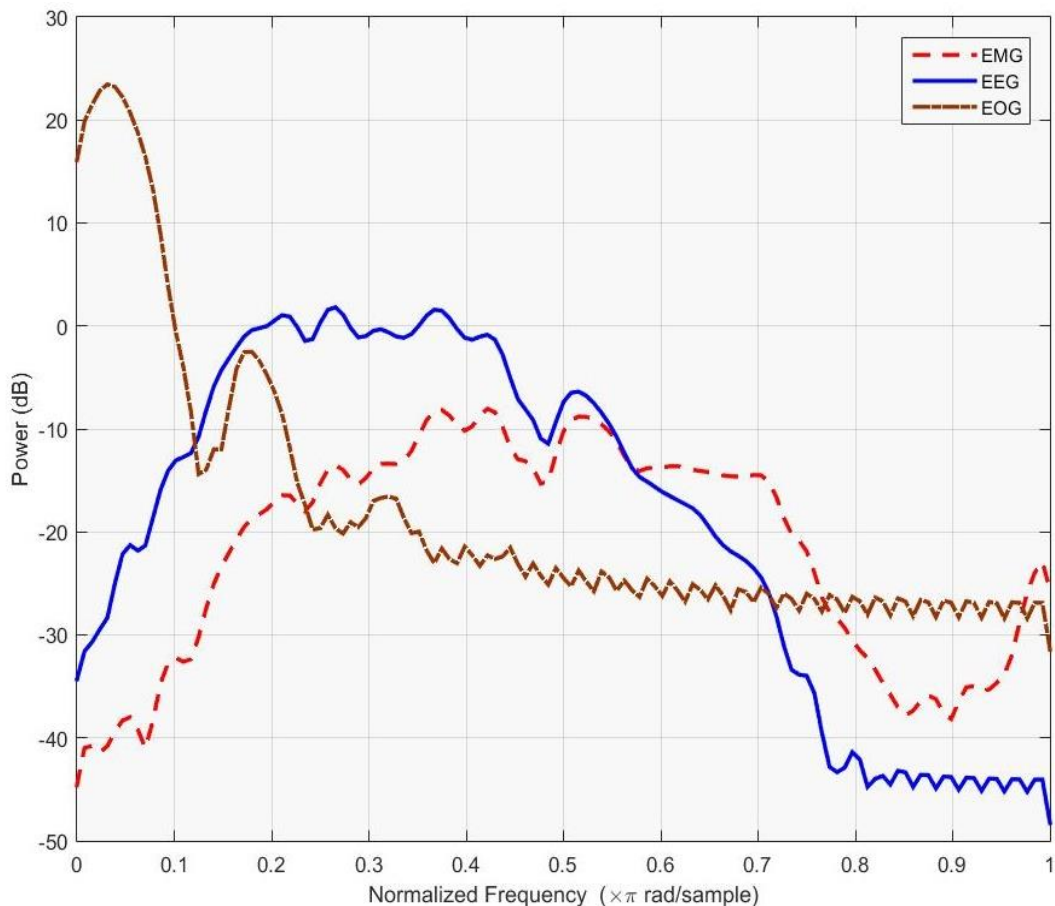


Figure 4-6. Overlapping noises in EEG signal.

There are number of filtering techniques that can be used to remove noises in the EEG signals. One of the popular filtering technique is the adaptive filter. The adaptive least mean square (LMS) filter is an automatic filtering process which automatically adjusts its filter weight coefficients to minimise the error and optimise the output signal (Ahirwal, Kumar & Singh 2014; Ram et al. 2012). The LMS algorithm is less complex in computation for filtering process (Foo 2006;

Jianbo et al. 2010; Kavitha, Lau & Premkumar 2007; Wang et al. 2009). The adaptive LMS filter technique is used in this research to carry out the filtering work in the EEG signal. The Bayesian student-t distribution is introduced for automatic adjustment of the filter weight step size. The combination of adaptive LMS filter and the Bayesian student-t is called the Bayesian adaptive LMS filter. A simple diagram of the Bayesian adaptive filter is shown in Figure 4-7(a) (adapted from Ram et al. 2012).

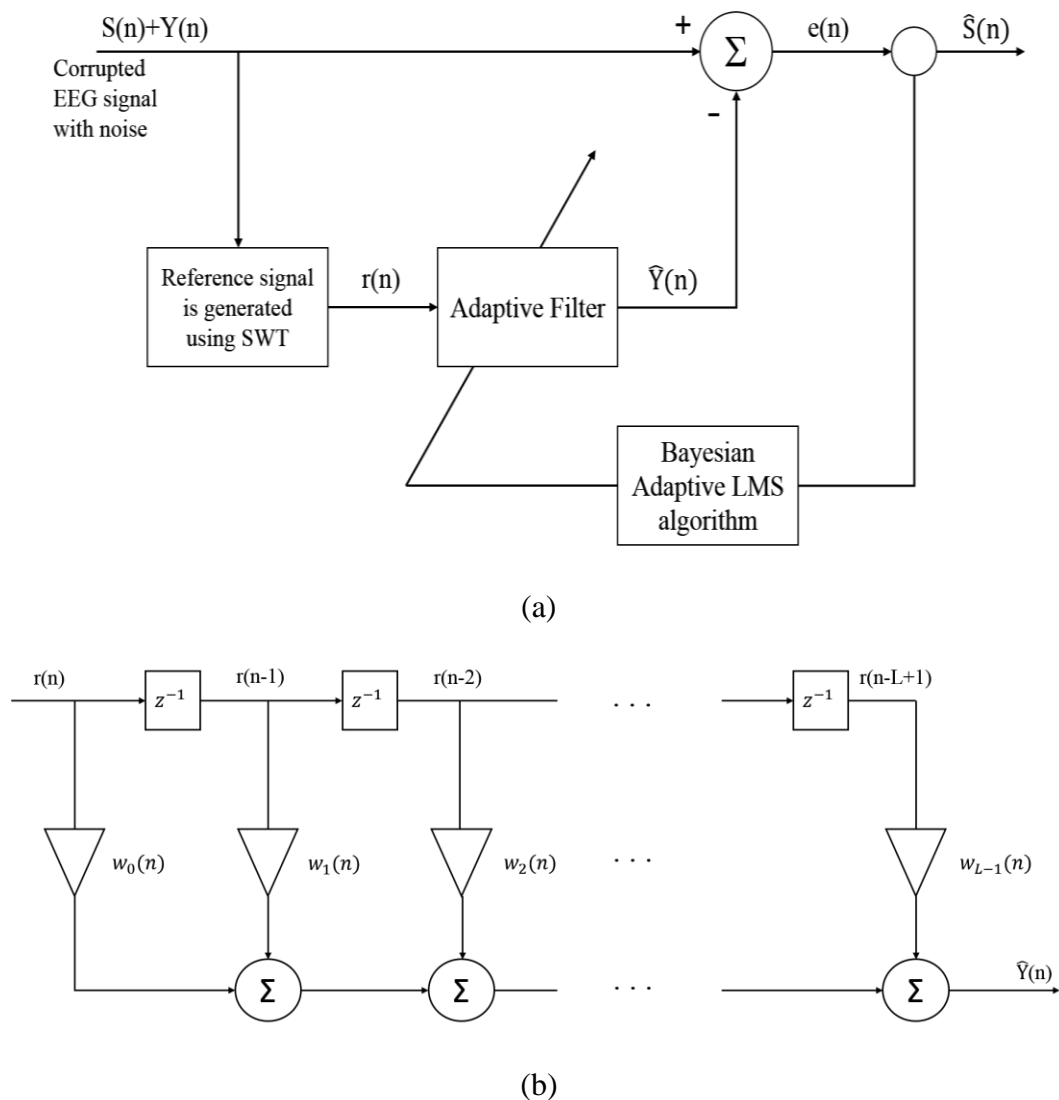


Figure 4-7. (a) Bayesian adaptive LMS filter diagram. (b) The FIR filter structure

Figure 4-7(a) shows that the contaminated EEG signal with noise $S(n) + Y(n)$ is fed into SWT. The SWT is employed to generate reference signal $r(n)$ for the adaptive LMS filter. The reference signal $r(n)$ is fed into the adaptive filter to compute the $\hat{Y}(n)$. The adaptive filter output is computed based on the FIR filter. The FIR filter structure is depicted in Figure 4-7 (b). The FIR filter is also known as a tapped-delay line filter, where z^{-1} is the unit delay and the $w_i(n)$ is a gain within the system (Madisetti 2009). Filter weight coefficient $W(x)$ is computed along with the $r(n)$ to derive the output of the adaptive filter. The output of the adaptive LMS filter is given by:

$$\hat{Y}(n) = \sum_{i=0}^L w_i(n)r(n-i) \quad 4-6$$

$$\hat{Y}(n) = W^T(x).r(n) \quad 4-7$$

$$w_i(n+1) = w_i(n) + m_n \cdot e(n).r(n) \quad 4-8$$

$$e(n) = (S(n) - Y(n)) - W^T(x).r(n) \quad 4-9$$

where L is the filter order, $i=0, 1, 2, 3, \dots, L$; m_n is the filter weight step size. Then, $\hat{Y}(n)$ is subtracted from $S(n) + Y(n)$, which is the contaminated EEG signal. The estimation of the recovered EEG signal can be defined in the equation below:

$$\hat{S}(n) = (S(n) + Y(n)) - \hat{Y}(n) \quad 4-10$$

The updated filter weight coefficient $w_i(n+1)$ is computed iteratively to minimise the error in the signal. Fast convergence in filter adaptation could be reached by

choosing the right value for filter weight step size (m_n). The m_n plays an important role in the adaptation process and for obtaining the best performance of the adaptive filter (Madisetti 2009). This research introduced a novel technique for automatic m_n adaptation which is calculated by taking the distribution of the contaminated EEG signal ($S(n)+Y(n)$) and then using the probability density function to compute its density function. The student-t distribution of the contaminated EEG data with ν degree of freedom can be define as:

$$P(x|\nu) = S(x|\mu, \lambda, \nu) \quad 4-11$$

$$\mu = \frac{1}{n} \sum_{i=1}^n x_i \quad 4-12$$

The parameter λ is called the student-t precision with the mean μ . The probability densities function of student-t distribution is as follows:

$$P(x|\nu) = \frac{\Gamma\left(\frac{\nu+1}{2}\right)}{\Gamma\left(\frac{\nu}{2}\right)} \left(\frac{1}{\pi\nu}\right)^{\frac{1}{2}} \frac{1}{\left(1 + \frac{x^2}{\nu}\right)^{\frac{\nu+1}{2}}} \quad 4-13$$

$$Psm = \max[P(x)] \quad 4-14$$

where ν is the degree of freedom. The $\Gamma(\cdot)$ is the Gamma function, and P is the probability density function of the student-t distribution with data x and the ν degrees of freedom. Student-t distribution is defined as a mixture of Gaussian distribution and Gamma prior with a shared precision and means (Bishop 2006; Christmas 2013; Christmas 2014; Christmas & Everson 2011). The Psm is defined as the maximum value of the density function of the Student-t distribution.

The LMS filter weight step size parameter is derived from the Student-t distribution by taking the density function of an epoch of EEG data. The density function in Equation 4-12 is then used as a filter weight step size, this can be defined as:

$$m_n = \max(P(x|v)) \quad 4-15$$

Therefore, filter weight adaptation in Equation 4-8 can be rewritten as:

$$W(x+1) = W_i(n) + \max(P(x|v)) \cdot e(n) \cdot r(n) \quad 4-16$$

4.4 Experimental results and analysis

The above filtering techniques are applied to the recorded EEG signal to remove the unwanted noise. These signals are processed at every epoch with a window size of 256 samples using the sliding windows technique. The signal was shifted every second with an overlap of 50%. Figure 4-8 shows the recorded EEG signals before filtering.

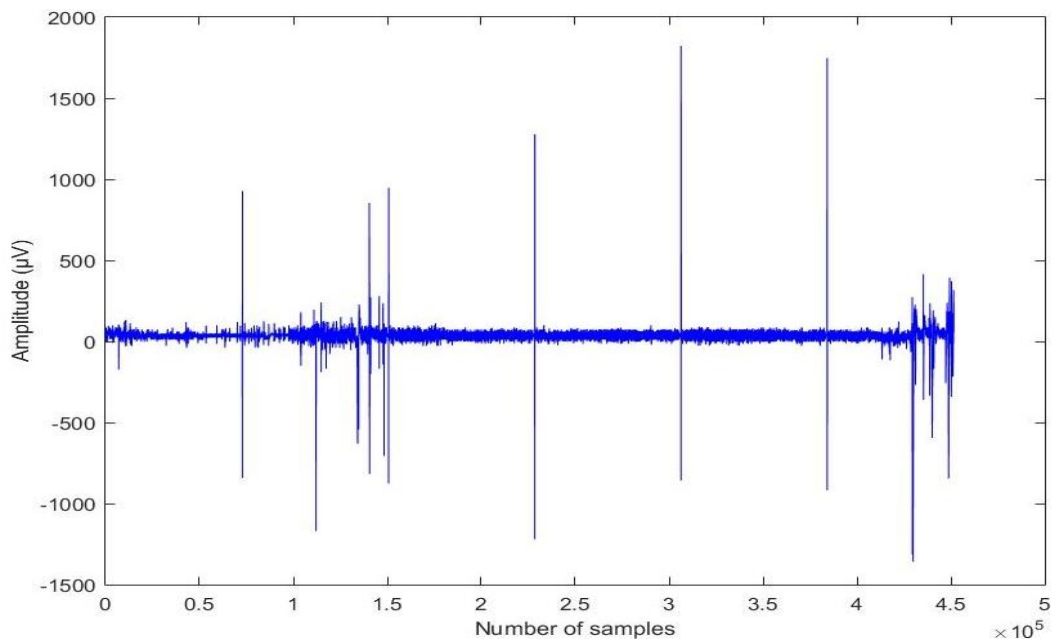


Figure 4-8. EEG raw signal was recorded for over one hour.

4.4.1 Result of the SWT filtering technique

The filtering results using the SWT technique is shown in Figure 4-9 and 4-10. The results show that the filtering process is able to restore the amplitude of the EEG signal. Furthermore, Figure 4-10 shows the EEG signal spectrum before and after the filtering process. The EEG signals spectrum in Figure 4-10 tells us that the high frequency and low frequency noise have corrupted the EEG signal. The EEG spectrum after filtering process shows that the filtering process is able to remove these noise.

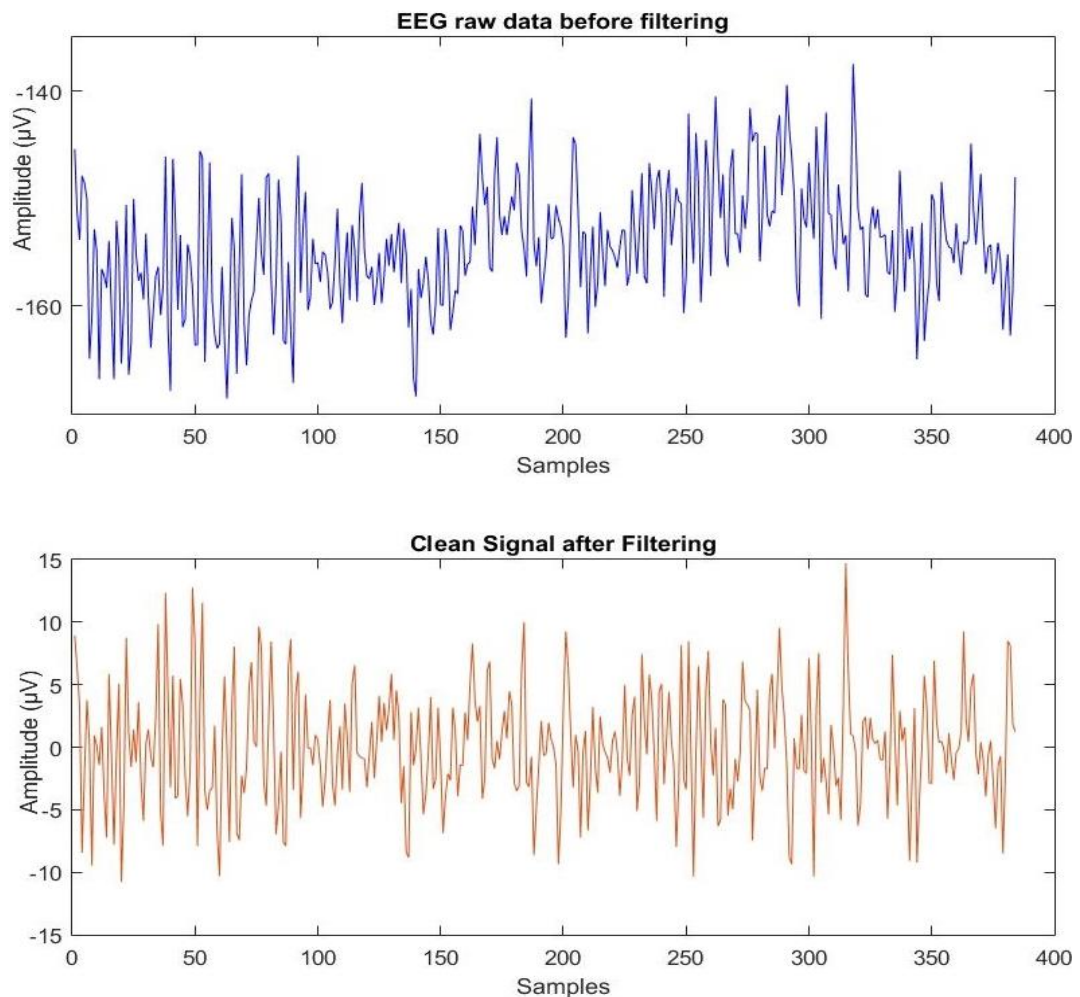


Figure 4-9. The result of signal filtering using SWT.

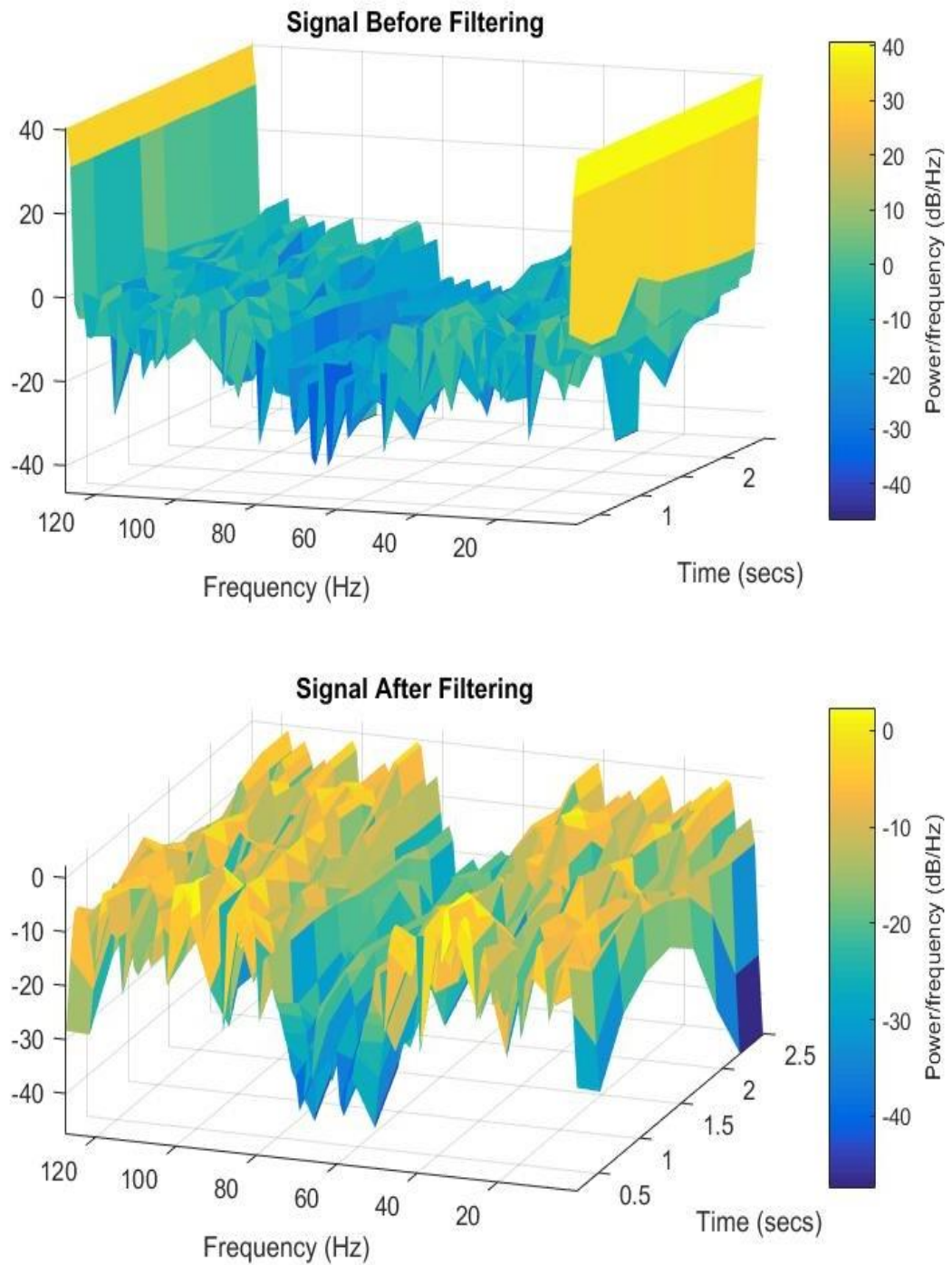


Figure 4-10 EEG signal spectrum before and after filtering process.

The relationship between the signal before and after filtering is presented in the cross correlation and the coherence figures in Figure 4-11. The cross correlation figures indicate that the two signals are closely correlated. The highest peak of the cross correlation in Figure 4-11 is zero. Further investigation using the coherence estimation and cross spectrum is revealed the correlation between both signals. Coherence estimation and cross spectrum phase indicated which frequency are both signals correlated. Figure 4-12 shows the spectral coherence and cross spectrum between the signal before and after filtering. The figure confirms that the frequency listed in the coherence figures are correlated between the signals before and after filtering process.

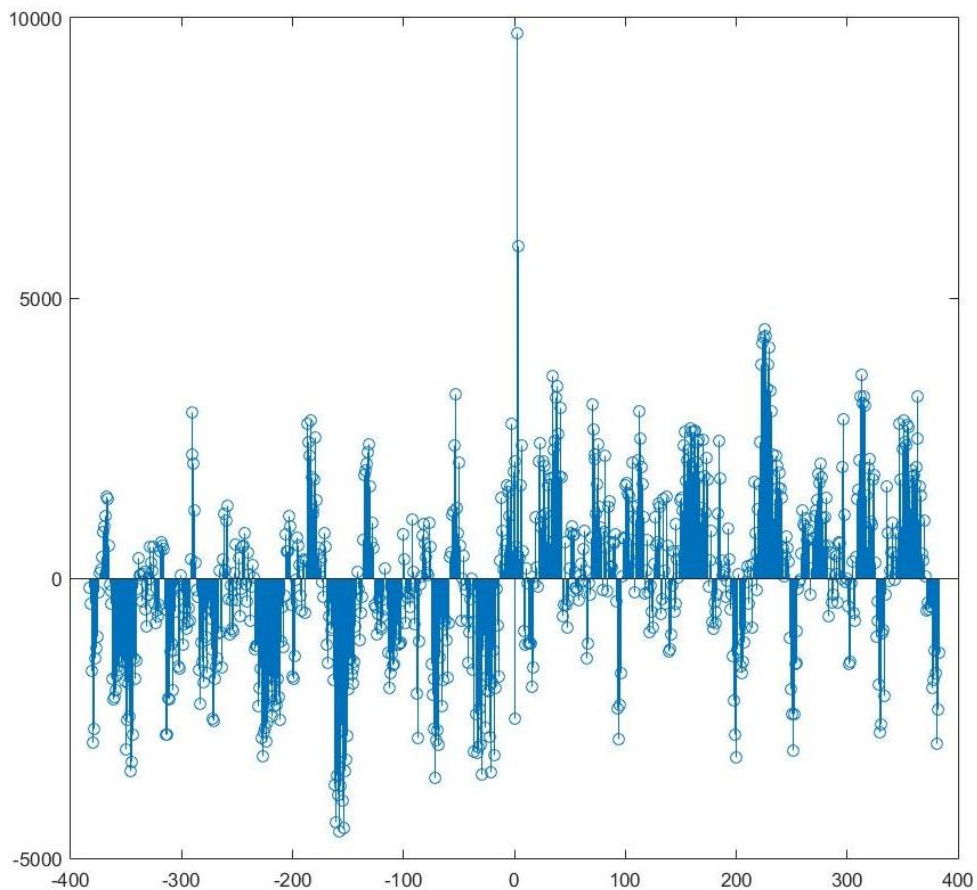


Figure 4-11. Cross correlation between the signal before and after filtering.

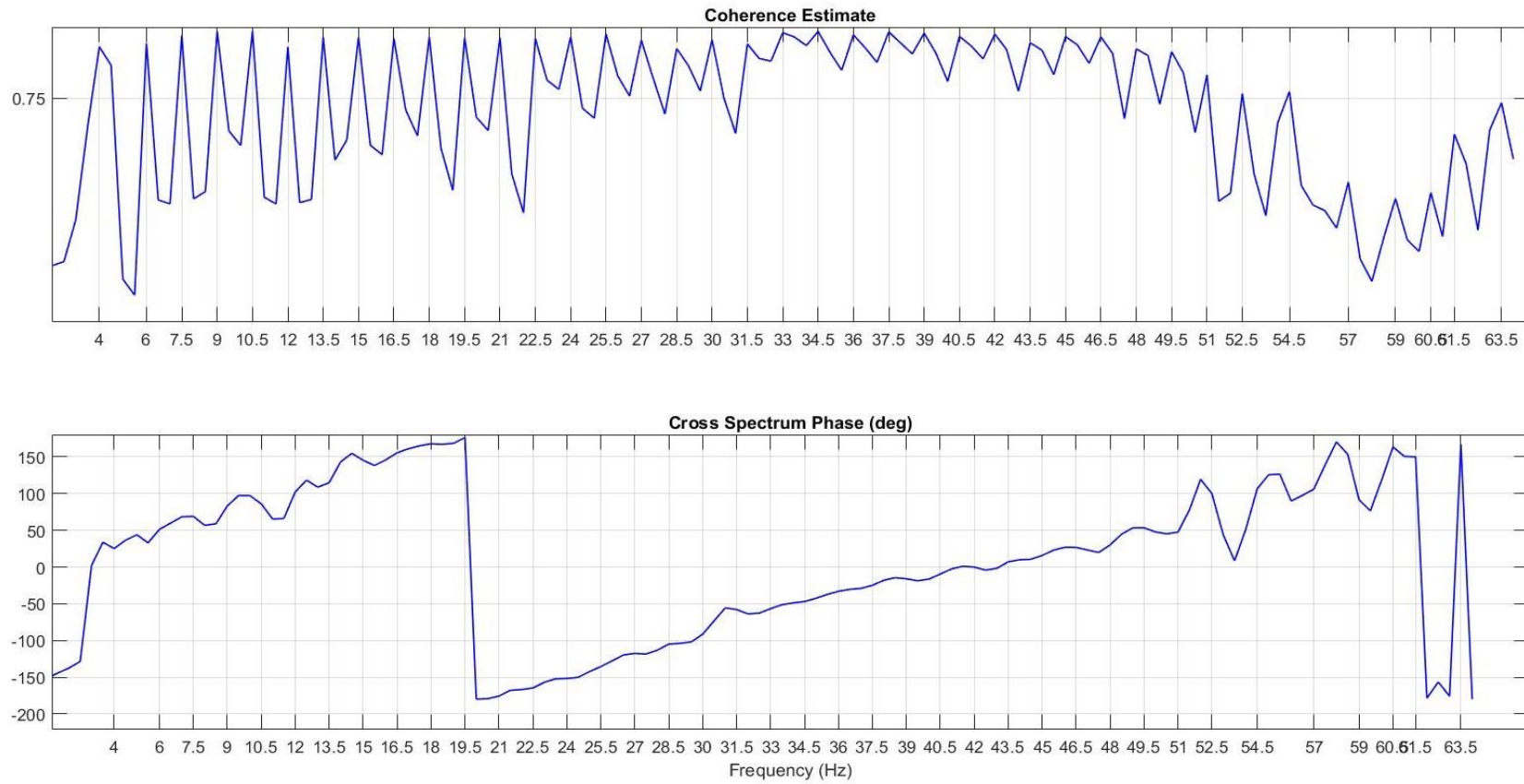


Figure 4-12. Coherence estimate and the cross spectrum phase.

4.4.2 Results of the Bayesian Adaptive LMS Filter

To compare the filtering technique between the SWT and the Bayesian adaptive filter, both filtering techniques use the same raw EEG signals in analysis. Figure 4-13 shows the EEG signal before and after filtering using the Bayesian adaptive LMS filter. It shows that the high frequency and low frequency noise in the signal has been removed using the Bayesian adaptive filter.

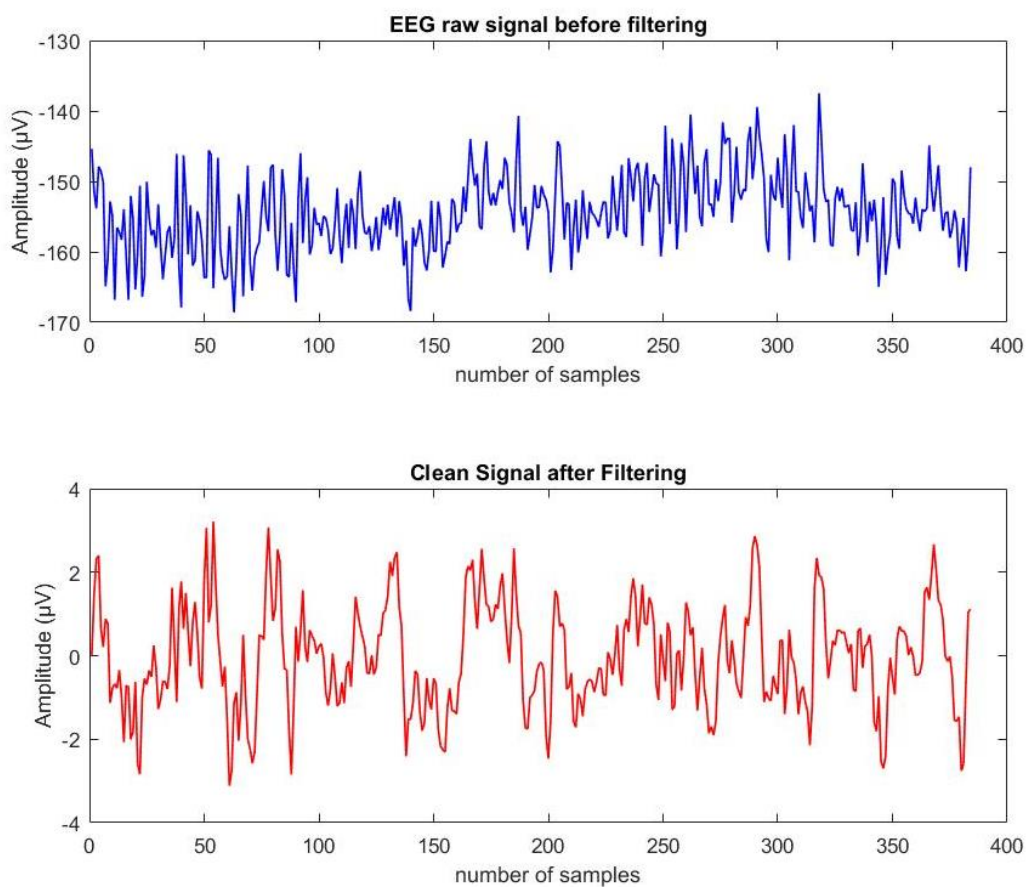


Figure 4-13. EEG signal filtering using Bayesian adaptive LMS filter.

The spectrum graph on Figure 4-14, shows the EEG signal spectrum before and after the filtering process. The bar on the right hand side indicates the signal power.

High frequency and low frequency noise in the signal have been removed and the signal power corrupted by the noise has also been reduced.

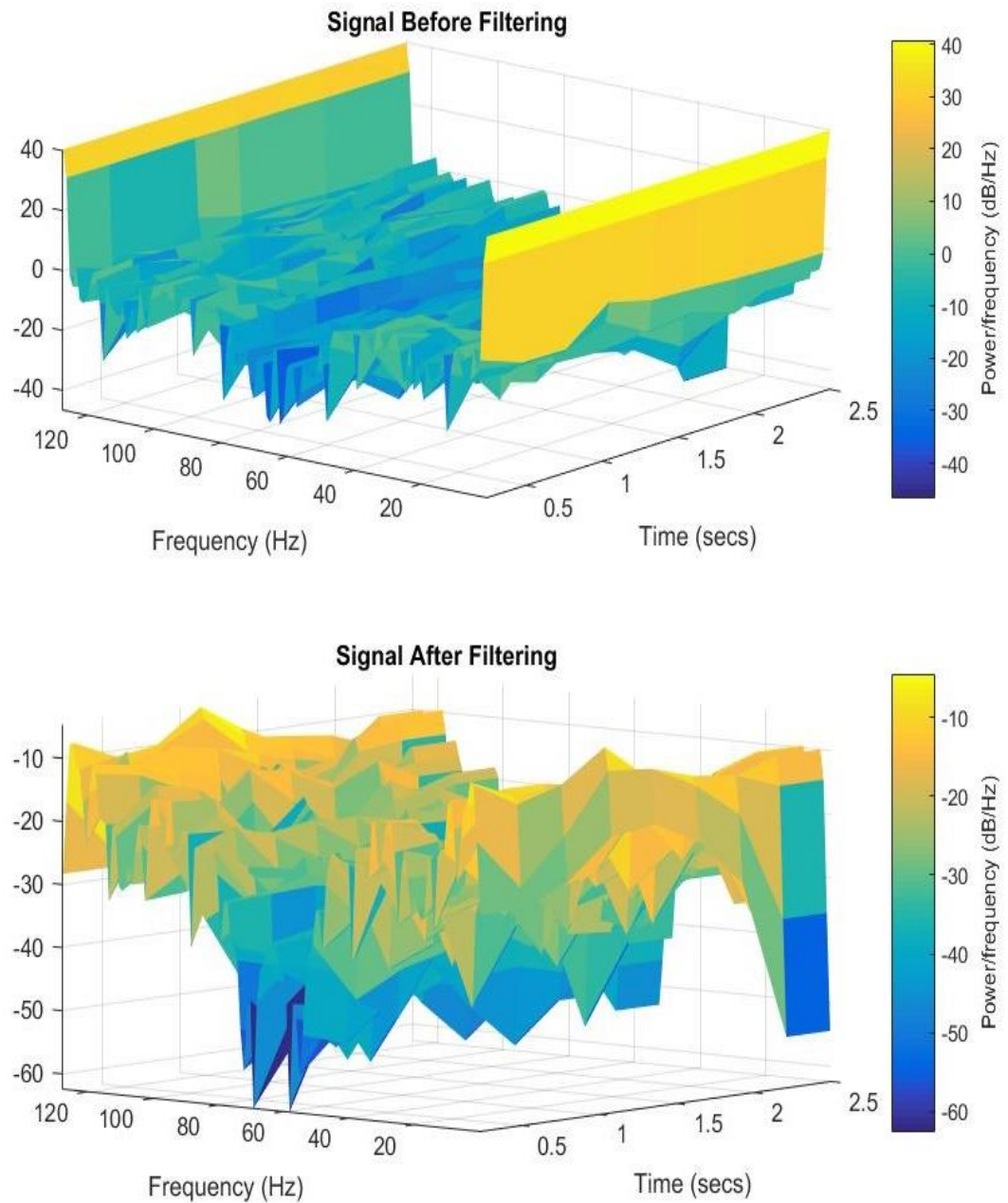


Figure 4-14. EEG signal spectrum before and after the Bayesian adaptive LMS filtering process.

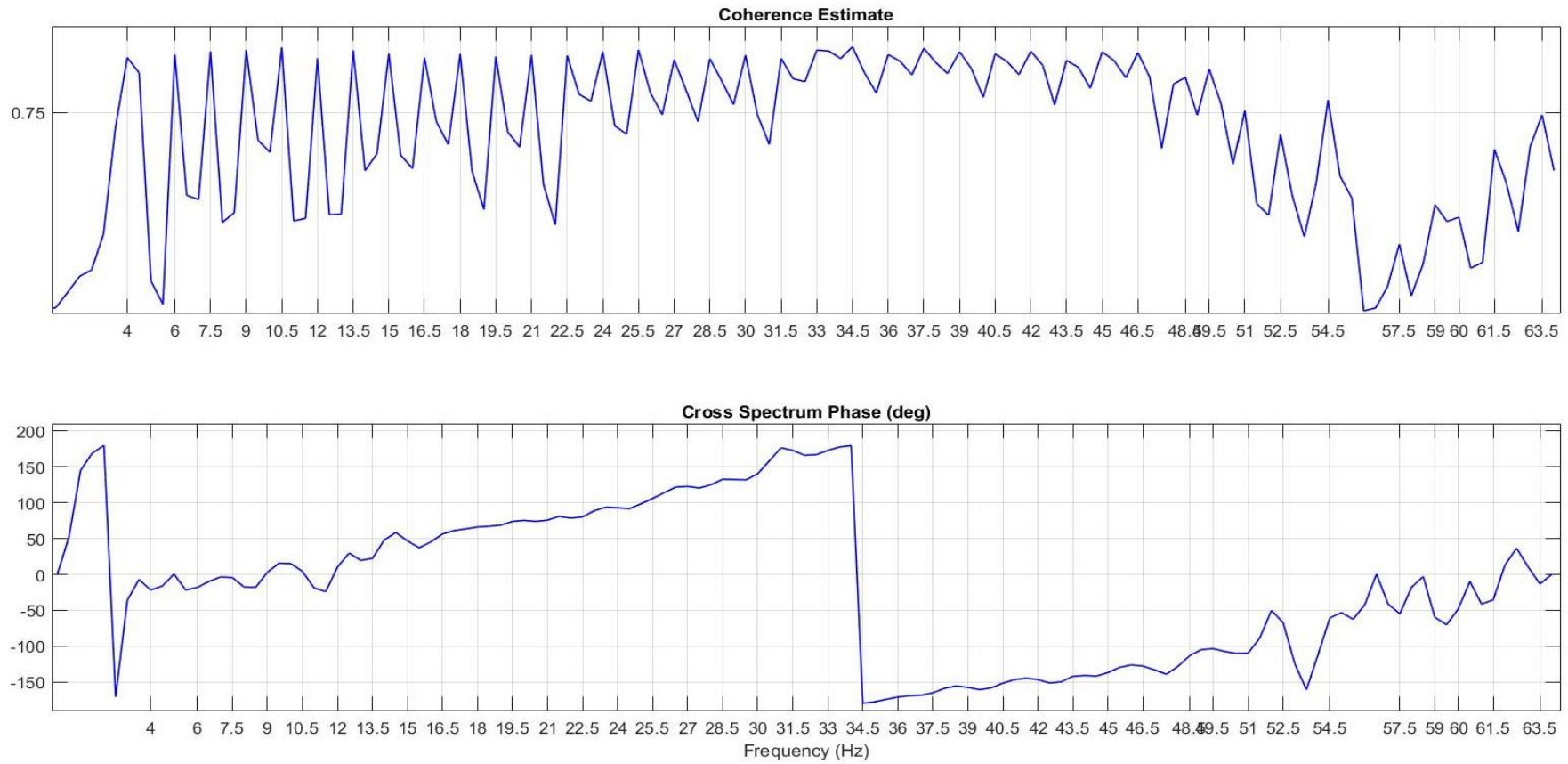


Figure 4-15. Signal coherence between two signals.

The coherence analysis indicates that the signal after the filtering processes still contains information similar to the raw EEG signals. Figure 4-15 shows the coherence between the signal before filtering and the signal after filtering. It clearly shows that the EEG signal frequencies from approximately 0.5 Hz to 63 Hz are retained during the filtering process. Signal power can be seen in Figure 4-16. The blue line plotted in the figures shows the EEG signal after the filtering process, and the black line colour plot shows the EEG signal before the filtering process.

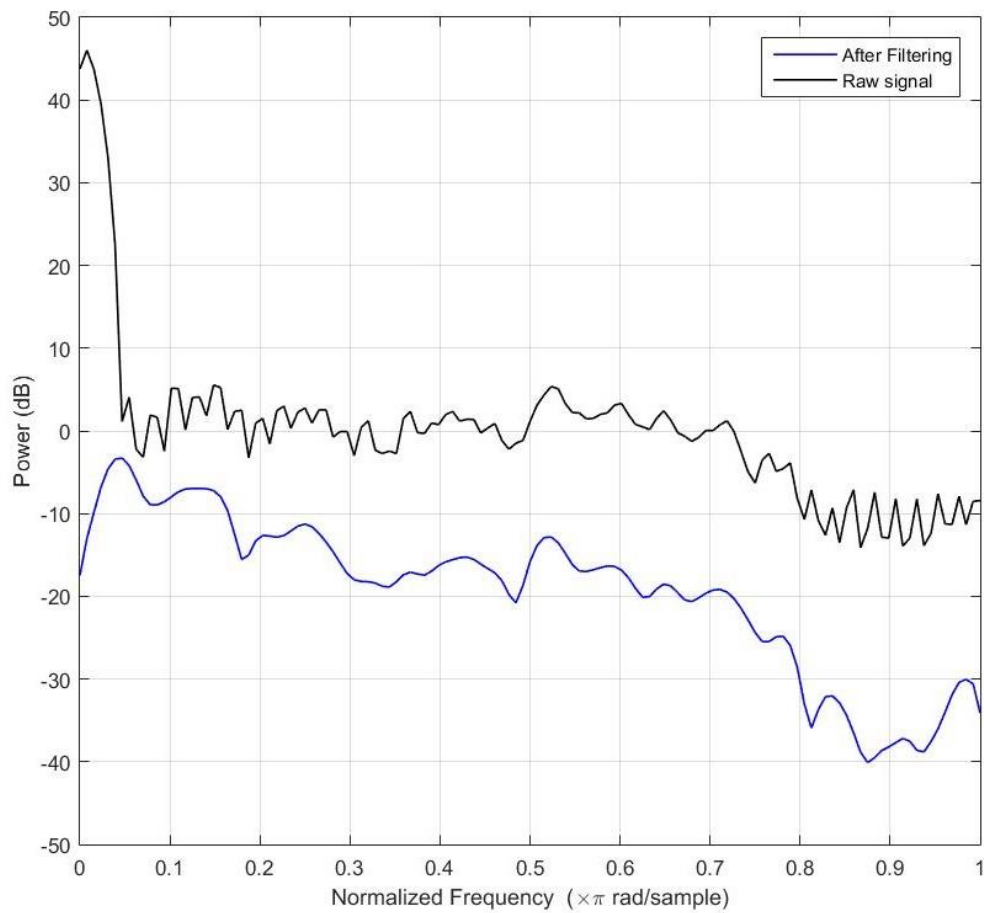


Figure 4-16. Comparison of the EEG signal power before and after filtering.

4.4.3 Comparison of the filtering techniques

Both filtering techniques introduced in this chapter show their capability for removing the noise underlying EEG signals. The first technique is SWT, which is not only able to remove noise, but is also useful for separating the EEG signal into different frequency bands. The SWT is also used to find the EEG signal frequency range for the $r(n)$ input in the Bayesian adaptive filter. Figure 4-17 shows the comparison of the EEG signal using the two different filtering techniques.

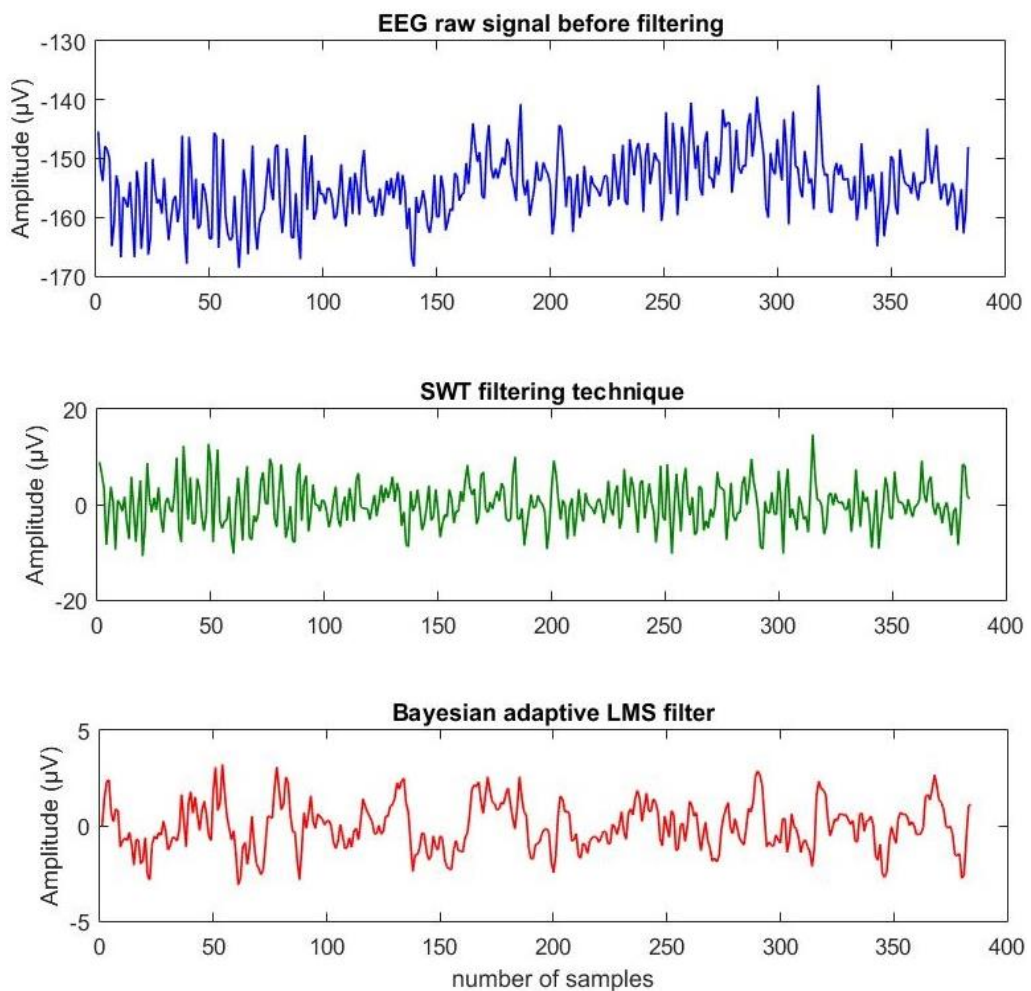


Figure 4-17. Comparison of the EEG signal filtered with the SWT and Bayesian adaptive filters.

Both filtering techniques retain the frequency component of the EEG signal. However, the SWT method has a high signal power compared with the Bayesian adaptive LMS filter. This indicates that some of the noise power is still affecting the SWT filtering results. Figure 4-18 shows the signal power from the raw EEG signal, Bayesian adaptive filter, and the SWT filter. The red line is the raw EEG signal before filtering, the black line is after the SWT filtering, and the blue line is after the Bayesian adaptive LMS filtering.

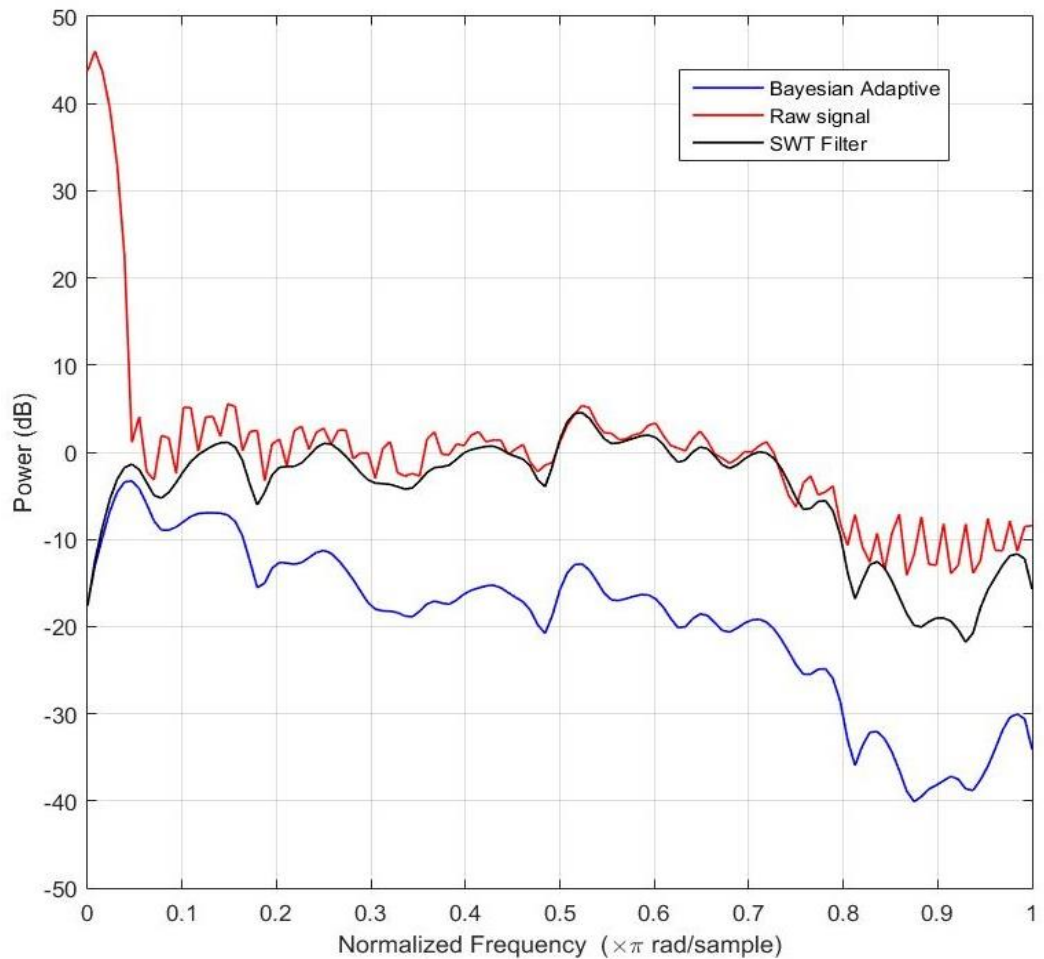


Figure 4-18. EEG signal power between the raw signal, Bayesian adaptive LMS filter, and the SWT filtering technique

4.5 Summary

The recorded EEG signal data not only includes pure EEG signal but also the noises. The noises corrupted the EEG signal and this could affect the EEG signal analysis. Therefore, the EEG signal filtering is very important before further analysis of the signals. This chapter has presented two EEG signal filtering techniques. The first filtering technique is the SWT filter and the second technique is Bayesian adaptive LMS filter.

The SWT filtering technique is able to remove noises from the EEG signals. By comparing the SWT result with the raw signal, it is suggested that the filtering technique not only removes the noises but also retains frequency information from the raw signal. In addition, the SWT is used to separate the EEG signal into different frequency bands.

The Bayesian adaptive LMS filter is a novel technique presented in this chapter. The filtering technique employs the Bayesian Student-t distribution to find the filter weight parameter for the LMS filter. The Bayesian adaptive LMS filter is able to remove the unwanted signal or noises from the EEG signals. The results shows that the outcome of the filter is better compared with the SWT filtering technique. It is also able to remove noises such as EMG, EOG and power line noises from the signals. The output signal after the filtering indicates that the Bayesian adaptive LMS filter technique is able to remove the noise and retain frequency information from the recorded EEG signals.

5 DEPTH OF ANAESTHESIA ASSESSMENT USING STRONG ANALYTICAL SIGNAL ANALYSIS

This chapter applies the strong analytical signal technique to extract EEG signal information for DoA. The method is simpler with less computations comparing to the method currently used in DoA monitors.

5.1 EEG feature extraction using the strong analytical signal technique

The EEG signal is decomposed into five bands as shown in Table 5.1. The information on each frequency band of the EEG signal is analysed using the strong analytical signal technique. Table 5.1 shows different levels of signal decomposition which corresponds to the EEG frequency bands. Detail level one (D_1) corresponds to frequency 50-120 Hz, detail level two (D_2) corresponds to frequency 30 to 50 Hz, detail level three (D_3) corresponds to frequency 20 to 30 Hz, detail level four (D_4) corresponds to frequency 10 to 20 Hz, detail level five (D_5) corresponds to frequency 6 to 10 Hz, and the approximation level five (A_5)

corresponds to frequency 0 to 6 Hz. In most DoA assessment, four different frequency bands are employed. These frequency bands are delta (δ) 0-4 Hz, theta (θ) 4-8 Hz, alpha (α) 8-13 Hz, and beta (β) 13-30 Hz (Kortelainen & Seppänen 2013; Nguyen-Ky et al. 2012; Rampil 1998). In this study, the five levels of SWT decomposition in Table 5-1 have been chosen to analyse the new DoA.

Table 5-1. Signal decomposition levels and their corresponding frequency bands

Decomposition Level	Frequency (Hz)
D ₁	50 - 120
D ₂	30 - 50
D ₃	20 - 30
D ₄	10 - 20
D ₅	6 - 10
A ₅	0 - 6

The strong analytical signal analysis is employed to extract information from the decomposed signals. It is called as a strong analytical signal technique as the real function $f(t)$ and its Hilbert Transform $\hat{f}(t)$ are strongly related (Kschischang 2006). The Hilbert Transform of $\hat{f}(t)$ is the convolution of the $f(t)$ and $1/\pi t$. The Hilbert Transform is defined as:

$$\hat{f}(t) = f(t) * \frac{1}{\pi t} \quad 5-1$$

$$\hat{f}(t) = \frac{1}{\pi} P \int_{-\infty}^{\infty} \frac{f(\tau)}{t - \tau} d\tau \quad 5-2$$

It is to be noted that the Hilbert Transform has an inappropriate integral value because it has an integrand singularity and a limit to infinity. Therefore, P (the Cauchy principle value integral) is placed in front of the integral (Kschischang 2006). Equation 5-2 can be redefined as follows:

$$\hat{f}(t) = \frac{1}{\pi} \lim_{\varepsilon \rightarrow \infty^+} \left(\int_{t-\frac{1}{\varepsilon}}^{t-\varepsilon} \frac{f(\tau)}{t-\tau} d\tau + \int_{t+\varepsilon}^{t+\frac{1}{\varepsilon}} \frac{f(\tau)}{t-\tau} d\tau \right) \quad 5-3$$

As stated by Kelley (2003); Kelley (2012), the EEG signal pattern changes from low amplitude to high amplitude and from high frequency to low frequency as the dosage of the anaesthetic agent administered to the patient increases. This changing pattern is the basis of EEG signal using the strong analytical signal analysis technique. Using the Hilbert Transform, the instantaneous amplitude and instantaneous phase of EEG signal in the time domain can be described as:

$$A(t) = \sqrt{f^2(t) + \hat{f}^2} \quad 5-4$$

$$\varphi(t) = \arctan\left(\frac{\hat{f}(t)}{f(t)}\right) \quad 5-5$$

where $A(t)$ is the instantaneous amplitude; $\varphi(t)$ is the instantaneous phase in the time domain.

5.2 Features extraction and DoA index development

The recorded EEG signal is shifted every second using a sliding window technique. The EEG signal parameter is extracted and analysed every second. The sampling rate is 128 samples per second and the overlap is 25 % of the window size. For a

given decomposed signal at level j , the amplitude of the signal $A_w(t)$ and the instantaneous phase $\varphi(t)$ are analysed. The detailed procedure is shown as follows:

- Find the mean amplitude of the signals:

$$A_w = \text{Max}_{(peak)} - \text{Min}_{(peak)} \quad 5-6$$

$$\mu A_w = \frac{1}{N} \sum_{w=1}^N A_w(t) \quad 5-7$$

where μA_w is the mean instantaneous amplitude, N is the number of observations, and $\text{Max}_{(peak)}$ and $\text{Min}_{(peak)}$ are the maximum and the minimum amplitude of the signals.

- The mean instantaneous phase:

$$\mu \varphi_w = \frac{1}{N} \sum_{w=1}^N \varphi_{wdj} \quad 5-8$$

where $\mu \varphi_w$ is the mean instantaneous phase from the signals. It is computed from the instantaneous phase on each decomposition level φ_{wdj} .

The amplitude and instantaneous phase are derived from every epoch and recursively computed through the whole signal. The mean amplitude and mean instantaneous phase are obtained from all decomposition levels. The complex

modulus (C_φ) is computed from the mean instantaneous phase. The C_φ is defined as:

$$C_\varphi = \sqrt{\left(\text{real}(\mu\varphi_w(t))^2 + \text{imag}(\mu\varphi_w(t))^2\right)} \quad 5-9$$

The new DoA index is derived from the sum of the mean range amplitude A_w of the signals and the mean complex modulus of the instantaneous phase divided by two as computed using Equations 5-10 and 5-11. The normalisation of the signal is applied to the newly calculated DoA value. The new DoA index also includes the signal amplitude parameter estimation; as the amplitude of the EEG signal increases, the patients lose consciousness.

Computation of the new DoA is shown as follows:

- Computing the mean amplitudes of D1, D2, D3, D4, D5, and A5

$$\text{newD} = \frac{\mu A_w + \mu(C_\varphi)}{2} \quad 5-10$$

$$\text{newD} = \frac{\frac{1}{N} \sum_{w=1}^N A_w + \frac{1}{N} \sum_{w=1}^N \mu(C_\varphi)}{2} \quad 5-11$$

with the normalisation and scaling properties is as follows:

$$\text{newDoA} = \frac{\mu A_w}{100 - rA} \times \text{newD} \quad 5-12$$

$$0 \leq \text{newDoA} \leq 100 \quad 5-13$$

where rA is the peak to peak amplitude of one EEG epoch before decomposition, and μA_w is the mean instantaneous amplitude.

5.3 Results

The DoA index is evaluated using the 20 EEG data sets, and the results were compared with that of the wavelet entropy technique and the BIS index. Figure 5-1 shows the comparison results between the new DoA and the Wavelet Entropy method by Zhiqian (Zhiqian, Fuying & Jianfeng 2005). The results show that, the wavelet entropy (blue line) has the same trend as the new DoA when the monitoring started. From the start to approximately 150 seconds, these two methods display similar trends. Afterwards, the new DoA level and the entropy begin to have slightly different values. The new DoA decreases to around 30. Meanwhile, the Wavelet Entropy level decreases to around 60 and then starts to fluctuate. The wavelet entropy index shows an increasing value when the sevoflurane and nitrous oxide were administered to the patients. The DoA normally decreases when the sevoflurane and Nitrous oxide was administered.

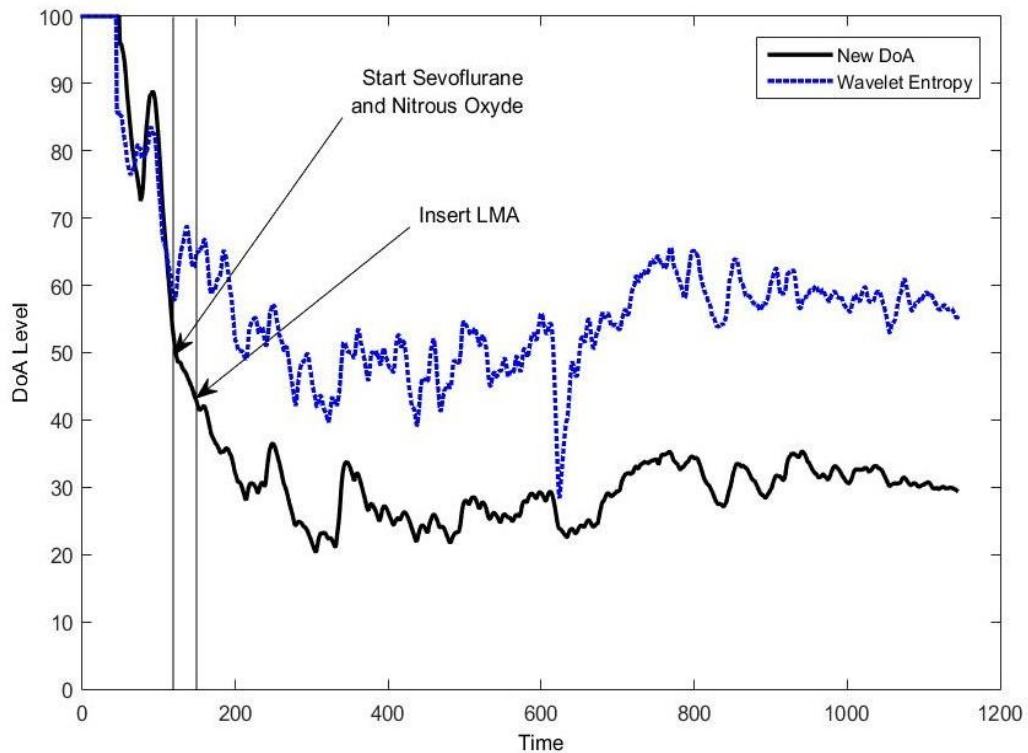


Figure 5-1. Comparisons between the new DoA and the Wavelet entropy method.

One of the disadvantages of the BIS index monitor is time delay in processing the index. The BIS monitor has a time delay of around 15 to 30 seconds between computing and displaying the DoA index (Zanner et al. 2009). Figure 5-2 shows comparisons between the new DoA index and the BIS index. The blue line is the new DoA and the red dashed line colour is the BIS index. The new DoA using the Hilbert based algorithm is fast in detecting the changing pattern of the EEG signal. The computation is simple; therefore, the computation time is faster than the BIS index. The new DoA index is about 50 seconds ahead of the BIS, as shown in Figure 5-2. The figure also shows that in the early stage at approximately 80 seconds after the recording starts, the new DoA index displayed a sudden decrease (from approximately 100 to about 73 within approximately 30 seconds) compared to the decrease in the BIS index (from approximately 97 to about 83 within approximately 3 seconds), marked with circle in Figure 4. The sudden decrease and peak (marked with circle) in the new DoA index is a response to an effect called the paradoxical delta arousal. The paradoxical delta is an unexpected slowing of EEG signals during anaesthesia (Freye & Levy 2005).

Figure 5-2 further shows that the response of the new DoA index is closely related to the clinical situation where the consciousness of the patient decreases as the effect of anaesthetic drugs increases. In the operating theatre, prior to insertion of the laryngeal mask airway (LMA), the patient must reach a sufficiently unconscious level to be able to relax the jaw muscle and to prevent movement and coughing (Dutt, Joad & Sharma 2012). The LMA is inserted about 30 seconds after the sevoflurane and nitrous oxide were given to the patient. Even though the patient was unconscious, the new DoA index was able to detect the changes when the LMA was inserted. The new DoA method is also able to detect patients' responses as shown by the slightly increasing DoA level (at approximately 151 seconds) when the LMA is inserted to the patient's.

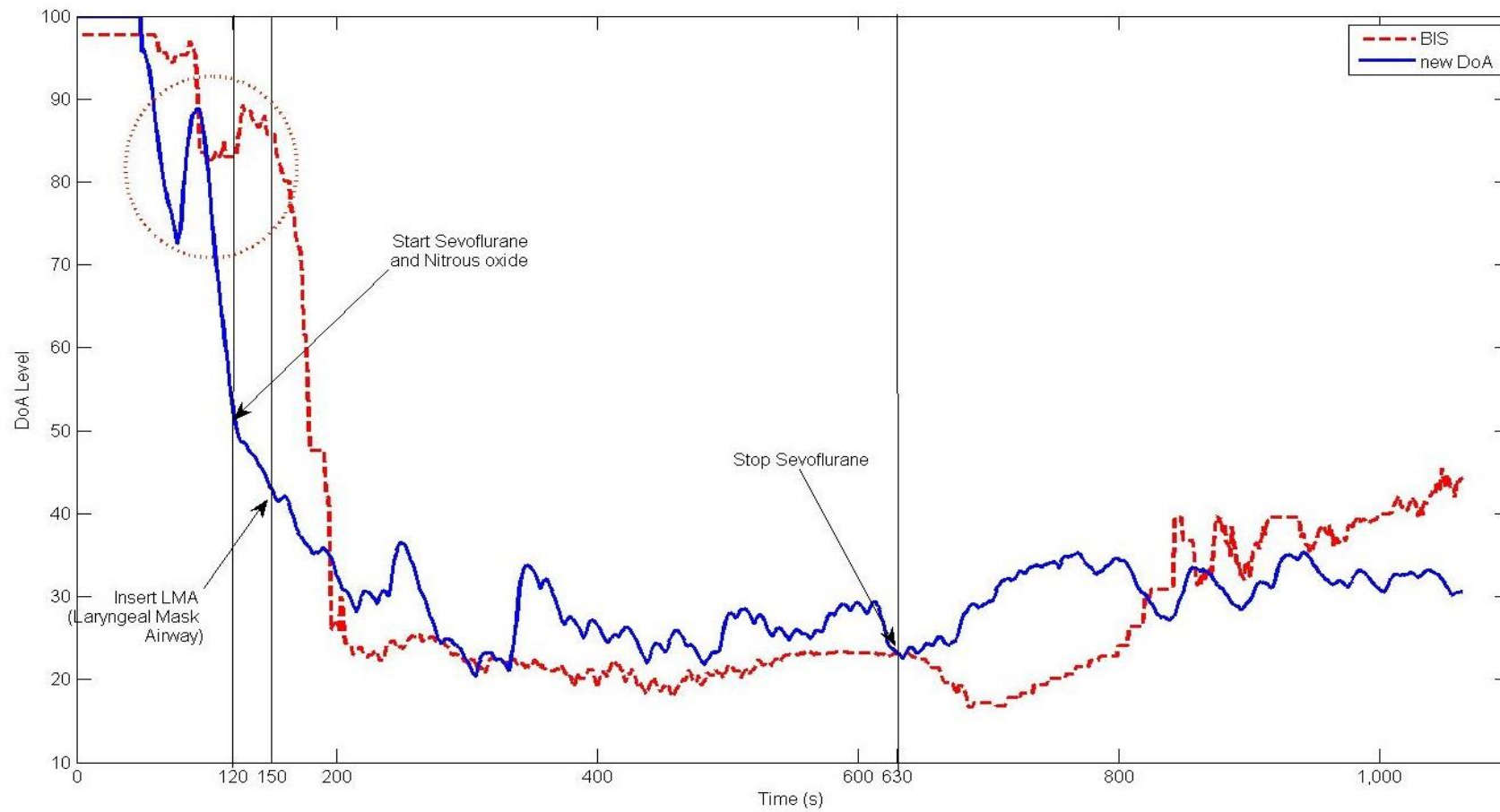


Figure 5-2. Comparisons between the new DoA index and the BIS index.

As also shown in Figure 5-2, at approximately 630 seconds the administration of the sevoflurane drugs ceased. The Sevoflurane is an anaesthesia maintenance drug given to maintain the level of unconsciousness during the operation. Shortly after the sevoflurane ceased, the patient began to gain consciousness, represented by the increasing of DoA level. In contrast, the BIS index dropped when the sevoflurane was stopped and then gradually increased to approximately 40. After 1000 seconds, there was no further recording. It was assumed that the patient began to gain consciousness and recover from anaesthesia.

Figure 5-3 shows the time delay between the BIS index and the new DoA. The new DoA is represented by the blue line and the BIS index is red. The result shows that the BIS index has a time delay of around 100 seconds behind the new DoA. As seen in Figure 5-3, after administering midazolam (3mg) the BIS index is taking some time to response. In addition, the effects of fentanyl and propofol in central nervous system create rapid changes in brain metabolism (Gelb et al. 2009; Sloan & Heyer 2002).

The effect of rapid changes in the central nervous system should be reflected in the changing pattern in BIS index instantly. However, Figure 5-3 shows the BIS index response a little bit late compared to the new DoA. After the anaesthesia induction with midazolam, the BIS level still shew the patient at the conscious level (in the awake stage). On the other hand, the new DoA shows that the patient is in the unconscious level. This result shows that the new DoA is responsive more in real-time than the BIS index.

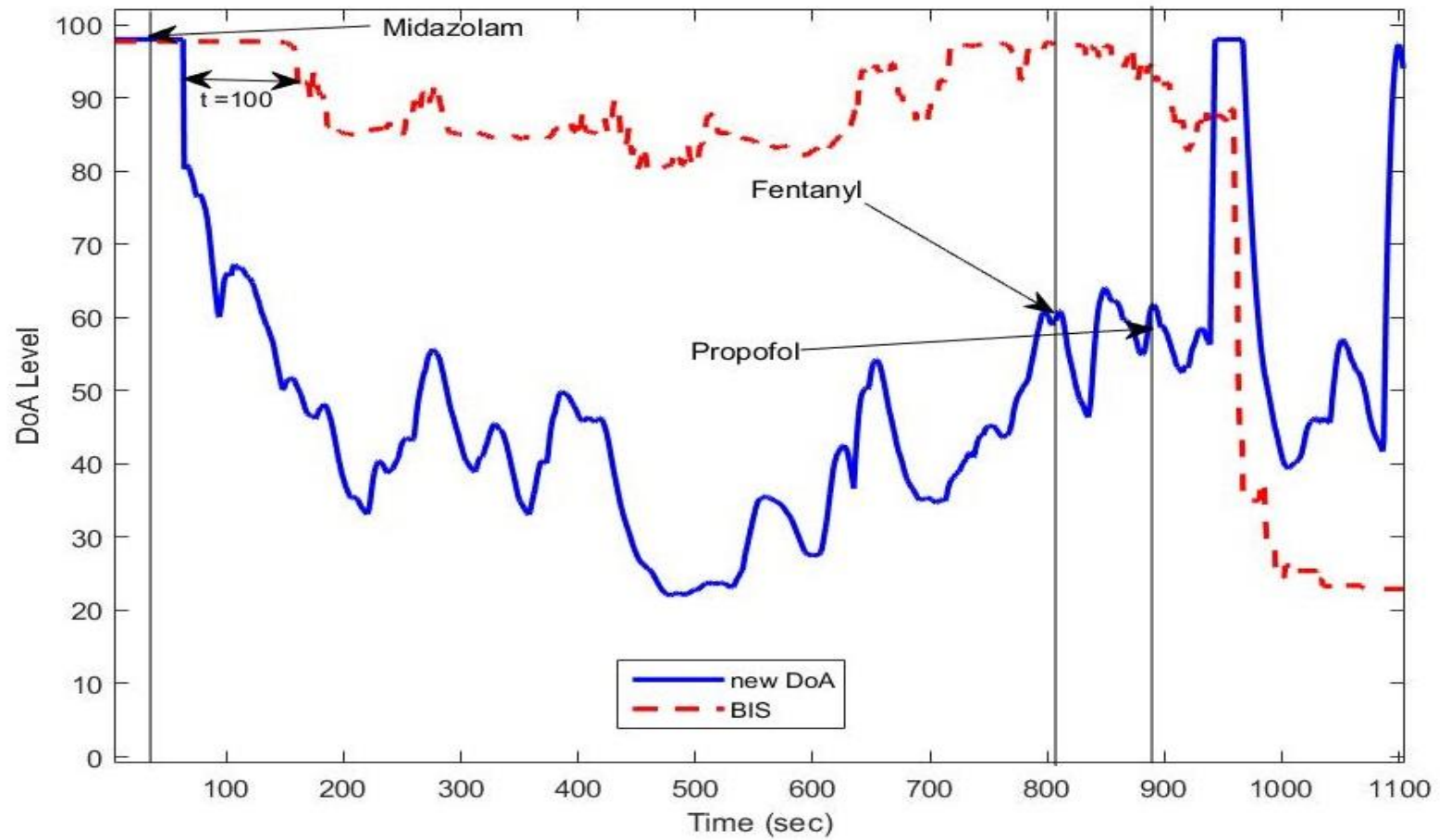


Figure 5-3. Time delay in BIS.

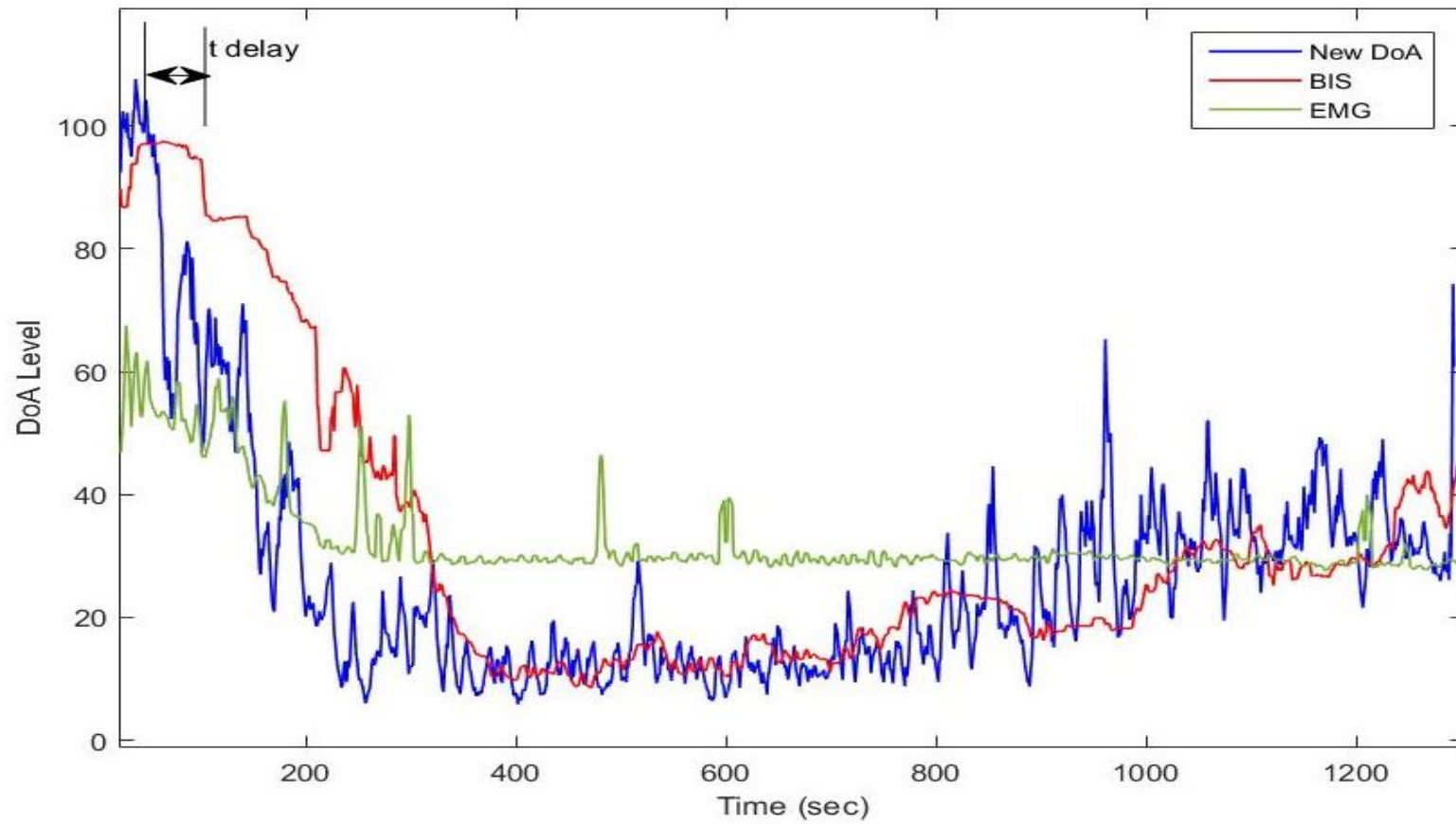


Figure 5-4. The comparison between new DoA and the BIS.

Figure 5-4 shows the BIS index time delay at around 40 seconds. The new DoA trend follows the BIS trends but the BIS index is 40 second behind the new DoA. Figure 5-4 also shows the patient response to some stimuli. The response is indicated in the increasing EMG signal value. The EMG signal is represented in a green line. It reveals that the new DoA is able to pick up some response from stimulation to the patient. At around 100 second from the start, the patient receives stimulation and the effect of this stimulation is the new DoA levels oscillates and slightly increased. On the other hand, the BIS index does not give any response to the stimulation, instead of gradually decreasing the BIS value.

BIS index time delay is displayed in Figure 5-5. Figure 5-5 shows the overall time delay of the BIS index to produce the DoA level. The new DoA index is ahead around 18 to 190 seconds to produce the index compared to the BIS. Data from Figure 5-5 indicates that patient number 19 time delay is the longest delay compared with the other patients, which is around 190 seconds. On the other hand, the short time delay data is from the patient number 17, which is 18 seconds.

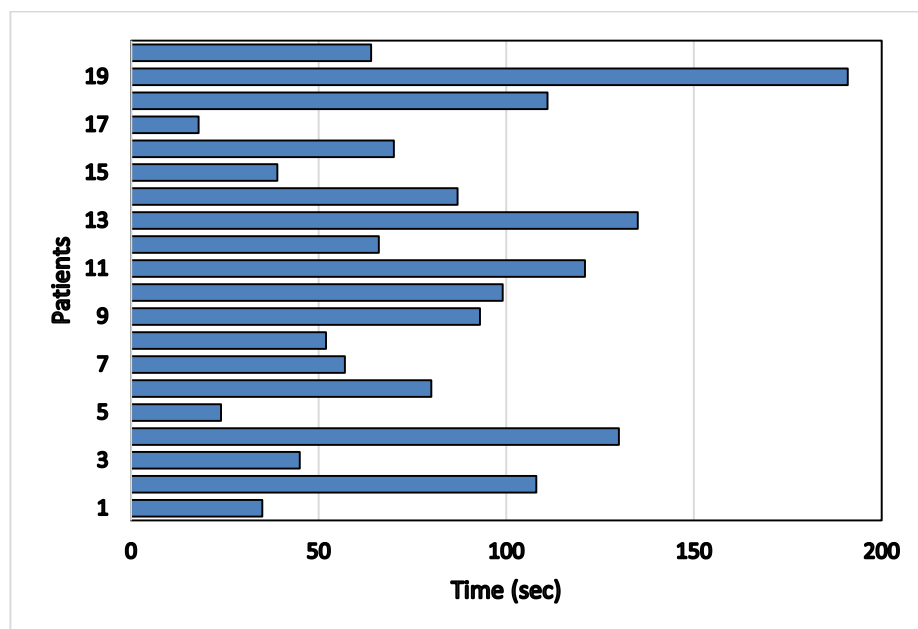


Figure 5-5. Time delay of the BIS index.

A cross correlation was performed to compare the results from the new DoA method and the BIS index. The correlation value r falls between -1 and 1. If the r value is close to 0, it indicates that the data has a weak correlation. If the r value is close to either -1 or 1, it indicates that the data are close to a linear relationship. The r value of -1 or 1 indicates that the data has a perfect linear relationship. Table 5-2 shows the cross-correlation between the BIS index and the new DoA index for 20 patients. Table 5-2 also shows that more than 85% of the sample has an r value more than 0.78 demonstrating that the BIS index and the new DoA index have a positive correlation. Therefore, the result indicates the new DoA method can be used as an alternative method to analyse the depth of anaesthesia.

Table 5-2. Correlation between the BIS index and the new DoA index for 20 patients

	Data	Correlation
Patient 1	2838	0.11
Patient 2	3191	0.86
Patient 3	5654	0.02
Patient 4	1656	0.87
Patient 5	2441	0.93
Patient 6	5856	0.89
Patient 7	1264	0.97
Patient 8	2889	0.90
Patient 9	4174	0.83
Patient 10	4977	0.89
Patient 11	6642	0.87
Patient 12	3308	0.94
Patient 13	3308	0.91
Patient 14	2198	0.88
Patient 15	5183	0.94
Patient 16	1415	0.92
Patient 17	4556	0.85
Patient 18	2875	0.21
Patient 19	2620	0.78
Patient 20	1064	0.91

To compare the BIS index and the new DoA index at different anaesthesia stages, a statistical analysis is applied. Table 5-3 shows the mean, standard deviation and correlation of the BIS and new DoA at different stages of anaesthesia. As shown in Table 5-3, the light anaesthesia stage and moderate anaesthesia stage have a higher correlation compared to the other stages. It is suggested that the BIS and new DoA are closely correlated during these two stages. On the other hand, the very deep anaesthesia stage shows the lowest correlation value. The low correlation value indicates that the prediction of the anaesthesia level between the BIS index and the new DoA index is less correlated.

Table 5-3. The mean, standard deviation and correlation in each anaesthesia stage

Anaesthesia stage	Mean	Standard deviation	Correlation
Awake	94.53	4.34	0.77
Light anaesthesia	79.01	6.60	0.91
Moderate anaesthesia (General anaesthesia)	43.78	2.96	0.94
Deep anaesthesia	30.79	4.14	0.86
Very deep anaesthesia (Isoelectric)	20.05	2.71	0.60

5.4 Summary

This chapter investigates the EEG signal and DoA using the strong analytical signal technique. The technique is based on the Hilbert transform and the amplitude detection technique. The method is employed to extract information of instantaneous phase and instantaneous amplitude and the envelope amplitude. The

results show that the feature extraction using the strong analytical signal is able to improve EEG signal interpretation for DoA monitoring as well as improve the computation time. The results also indicate that the new DoA can be used as an alternative for monitoring the DoA. The strong analytical signal analysis is a simple technique in EEG signal analysis.

6 BAYESIAN SPIKES ACCUMULATION TECHNIQUE TO ANALYSE ELECTROENCEPHALOGRAPH SIGNAL FOR DEPTH OF ANAESTHESIA ASSESSMENT

This chapter introduces a novel technique using Bayesian spike accumulation (BSA) to extract EEG signal parameters in time domain and to assess the depth of anaesthesia. The BSA method is based on the Bayesian Gaussian distribution. The BSA computes the probability number of spikes in the EEG signal. The likelihood function of the EEG signal is computed with the assumption that the signal is normally distributed.

6.1 Bayesian Method

Signal analysis based on the Bayesian method is an advanced technique for estimating the signal. The EEG signal parameter can be estimated with the Bayesian method (Nguyen-Ky, Wen & Li 2013, 2014). The EEG signal parameter is estimated using the prior and likelihood function. The unknown parameter θ is estimated from the EEG data $x=(x_1, x_2, \dots, x_n)$. Data (D_1, D_2, \dots, D_n) are the EEG

epochs extracted from the raw EEG signal using the sliding window technique. The Bayesian estimation theorem for the conditional probability estimation can be expressed as (Fienberg 2006; Heung-II & Seong-Whan 2013; Krieger et al. 2014; Valencia et al. 2014):

$$p(\theta|x) = \frac{p(x|\theta)p(\theta)}{p(x)} \quad 6-1$$

$$p(x) = \int_{\theta} p(x|\theta)p(\theta)d\theta \quad 6-2$$

where:

x is the observation data

$p(\theta)$ is the prior density of parameter θ

$p(x|\theta)$ is the likelihood function

$p(\theta|x)$ is the posterior distribution

$p(x)$ is the normalising constant

The prior is described as prior knowledge before analysing or observing the data. Updating the prior distribution θ through a number of iterations from the given data $x=(x_1, x_2, \dots, x_n)$ could give the best possible estimation of θ . The likelihood functions $p(x|\theta)$ is the probability of the observed data. Research by Nguyen-Ky, Wen and Li (2013) suggested that Gaussian probability distribution was able to give better estimation for the EEG signal analysis. Therefore, the Gaussian distribution has been chosen to estimate the likelihood function from the data x . Gaussian distribution or normal distribution for the continuous single variable x is

defined as (Dahlhaus 2000; Sykacek, Rezek & Roberts 2005) :

$$N(x|\mu, \sigma^2) = \frac{1}{\sqrt{(2\pi\sigma^2)}} \exp\left\{\frac{1}{2\sigma^2}(x - \mu)^2\right\} \quad 6-3$$

where: μ is the mean and σ^2 is the variance. Parameters μ and σ^2 in Gaussian probability distribution are normally determined by maximising the likelihood function (Bishop 2007). The maximum likelihood estimation for the Gaussian Parameter with respect to μ , is defined as:

$$\mu_{MLE} = \sum_{i=1}^n \frac{x_i}{n} \quad 6-4$$

The maximum likelihood for the σ^2 is defined as:

$$\sigma_{MLE}^2 = \frac{1}{n} \sum_{i=1}^n (x_i - \mu)^2 \quad 6-5$$

The posterior $p(\theta|x)$ from the Gaussian distribution in Equation 6-1 and the normalising constant independent θ in equation (2) can be rewritten as (Radtke et al. 2013):

$$p(\theta|x) \propto p(x|\theta)p(\theta) \quad 6-6$$

where the symbol \propto means "proportional to" posterior $p(\theta|x)$ is the normalising constant of the probability density function $\int p(\theta|x)d\theta = 1$ (Cooper & Herskovits 1992). Nguyen-Ky, Wen and Li (2013), in their paper tested several distributions for the histogram EEG data fitting. Their results suggested that the EEG signal distribution fits with Gaussian distribution.

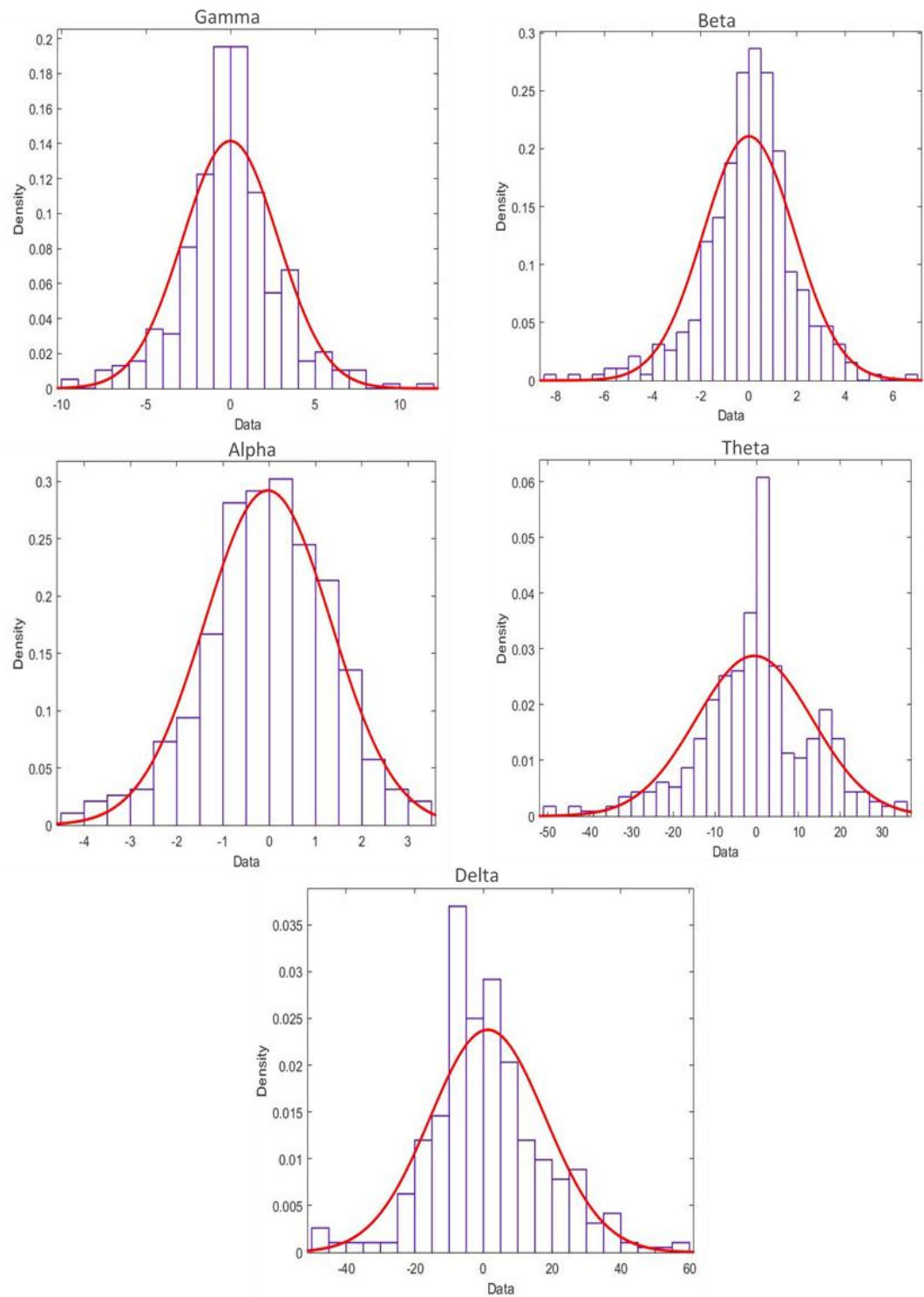


Figure 6-1. Histogram of the EEG signal in different frequency bands.

The EEG signal parameter in this research is estimated using the Gaussian probability density function. Figure 6-1 shows a histogram of the EEG signal in each frequency band. The testing and results from this research confirmed that the EEG signal distribution fits with the Gaussian distribution. Testing for the EEG signal histogram and distribution fitting is presented in Figure 6-1. The data for the histogram in Figure 6-1 is taken from the EEG awake signal and the signal is then separated into different frequency bands. The result shows the EEG signal in different frequency bands fitting with the Gaussian distribution.

6.2 Bayesian spike accumulation

The Bayesian spike accumulation technique was inspired by a number of methods used to analyse signal. Those methods only analyse and find the synchronisation of the signal spikes (Biswas, Khamaru & Majumdar 2014; Kloosterman et al. 2014; Nia & Huosheng 2012). Unlike these methods, the Bayesian spike accumulation technique assembles all the spikes and sums up the spikes. The Bayesian spike accumulation technique applies the Gaussian probability density distribution to each EEG signal on every epoch. The BSA is constructed from a vector with linearly spaced element. A vector space is defined based on the maximum and minimum value of EEG signals in each epoch (A). The parameter for the BSA is extracted from a Bayesian density function with known variance and unknown mean. It is computed as follows:

$$N(x|A, \sigma) = \frac{1}{\sqrt{2\pi}\sigma} \exp\left\{-\frac{1}{2\sigma^2}(x - A)^2\right\}$$

6-7

where: x is the vector of EEG data for one epoch, vector A is a one-dimension vector with a minimum boundary x_{min} and a maximum boundary x_{max} . $A=(x_{min},$

x_{max}) is the vector with linearly spaced element, and σ^2 is a variance from the data. The BSA value is calculated from the sum of spikes in the probability density function in each epoch. The BSA posterior value is defined as:

$$p(A|x, \tau) \propto p(A, x|\tau)p(\tau) \quad 6-8$$

$$BSA = \sum_{n=1}^N p_n(A|x, \tau) \quad 6-9$$

The posterior estimation on BSA is calculated based on the number of spike estimated on $N(x|A, \sigma)$ and the density value in the data (τ). The algorithm is implemented as follows:

- Find the maximum and minimum value in each epoch
- Create a vector with linearly spaced elements from the maximum and minimum value
- Compute the Gaussian probability distribution of the EEG signal as in Equation 6-7
- Find the total number of spikes
- The total number of spikes in each epoch can vary in each anaesthesia stage.

6.3 DoA with Bayesian Gaussian distribution

The DoA with BSA technique is computed by using the BSA parameter and the likelihood parameter from the EEG signal. The EEG signal is analysed by assuming that its distribution is Gaussian. The DoA value is obtained from the posterior value. The posterior from the EEG signal is estimated with the unknown mean μ and the known variance σ^2 . The likelihood function is computed using the probability density function with Gaussian distribution $p(x|\theta)$ and can be written as:

$$p(x|\theta) = N(x|\mu, \sigma) = \frac{1}{\sqrt{2\pi\sigma}} \exp\left\{-\sum_{i=1}^n \left(\frac{x_i - \mu}{2\sigma}\right)^2\right\} \quad 6-10$$

The prior density for the DoA assessment is derived from the BSA parameter. The prior $p(\theta)$ can be expressed as $p(\theta)=(A|x,\tau)$. Thus, the posterior estimation based on Equation 6-6 can be rewritten as:

$$p(\theta|x) \propto p(x|\theta)p(\theta) \quad 6-11$$

$$p(\theta|x) = \frac{1}{\sqrt{\sigma^2 + \sigma_n^2}\sqrt{2\pi}} \exp\left\{-\frac{1}{2} \frac{(x - \mu_n)^2}{\sigma^2 + \sigma_n^2}\right\} \quad 6-12$$

where: μ_n is the mean and σ_n^2 is the variance of μ . The sliding window technique is applied to analyse the EEG signal in every epoch. Each epoch is shifted every one second. For every observed data set $D(x_i)$ in one epoch, the likelihood function and the posterior of the data are analysed recursively. The DoA assessment is computed based on the posterior with the prior density parameter and the likelihood

parameter. An epoch posterior estimation can be seen in Figure 6-2. Figure 6-2 shows the posterior estimation analysis from the Bayesian Gaussian distribution. It shows that the low BIS value approximately 15 (very deep anaesthesia) has higher probability density. The lowest probability value is the awake data or equivalent to BIS value 97. The probability of the BIS 30 is around 0.025 which is the second highest value in the Figure 6-2.

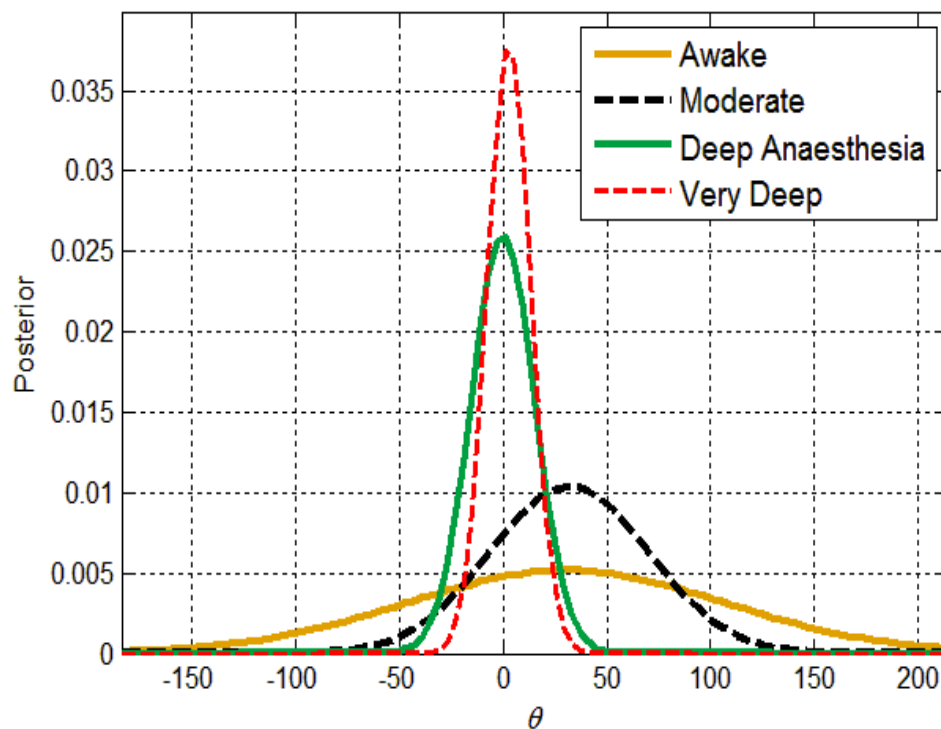


Figure 6-2. Posterior estimation for one epoch of observed data.

The experiment shows that the EEG posteriors are changing when the patient's consciousness level changes from awake to unconscious. In other words, the probability that patients do not response to stimuli increases as the anaesthetics affect the central nervous system. As shown in Figure 6-3, the probability of the patient's unconscious increases to 0.035 at BIS index 15 and the probability decreases to 0.005 at BIS 97 when the patient is awake. In addition, the probabilities are different in every single patient. However, the graphical trends

from awake to unconscious show the same tendency. In addition, Figure 6-4 shows the four stages of anaesthesia which are awake, light anaesthesia, general anaesthesia and deep anaesthesia. In this experiment, the EEG data is simulated from the different anaesthesia stages. The experiment confirmed that the different level of anaesthesia shows the different posterior values.

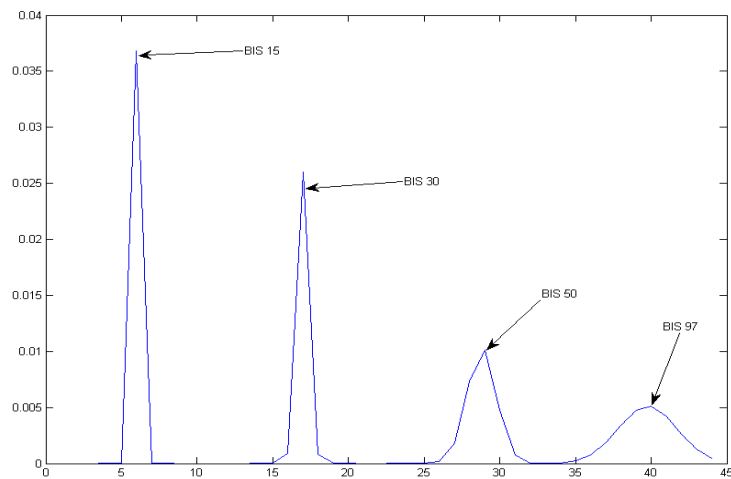


Figure 6-3. Probability response of patients in different level of anaesthesia.

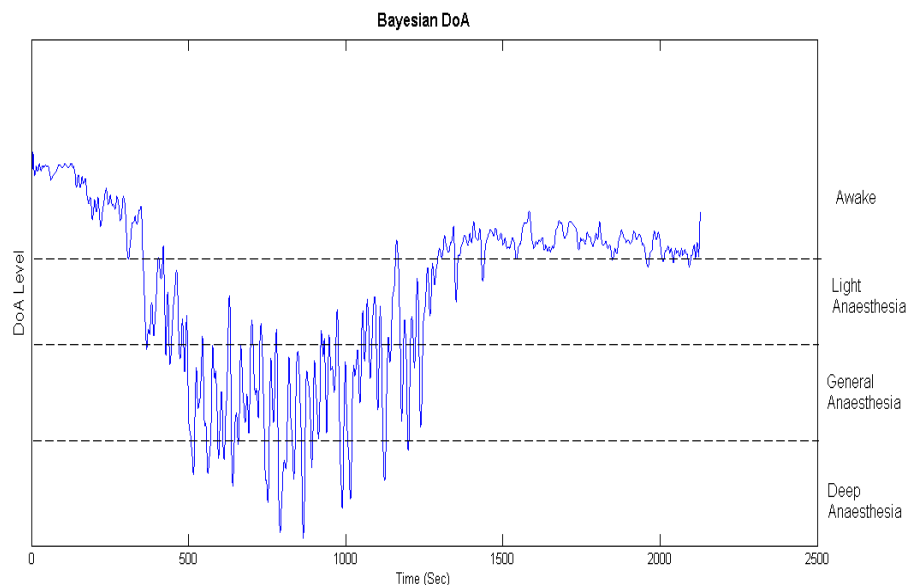


Figure 6-4. Four stages of anaesthesia which are awake, light anaesthesia, general anaesthesia and deep anaesthesia

6.4 Results and Analysis

6.4.1 Spike accumulation technique

Data from 20 adult patients are used in this experiment. The patients were administered with the anaesthetics drugs such as midazolam, alfentanil, fentanyl, and propofol. Twelve adult patients were administered with combination of midazolam, alfentanil and propofol and 8 patients received combination of midazolam, fentanyl and propofol. The experiment using the spike accumulation technique shows that there are decreasing numbers of spikes from the awake to deep anaesthesia stages. Data in Figure 6-5 was taken from awake patients. The awake data has the highest number of peaks compared to the other anaesthesia stages. Figure 6-5(a) shows the estimation from the awake data. As the anaesthesia level declines, the numbers of spikes also decline. Figure 6-5(d) shows the lowest number of spikes. The lowest numbers of spikes correlates with the BIS index 15.

The results show that spike accumulation is able to detect the changes in EEG signals as a response to anaesthetic drugs. Figure 6-5 indicates the basic pattern for analysing the EEG signal. Increasing effect of anaesthetic drugs to the patients (becomes unconscious) reflects the decreasing number of spikes in the EEG signal.

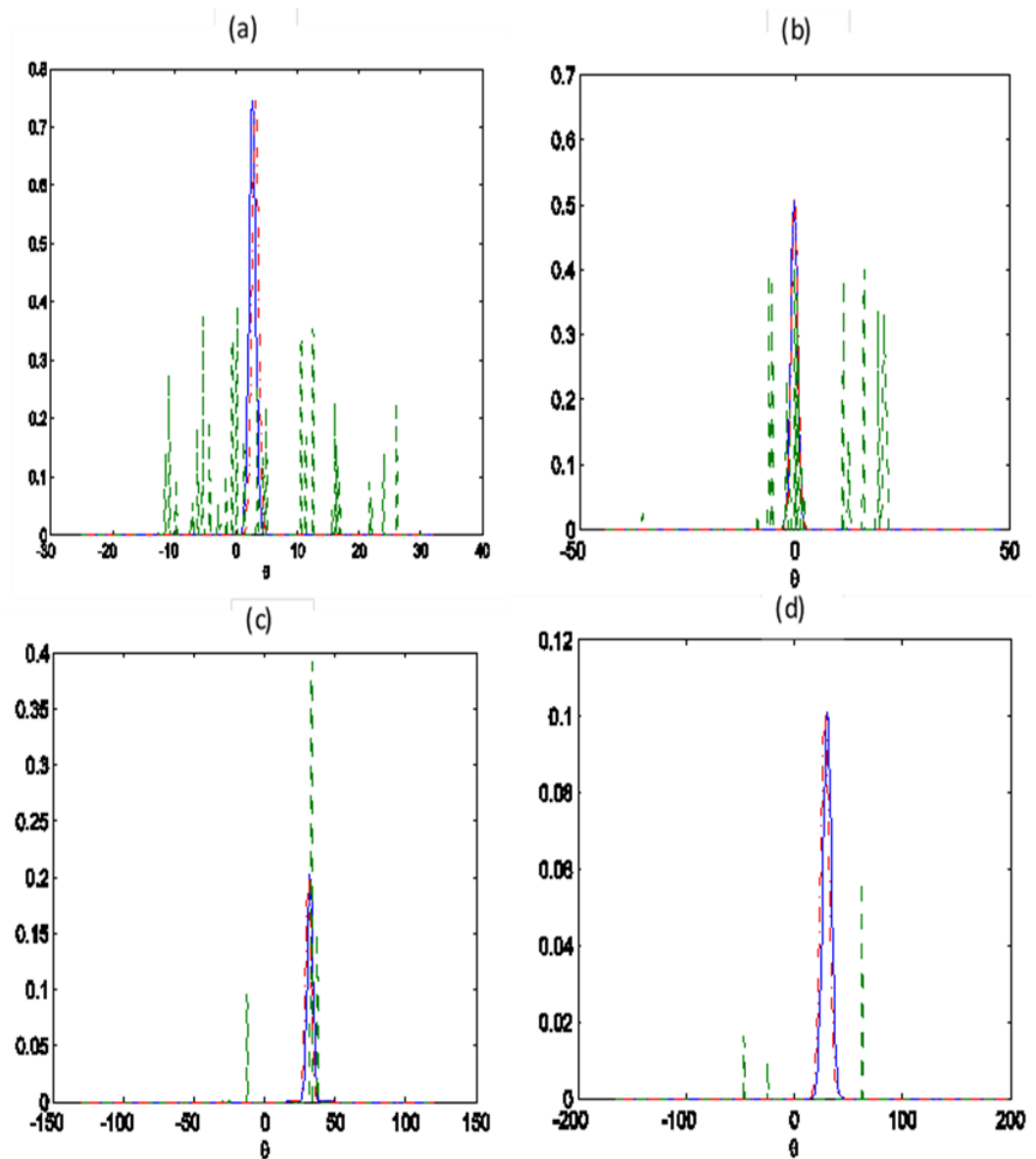


Figure 6-5. Different levels of anaesthesia (a) awake patient correlate with BIS 97, (b) moderate anaesthesia correlates with BIS 50, (c) deep anaesthesia correlates with BIS 30 and (d) very deep anaesthesia correlates with BIS 15.

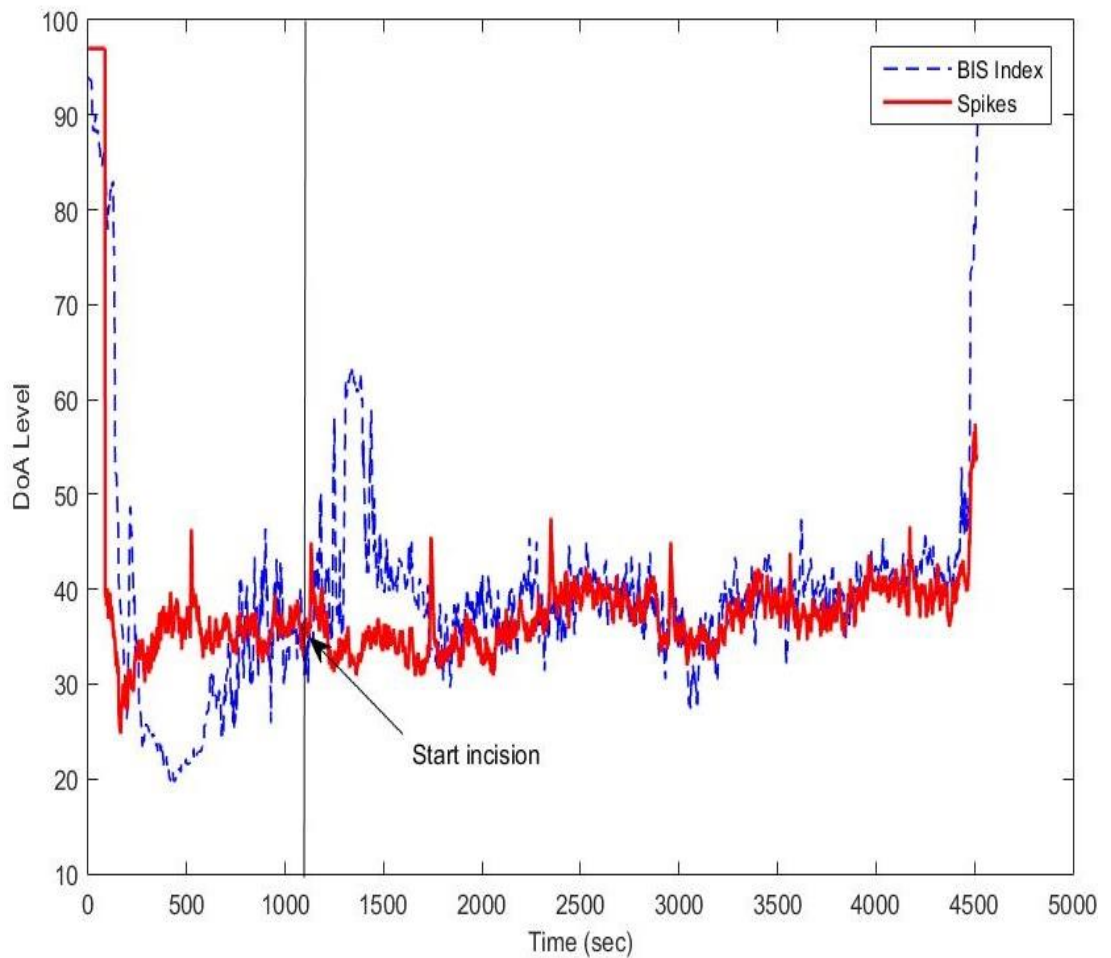


Figure 6-6. Comparison of the spike accumulation and the BIS index

Figure 6-6 shows a comparison between spike accumulation and the BIS index. It shows that the spike technique is able to detect different stages of anaesthesia levels. In addition, the spike accumulation and BIS index are able to give close results for DoA assessment. The spike accumulation is able to follow the BIS index pattern. The result also shows the spike accumulation response early compared to the BIS index. At around 1120 seconds the surgeon started the incision, the spike responded in real-time to the incision compared to the BIS index. Table 6-1 shows

the minimum, maximum, mean and standard deviation of the spike accumulation technique at different anaesthesia levels.

Table 6-1. Spike accumulation in different anaesthesia stage

	Minimum	Maximum	Mean	Std. Deviation
Awake	80.00	97.00	95.00	4.93
Moderate	60.05	64.91	62.67	1.66
General Anaesthesia	40.00	59.80	44.35	5.01
Deep Anaesthesia	20.01	40.00	33.96	4.86
Very Deep	17.30	19.99	19.02	0.72

The experiment also tested the EEG signal analysis using only the spike accumulation parameter. The result shows that the spike accumulation parameter gives a slightly different result compared to the BIS. Figure 6-7 shows the comparison of spike accumulation and the BIS index in patient number 6. In general, the spike accumulation is able to follow the BIS index pattern but, at around 200 seconds to 800 seconds the spike accumulation shows that the index is very different from the BIS. The BIS index dropped to deep anaesthesia level, on the other hand the spike accumulation is rising.

The experiment suggests that the spike accumulation parameter cannot be used to analyse the DoA by itself. The spike accumulation technique needs to combine with the maximum likelihood parameter and the probability density function parameters for DoA assessment.

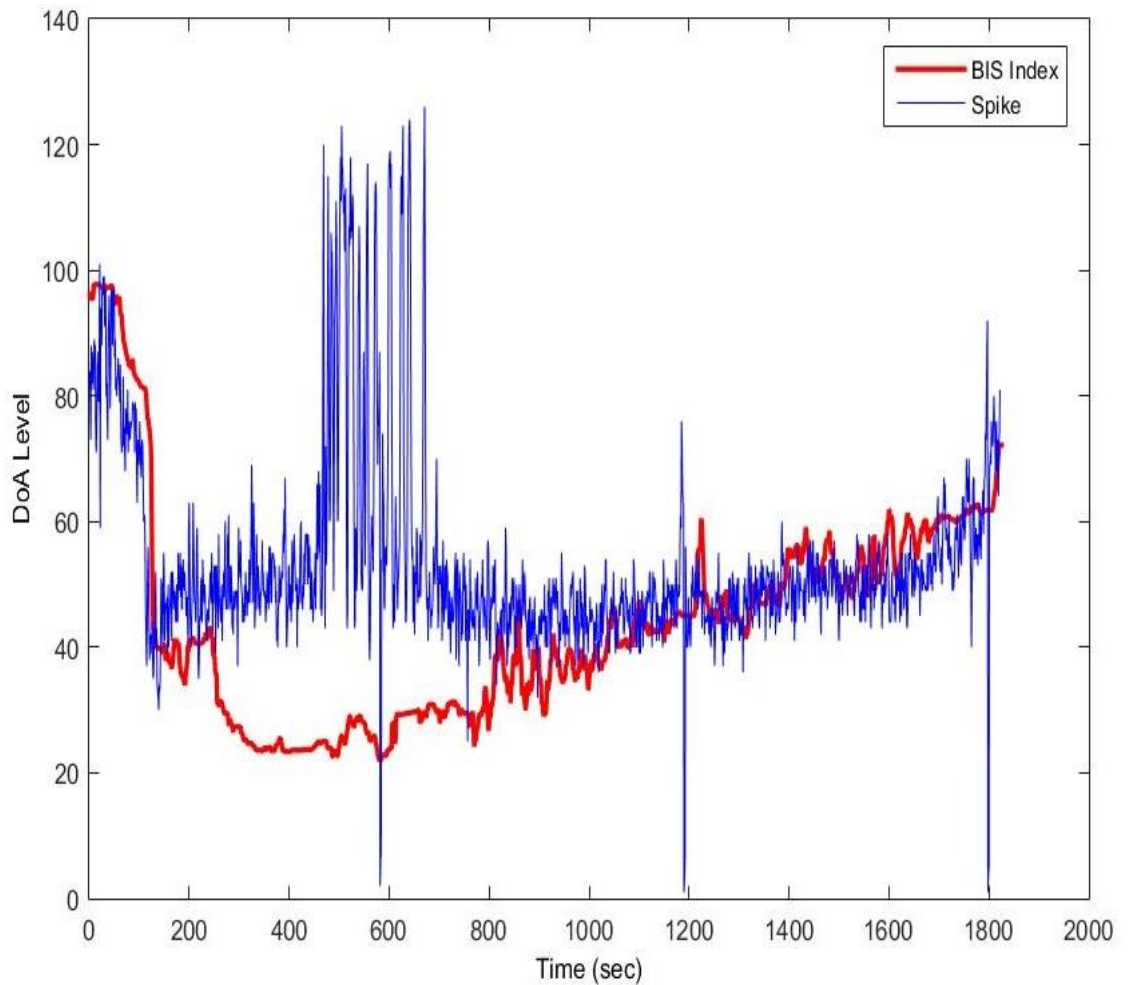


Figure 6-7. Comparison of spike accumulation and BIS index in patient number 6

6.4.2 Depth of anaesthesia using Bayesian technique

The new DoA index is the combination of the posterior Bayesian technique with BSA parameters and the Gaussian likelihood parameter. Figure 6-8 shows the comparison between the BIS index and the new DoA index. The EEG data used for simulation in Figure 6-8 is highly affected by the EMG signals. Figure 6-9 shows how the EMG signals affected the BIS index.

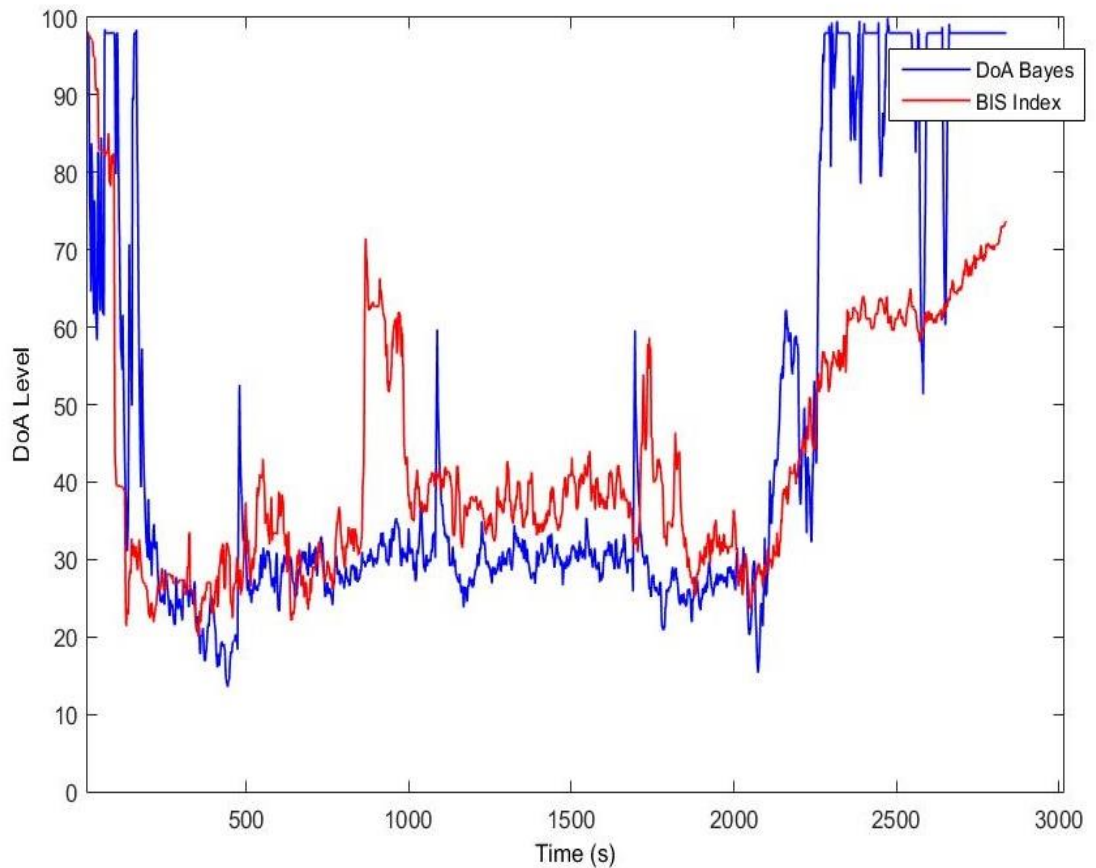


Figure 6-8. Comparison between BIS index and the DoA index based on Bayesian Gaussian distribution

The result in Figure 6-8 also shows that the new DoA index based on the Bayesian technique with the BSA parameters and the Gaussian likelihood parameter is not badly affected by the EMG signals. Figure 6-8 shows that the BIS index and the new DoA index trend look the same. As a comparison, Figure 6-9 shows the BIS index and the EMG signal. It indicates that the BIS pattern followed the EMG signal pattern. At around 865 second to 1008 second the BIS pattern looks the same as the EMG signal pattern. It is also indicated that the BIS index value is affected

by the EMG signal noise. Kelley (2012) reported that the BIS index value could be affected by EMG signals.

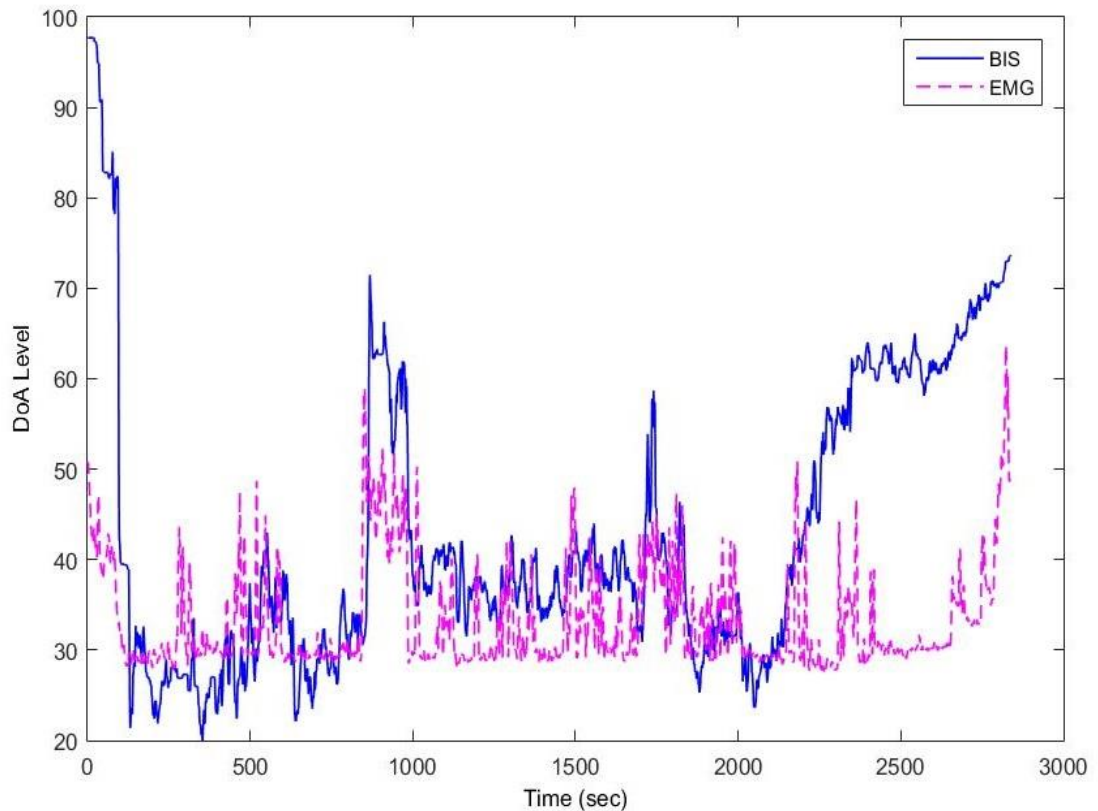
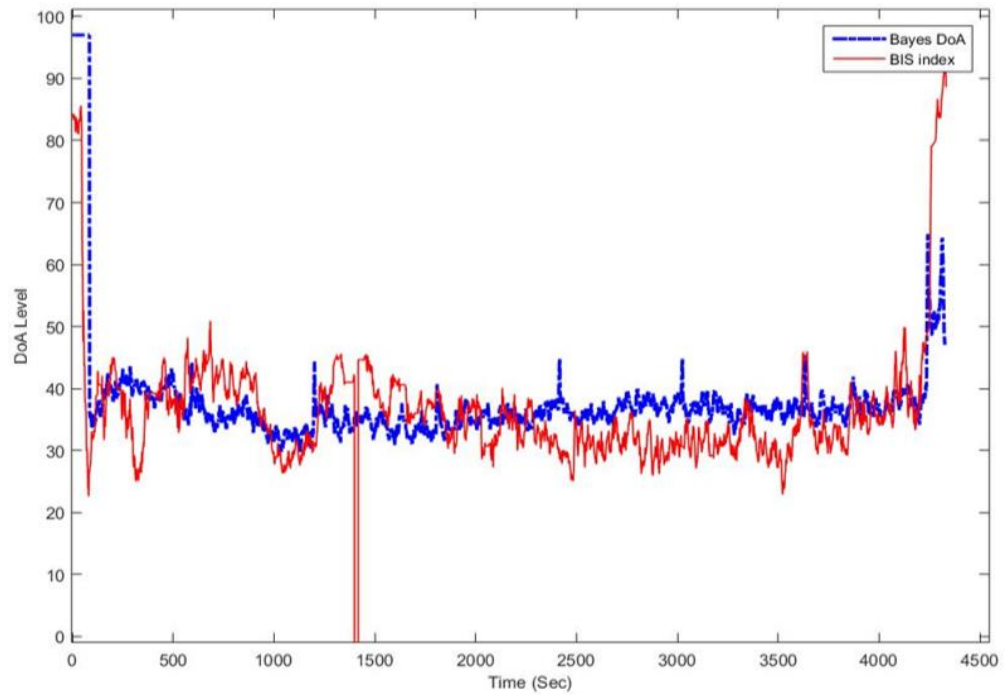
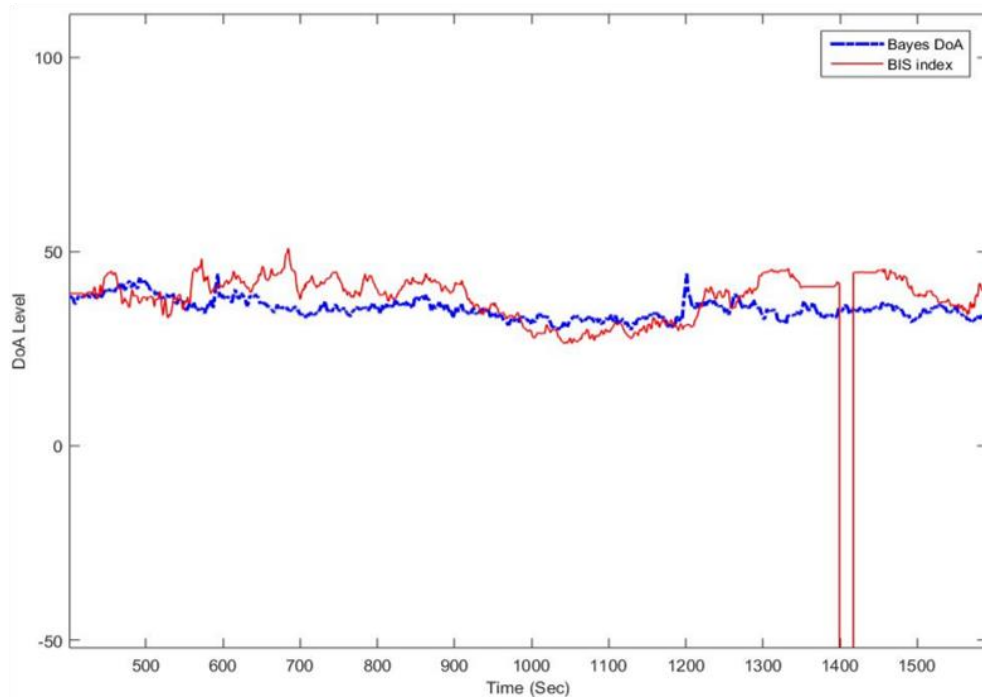


Figure 6-9. BIS index and the EMG signal

Figure 6-10a shows the comparison between the DoA based on Bayesian method (Bayes DoA) and the BIS index. It indicated that both Bayes DoA method and the BIS index are having a similar trend. However, in some point the BIS index value is drop and back-up again. On the other hand, DoA based on Bayesian is able to produce a valid DoA index. Figure 6-10 appears that the BIS index is unable to provide the DoA level for a period of time. Figure 6-10b is zoom-in of Figure 6-10a where the BIS did not produce any valid DoA value.



(a)



(b)

Figure 6-10 BIS index is unable to provide the DoA level. (a) Comparison between BIS and the DoA Bayes; (b) The section where BIS index is unable to produce the DoA level

The anaesthetist's records and observations are used to evaluate and validate the Bayes DoA result. The result is compared with the observation records to check the performance of the Bayes DoA. The data shown in Figure 6-11 was collected from patient number 19. Figure 6-11 shows the Bayes DoA, the BIS index and the arterial blood pressure from the same patient (systolic and diastolic).

In general, the arterial blood pressure increased when there are stimulations to the patient during the surgery (Gelb et al. 2009; Gul et al. 2015; Kazama et al. 1999; Momota et al. 2010). Figure 6-11 indicated that the blood pressure value is going up and then drop again. Systolic value is increasing from 115 mmHg to 135 mmHg during the stimulation.

The result in Figure 6-11 shows that the BIS index trend is relatively steady at 1000 seconds to 2500 seconds when the blood pressure increase. BIS index value is approximately 45 to 55 when the blood pressure increased. It indicates that the patient responded to the stimuli during the operation but the BIS index value did not show the changing response from the patient. On the other hand, the Bayes DoA indicates an increasing DoA level when patient's blood pressure is increasing. Bayes DoA value jump from approximately 50 to 70 in the time of stimulation. It is suggested that the Bayes DoA technique is able to detect the effect of stimulation on the patient. Therefore, the DoA index is able to identify the patient response during the operation.

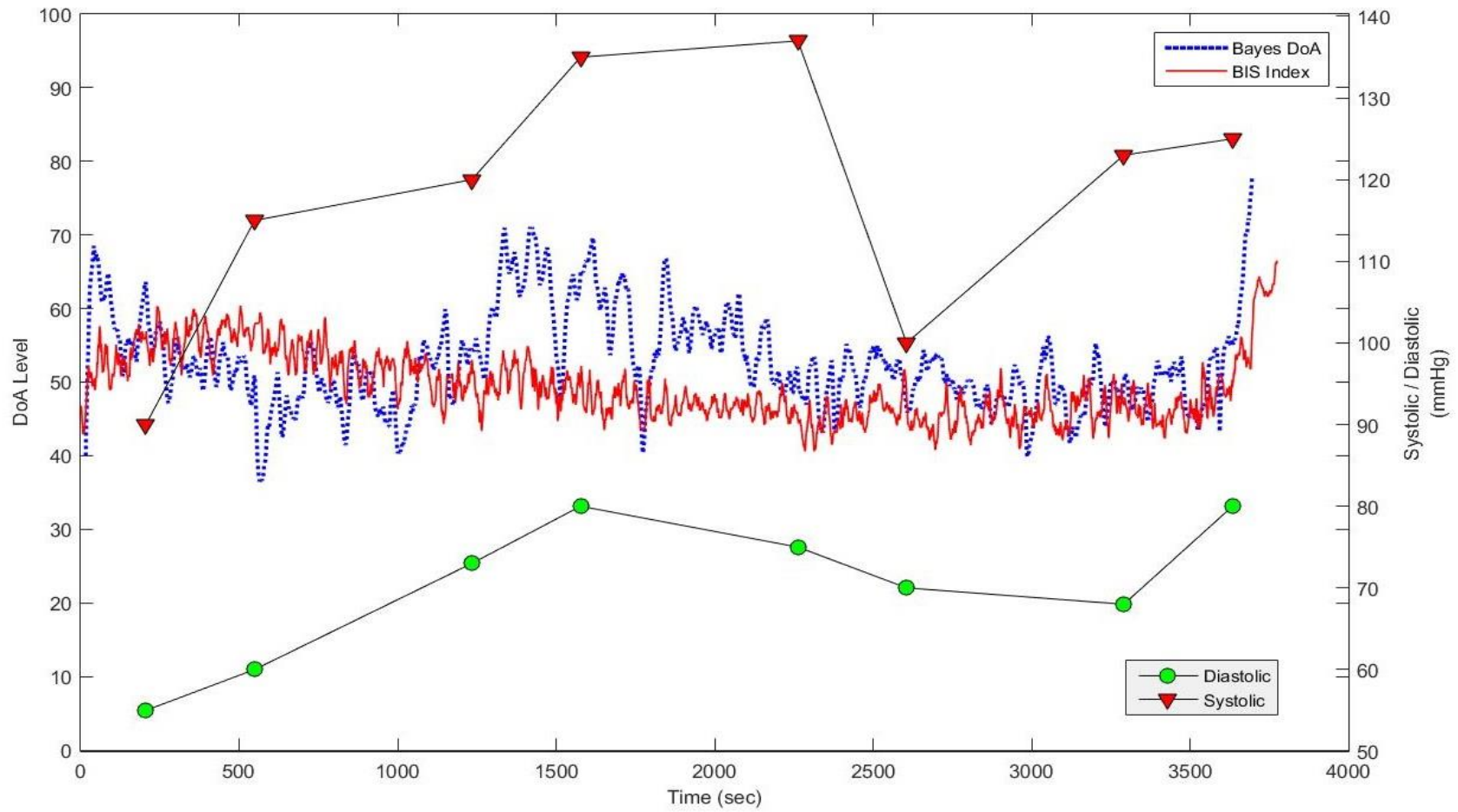


Figure 6-11. Patient's blood pressure and the comparison between the DoA Bayes and the BIS Index

6.5 Summary

This chapter introduced the EEG signal analysis in time domain. The EEG signal in time domain is divided into and analysed at every epoch (one epoch = 256 number of samples). Then, the EEG signal distribution is estimated in assuming the Gaussian distribution. In order to analyse the signal, a novel technique based on the Bayesian technique for extracting information from the EEG signal was presented.

The Bayesian spike accumulation technique was presented to extract the EEG signal information. The extracted information is used as parameters for DoA assessment. The DoA assessment introduced in this chapter employs the BSA parameter and density estimation parameter to calculate the DoA Bayes. The results show a close relationship between the estimation number of spikes in the signal and the effect of anaesthetic drugs.

7 ELECTROENCEPHALOGRAM SIGNAL ANALYSIS USING BAYESIAN APPROXIMATION WITH STUDENT- T DISTRIBUTION FOR DEPTH OF ANAESTHESIA MONITORING

This chapter introduces the depth of anaesthesia assessment method based on the EEG signal analysis using the Bayesian approximation with student-t distribution. The student-t distribution is able to improve the posterior even though there is an outlier in the distribution (Christmas 2014; Christmas & Everson 2011; Tipping & Lawrence 2005). The noises or outlier in the distribution can affect the depth of anaesthesia estimation. The depth of anaesthesia assessment is computed based on the posterior estimation on every epoch. The depth of anaesthesia value is derived from the maximum posterior density function.

7.1 Student-t distribution

Student-t distribution is formed by the Gaussian and Gamma distribution (Bishop 2006). Data analysis with the assumption Gaussian distribution is most likely

affected by the outlier (Bishop 2006; Christmas 2014; Tipping & Lawrence 2005). The posterior estimation based on Student-t distribution is not affected by the outlier compared with the Gaussian distribution. This advantage makes the student-t distribution more robust than the Gaussian. Figure 7-1 shows the robustness of the student-t distribution. The data shows the EEG sample with outlier. The outlier from the data affected the Gaussian distribution estimation and makes the Gaussian posterior lower than the Student-t distribution. The Student-t distribution maximised the probability estimation of the EEG data because it is less sensitive to the outlier (Bishop 2006).

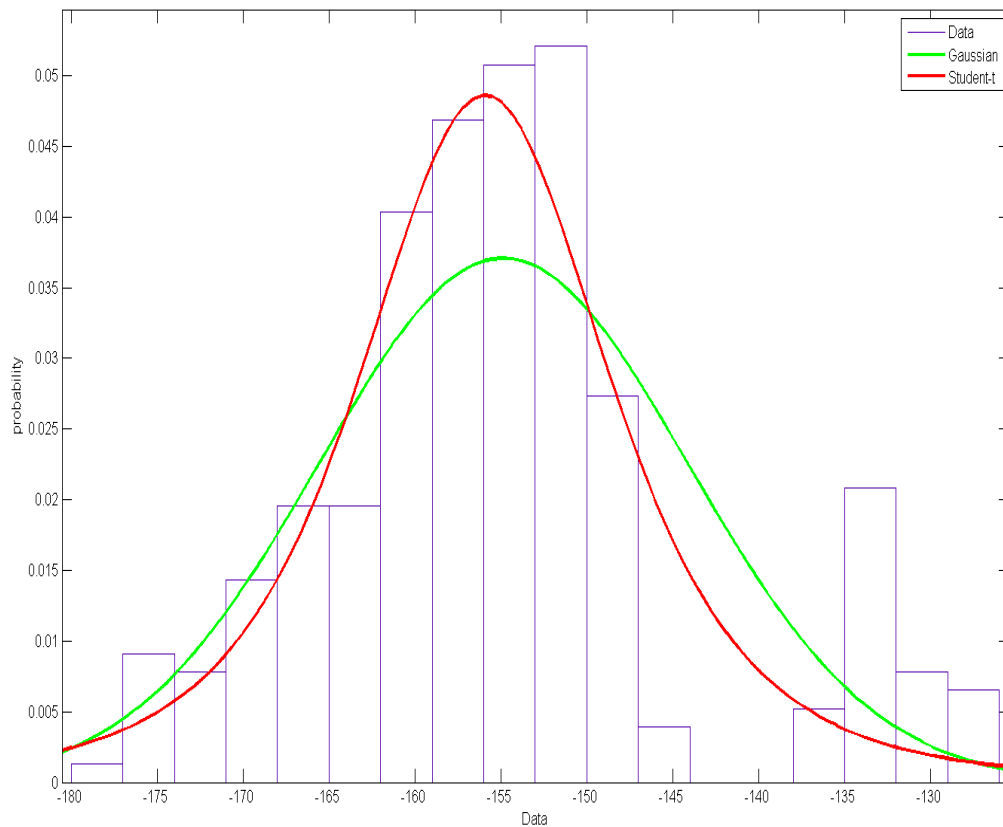


Figure 7-1. Data histogram shows the presence of outlier that can minimise the estimation. It is shows that the Student-t distribution can maximise the estimation

Suppose the EEG signal data in one epoch is $x = (x_1, x_2, \dots, x_n)$. The probability distribution of Student-t distribution P with ν degrees of freedom can be written as a fraction between standard normal random variable Y and the square root of Gamma random variable Γ .

$$P = \frac{Y}{\sqrt{\Gamma}} \quad 7-1$$

$$P(x|\nu) = S(x|\mu, \lambda, \nu) \quad 7-2$$

$$P(x|\nu) = \frac{\Gamma\left(\frac{\nu+1}{2}\right)}{\Gamma\left(\frac{\nu}{2}\right)} \left(\frac{1}{\pi\nu}\right)^{\frac{1}{2}} \frac{1}{\left(1 + \frac{x^2}{\nu}\right)^{\frac{\nu+1}{2}}} \quad 7-3$$

where ν is the degree of freedom, $\Gamma(\cdot)$ is the Gamma function, and P is the probability density function of the student-t distribution with data x . Student-t distribution is defined as a mixture of Gaussian $\mathcal{N}(x|\mu, \sigma^2)$ distribution and Gamma prior with a shared precision λ and mean μ (Bishop 2006; Christmas 2014). The precision λ is the inverse variance $\lambda = \frac{1}{\sigma^2}$. The probability density function of the Student-t can also be written as:

$$X(x|\mu, \lambda, \nu) \equiv \int_0^{\infty} \text{Normal}(x|\mu, (\lambda\eta)^{-1}) \text{Gamma}\left(\eta \middle| \frac{\nu}{2}, \frac{\nu}{2}\right) d\eta \quad 7-4$$

The likelihood function is estimated from the data x with parameter μ . The maximum likelihood estimation for one epoch of EEG data can be defined as:

$$p(x_i|\mu) = Student(x_i|\lambda, \mu) \quad 7-5$$

7.2 Depth of anaesthesia assessment using the student-t distribution

The depth of anaesthesia assessment based on the student-t distribution is derived from the density estimation of the EEG signal in every epoch. Density estimation of the student-t distribution is computed using Equation 7-3. The new DoA assessment based on the student-t distribution (nDoA Student) is calculated from the maximum value which is drawn from the posterior estimation. The depth of anaesthesia assessment is computed as follow:

$$S(x|\mu, \lambda, v) = \frac{\Gamma\left(\frac{v+1}{2}\right)}{\Gamma\left(\frac{v}{2}\right)} \left(\frac{1}{\pi v}\right)^{\frac{1}{2}} \frac{1}{\left(1 + \frac{x^2}{v}\right)^{\frac{v+1}{2}}} \quad 7-6$$

The Bayesian estimation is computed based on the parameter function from Equation 7-8 and the likelihood function in Equation 7-5. The posterior distribution can be defined based on the Bayesian theorem as below:

$$p(v|x) \propto p(x|v)p(v) \quad 7-7$$

$$DA = \max[p(v|x)] \quad 7-8$$

$$0 < DA < 1$$

7-9

The DA value is between 0 and 1. Value 0 represents the isoelectric or very deep anaesthesia and the value 1 represents the awake stage. The new depth of anaesthesia index is derived from the best fit line between BIS index and the nDoA student. The linear function of the new depth of anaesthesia assessment is defined as:

$$snDoA = 1.2e^2 \cdot DA + 6.4$$

7-10

Depth of anaesthesia is divided into five stages. Table 7-1 shows the anaesthesia stages and its corresponding values. Figure 7-2 shows the initial value of depth of anaesthesia assessment computed using Equation 7-9.

Table 7-1. Five stage depth of anaesthesia value

Anaesthesia stage	DA Value
Awake	$0.8 \leq DA \leq 1$
Light anaesthesia	$0.6 \leq DA < 0.8$
Moderate anaesthesia	$0.4 \leq DA < 0.6$
Deep anaesthesia	$0.2 \leq DA < 0.4$
Very deep anaesthesia	$0 \leq DA < 0.2$

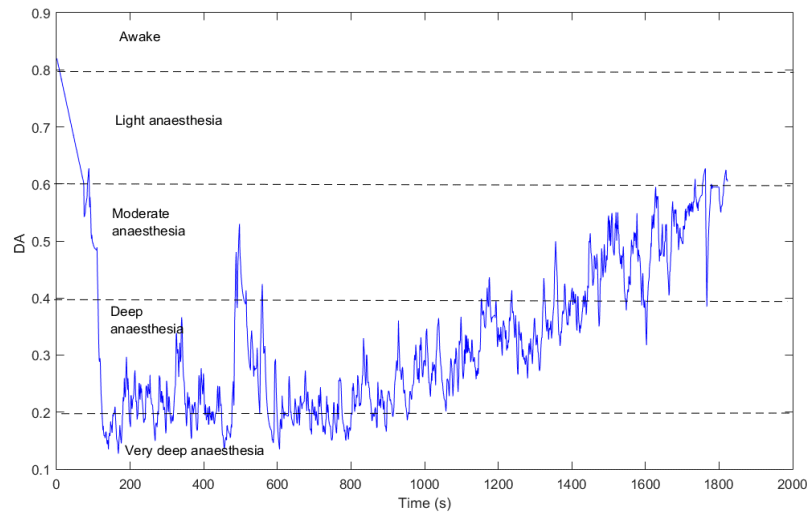


Figure 7-2. Posterior distribution value

7.3 Experimental results and analysis

Recorded data from 22 patients are used in this experiment. The patients were induced with the suitable amount of anaesthetic drugs, such as combination of midazolam, alfentanil or fentanyl, and propofol. Desflurane or sevoflurane in combination with Nitrous Oxide (N₂O) and oxygen are used for anaesthesia maintenance. Figure 7-3 shows the comparison of the BIS index, nDoA student and the DoA bayes. The red line is the BIS index value, green line is the nDoA student and the blue line is the DoA Bayes. Figure 7-3 shows that the DoA assessment using the student-t distribution and Gaussian distribution follows the BIS index trend. The DoA assessment based on the Student-t distribution is closer to the BIS index trend. Moreover, the result indicates that the nDoA student is more robust compared with the BIS index and the Bayes DoA. The nDoA student is faster in computation, responds quickly to the drug effect on the patients, and reduces the time delay in providing the index. At around 430 seconds, the patient received another 50 mg/kg propofol to maintain the anaesthesia. The effect of this drugs in the patient's central nervous system is reflected in the decreasing value of nDoA student index.

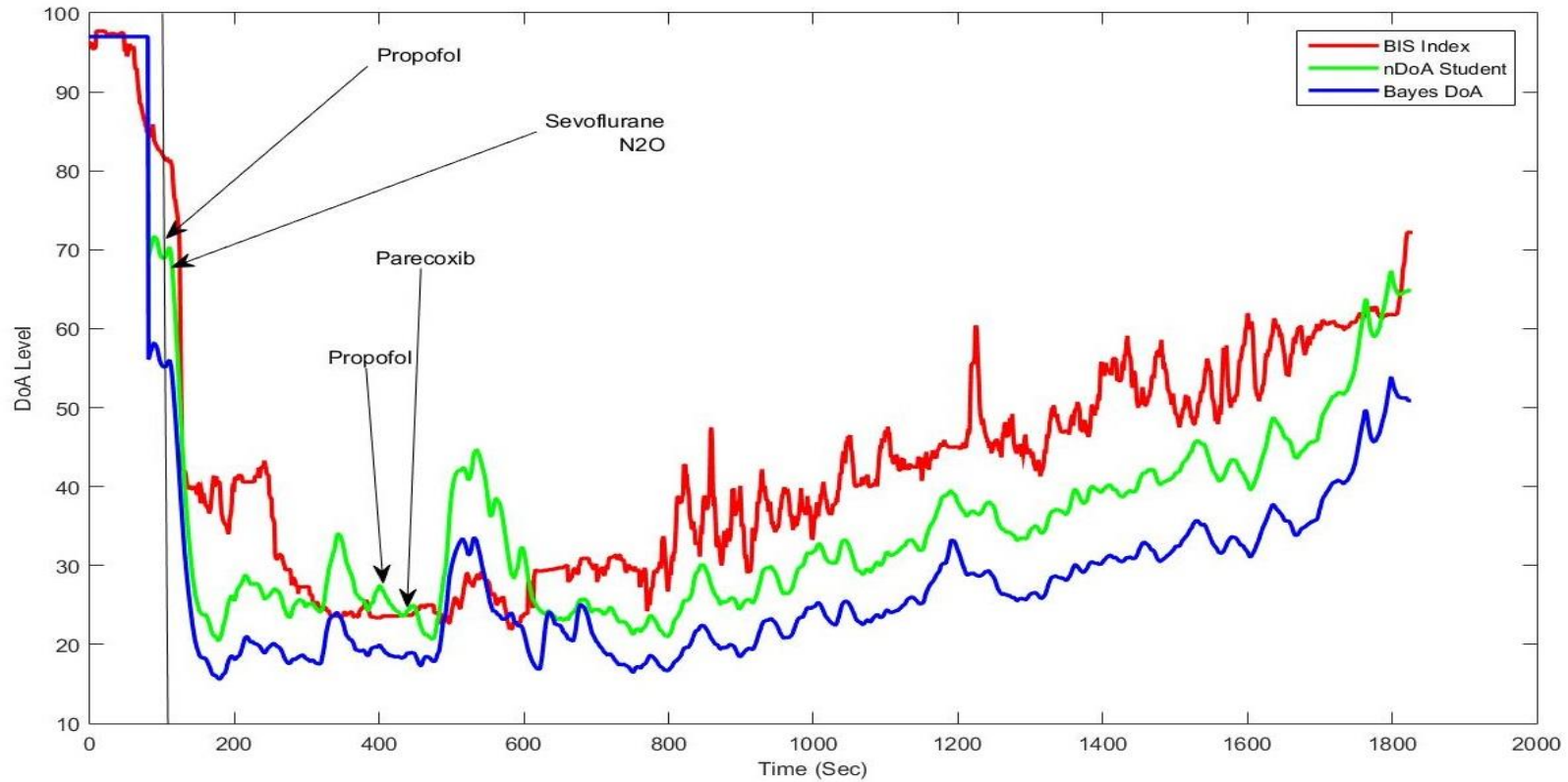


Figure 7-3. Comparison between BIS index, anaesthesia assessment using Student-t distribution and Gaussian distribution

The results in Figure 7-4 are based on the data of patient number 18. It shows the trend of the BIS index and the DoA assessment using student-t distribution. The nDoA student in Figure 7-4 is represented as a blue line and the BIS index is in a red. It shows that the nDoA student is able to follow the BIS index value. The correlation between the BIS index and the nDoA student is presented on Figure 7-5. Figure 7-5 shows a scatter plot with marginal histogram of the BIS index against the nDoA student. From the histogram and scatter plot we can see that both methods have a strong correlation.

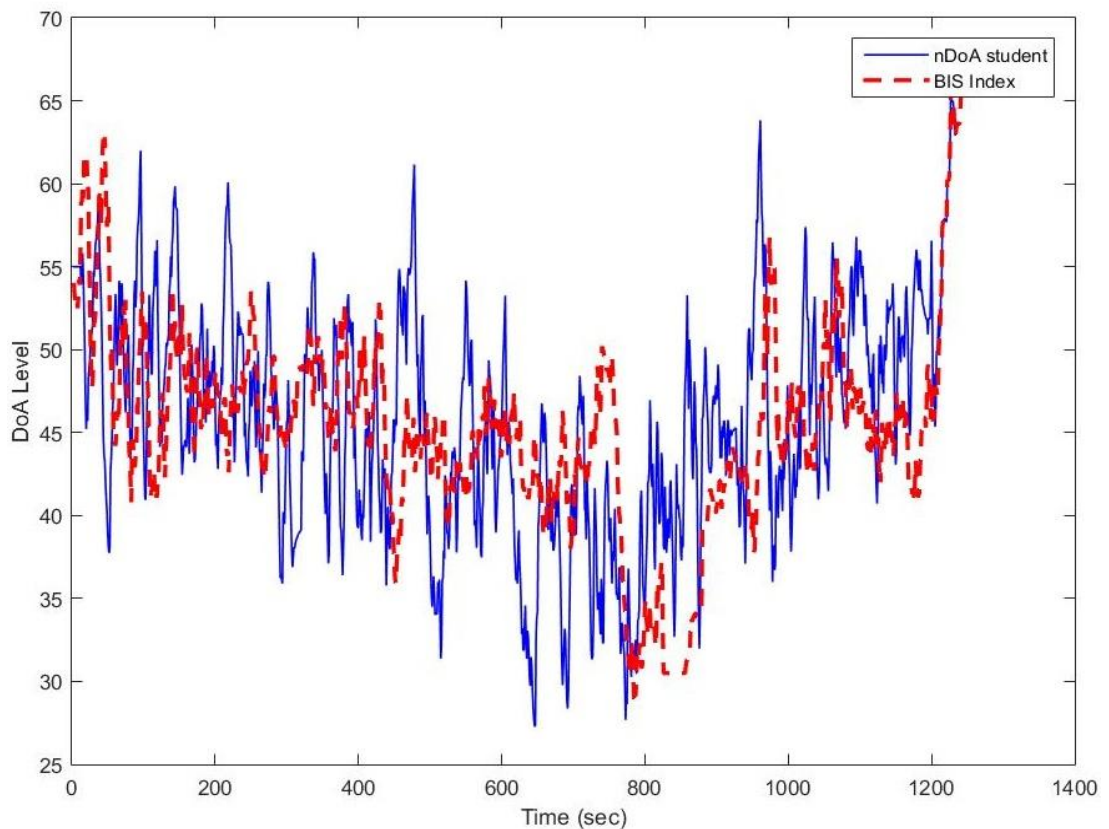


Figure 7-4. Comparison between new depths of anaesthesia based on student-t distribution and BIS index

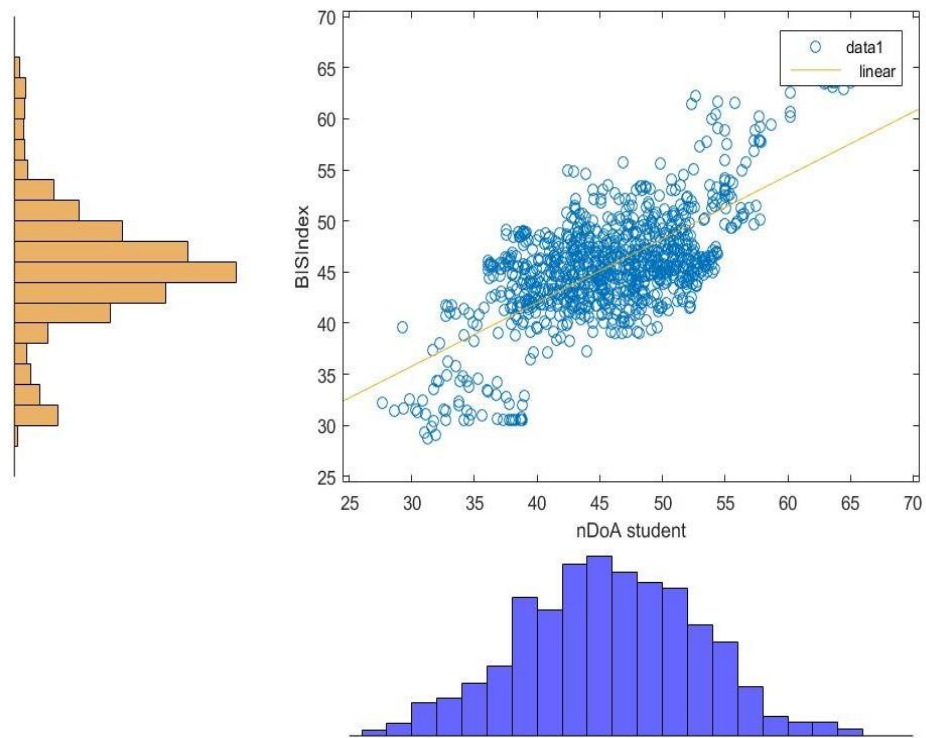


Figure 7-5. Scatter Plot with marginal histogram

The BIS index does not always give a valid DoA index value. There are number of cases where the BIS index fails to give the depth of anaesthesia values. Being unable to provide the depth of anaesthesia level can be dangerous because, in the modern operating room, the anaesthetic drug delivery to the patient is based on the DoA monitor and anaesthetist observation. The DoA monitor itself is a tool for the anaesthetist to justify patient's condition. Figure 7-6 shows that the BIS index failed to provide the DoA level. In Figure 7-6 (a), the BIS index is unable to provide the index for about 49 seconds. Figure 7-6 (b), shows the zoomed section of the Figure where the BIS index could not provide the number. On the other hand the nDoA student is able to provide the depth of anaesthesia level. This is a proof that the nDoA level is a robust in assessing the EEG signal for DoA assessment.

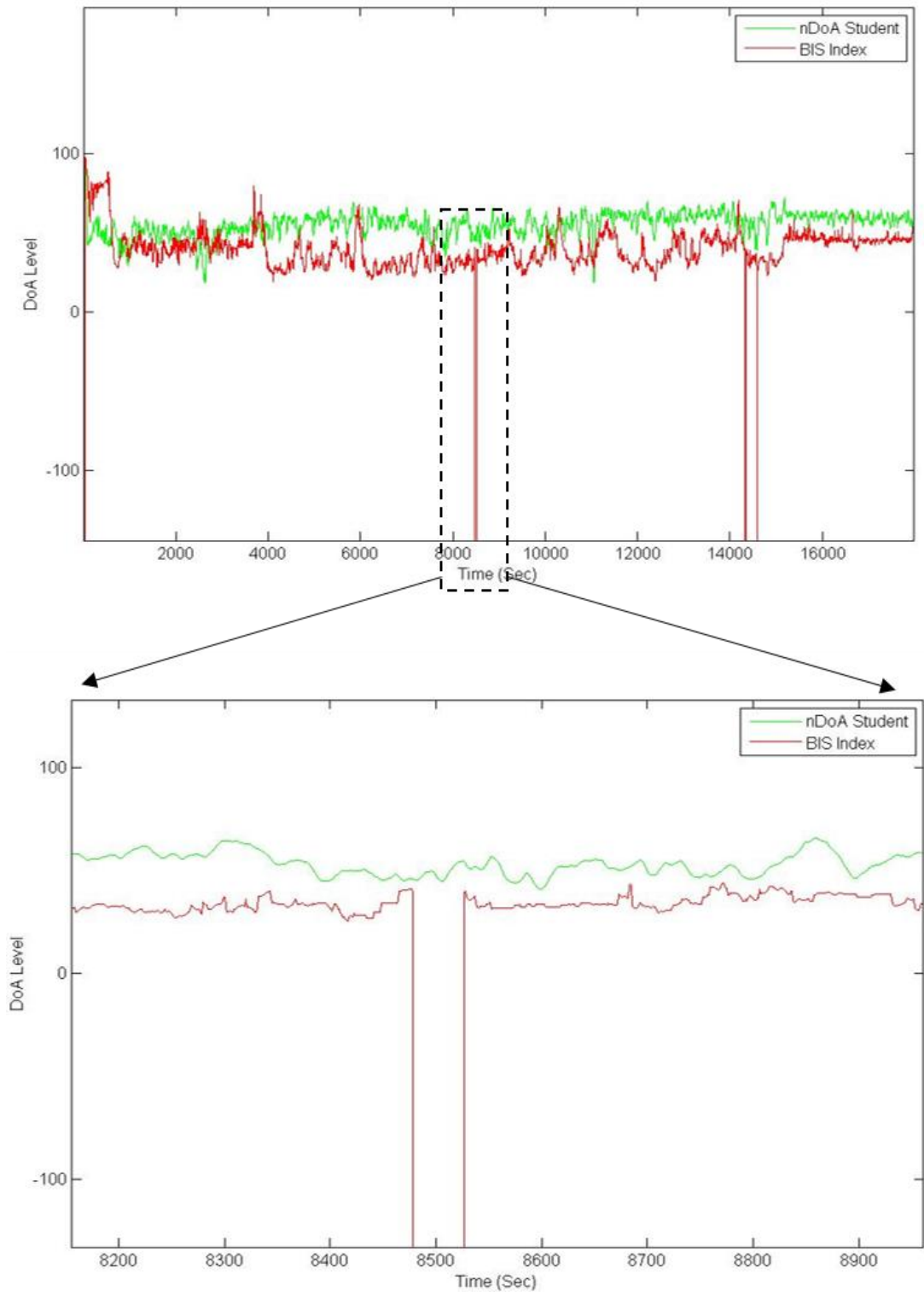


Figure 7-6. (a) BIS index is unable to provide the DoA level and the DoA based on the student-t distribution is able to give the DoA level. (b) Zoomed image of BIS index

The comparison of the DoA assessment between the BIS index and the nDoA student is depicted in Figure 7-7. The BIS index trend and the nDoA student trend are slightly different. For example, in around 1200 seconds the sevoflurane and the nitrous oxide were beginning to be administered to the patient. It was expected that after the hypnotic drugs are delivered to the patient, the DoA level would drop. However, in this case the BIS index level was increased. On the other hand, the nDoA student level is falling after the sevoflurane started to administer to the patient.

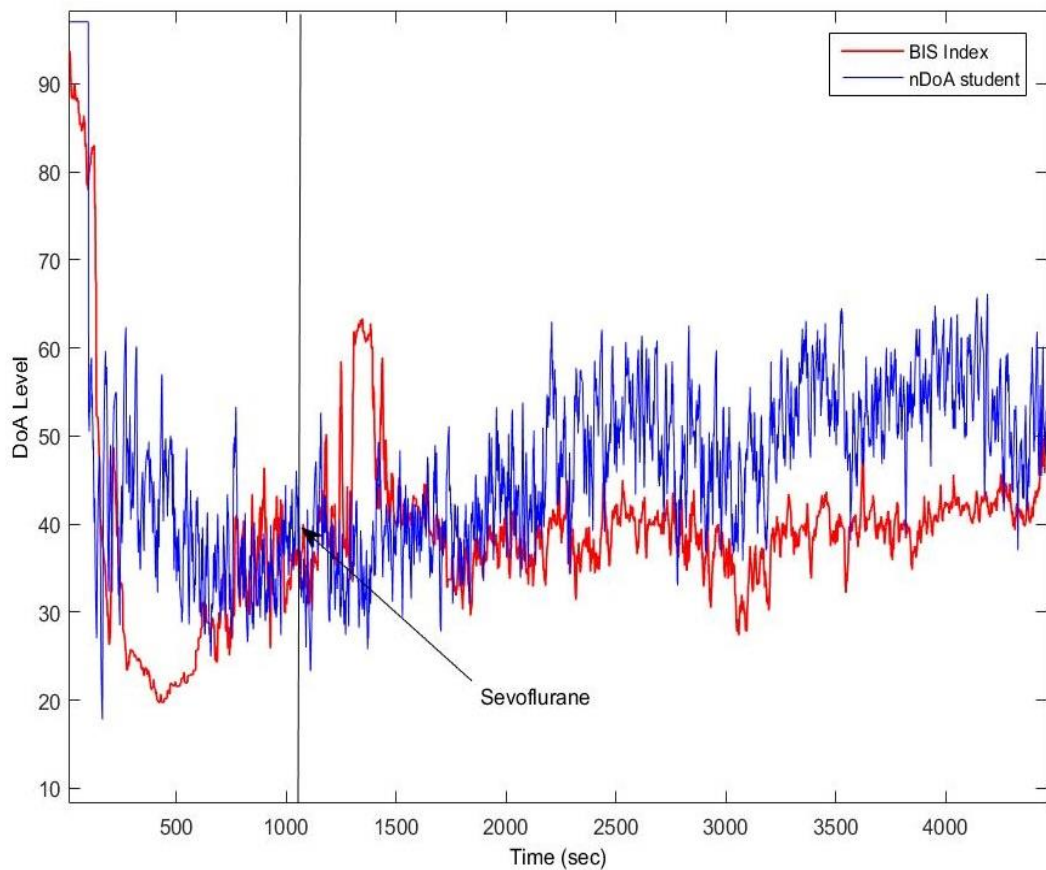


Figure 7-7. The Comparison between BIS and the nDoA

The nDoA student result is compared with the DoA based on BSA technique. The DoA results from both techniques show the same trend. However, the nDoA student is smoother compared to the DoA based on BSA technique. Figure 7-8

shows the comparison between the nDoA student and the Bayes DoA based on BSA technique. The blue line is the nDoA student and the red colour is the Bayes DoA based on BSA technique.

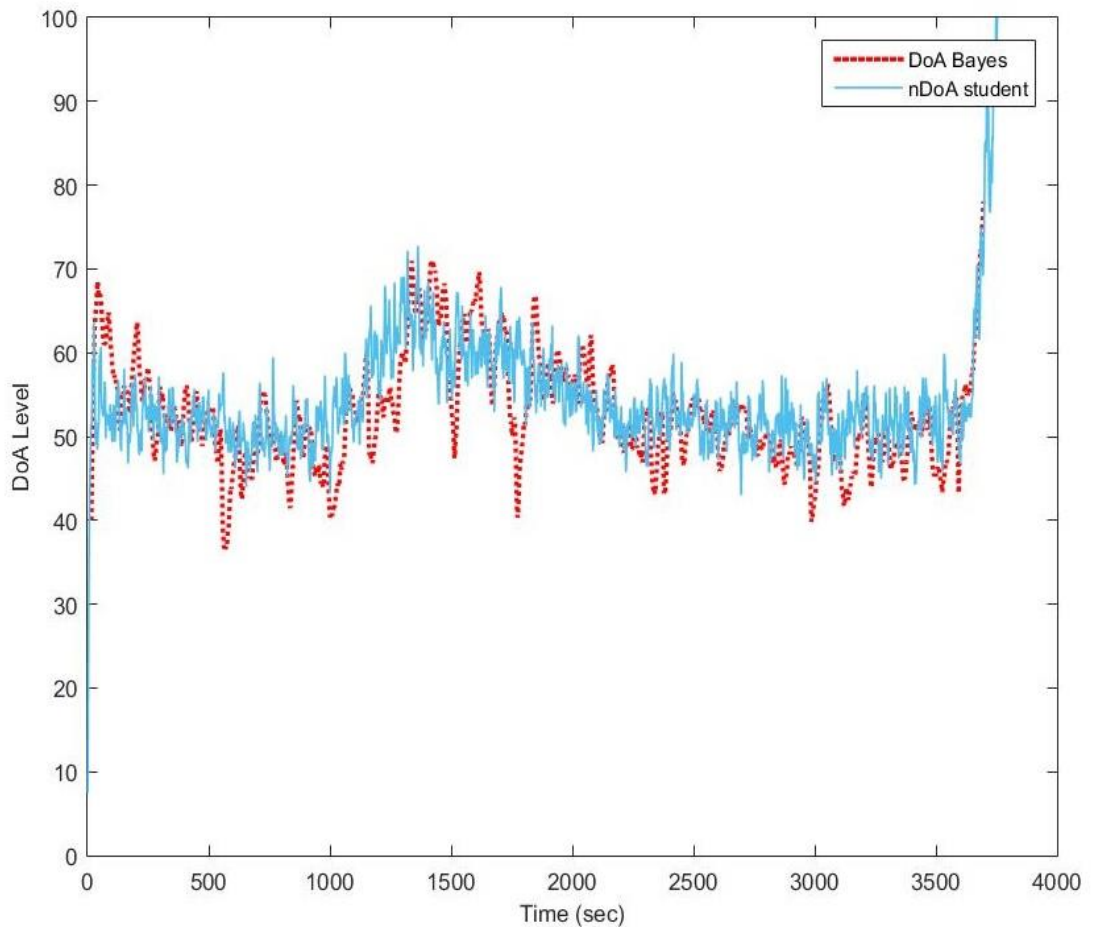


Figure 7-8. Comparison between nDoA student and the DoA Bayes based on BSA technique

One of the drawbacks of the BIS index is the time delay in index production. The DoA based on student-t distribution can produce an index faster than the BIS index. The transition time from conscious to unconscious is calculated to find the time delay of the BIS index. Figure 7-9 displayed the transition period from consciousness to

unconsciousness where the time delay for the BIS index is calculated. The data transition period of consciousness to unconsciousness from 21 patients is computed and then analysed using statistical analysis.

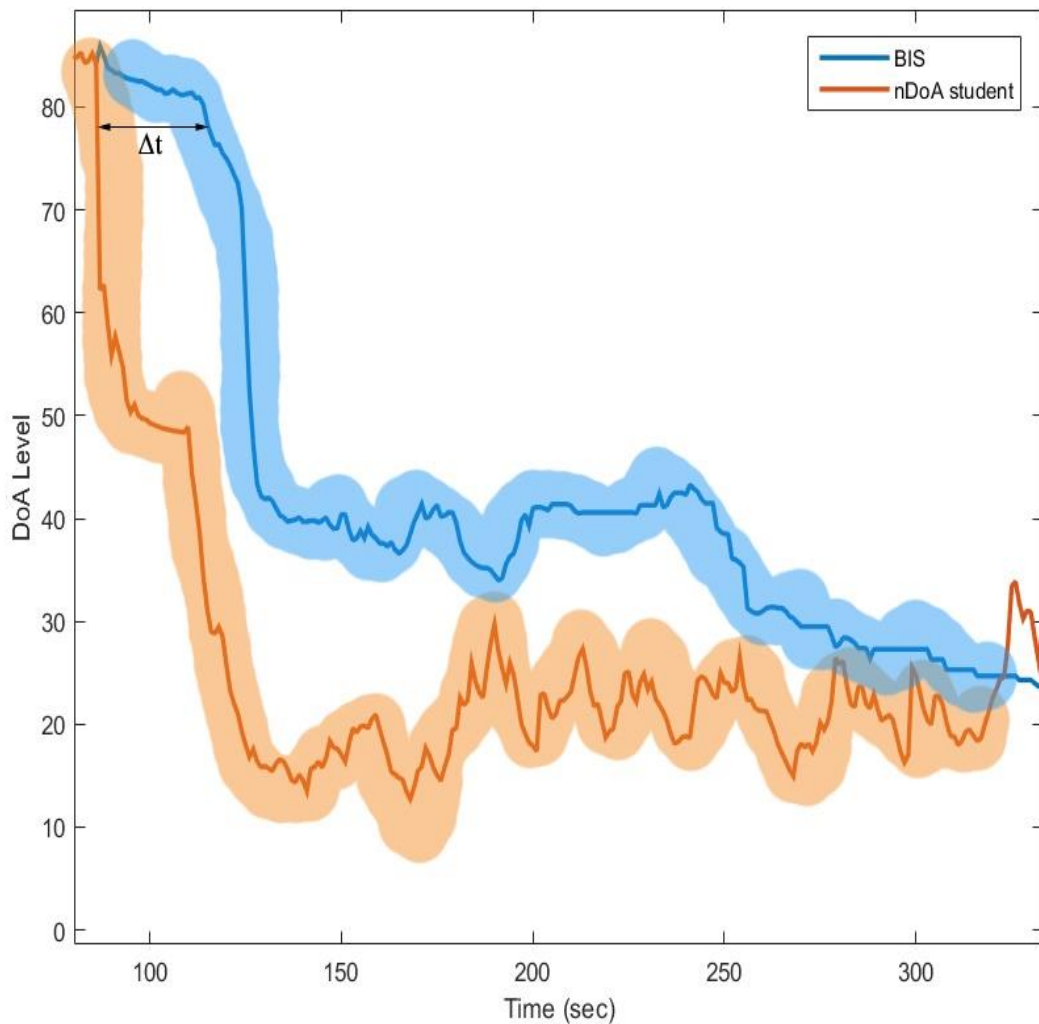


Figure 7-9. Transition period to calculate the time delay

The time delay is analysed in statistics. Data from 21 patients is analysed using the descriptive statistics test and the one-sample statistics test. The time delay data in bar chart from 21 patients is displayed in Figure 7-10. Table 7-2 shows the descriptive statistics of BIS index time delay. Statistical analysis indicates that the mean value of the time delay from the 21 patients is 41.41 seconds. The time delay

of around half of the sample is 36 seconds behind the nDoA student index. The standard deviation of the BIS time delay is 18.651 seconds. By using the M-estimator based on the Tukey's Biweight, the time delay of the BIS index is 33.40 seconds.

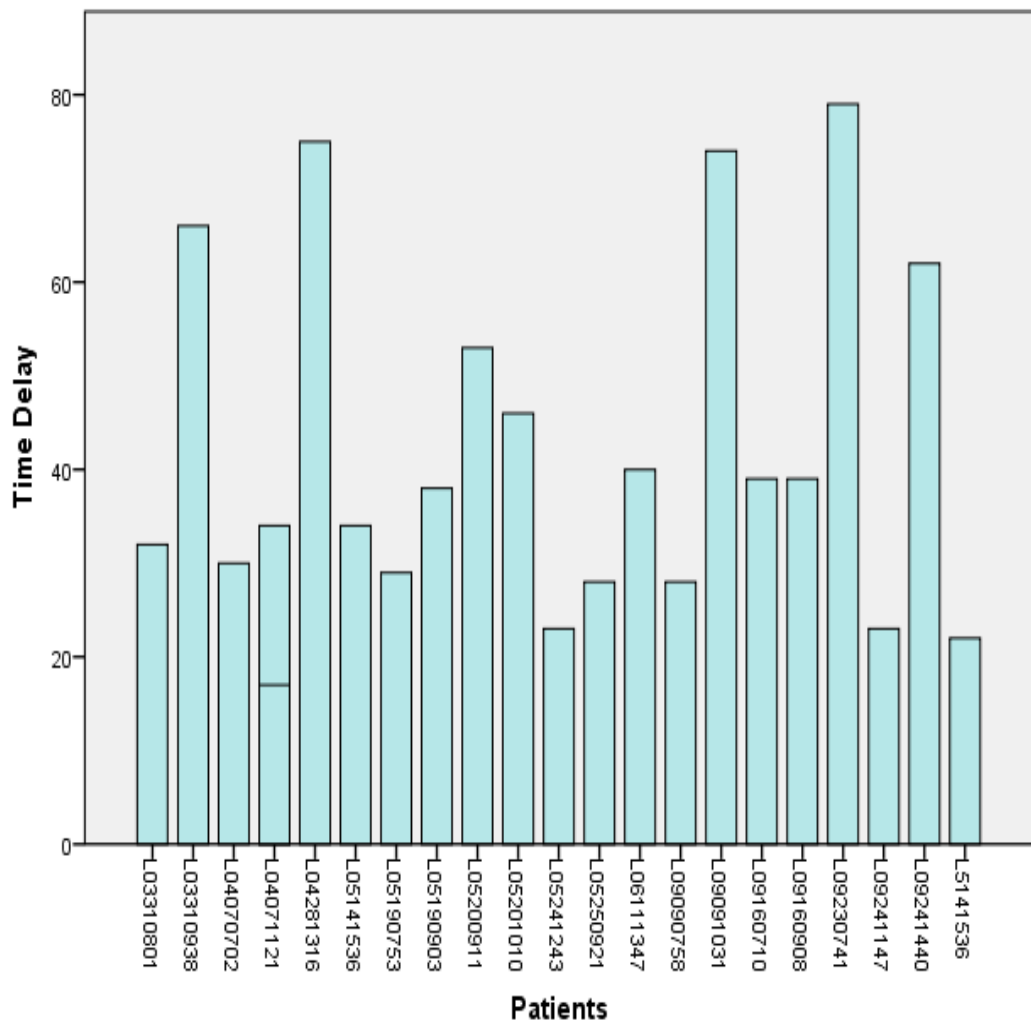


Figure 7-10. Time delay data from the patients

Table 7-2. Descriptive statistics of BIS index time delay

		Statistic	Std. Error	
Time Delay	Mean	41.41	3.976	
	95% Confidence Interval for Mean	Lower Bound		33.14
		Upper Bound		49.68
	5% Trimmed Mean	40.67		
	Median	36.00		
	Variance	347.872		
	Std. Deviation	18.651		
	Minimum	17		
	Maximum	79		
	Range	62		
	Interquartile Range	27		
	Skewness	.861		.491
	Kurtosis	-.438		.953

The time delay analysis results in this research are compared with the results from Zanner et al. (2009). Zanner et al. (2009) reported that time delay from awake to general anaesthesia stage was 25 seconds. A one-sample statistical test is used to compare the 25 seconds delay from Zanner with the result from the nDoA student-t. The time delay mean between the BIS index and nDoA student is compared with the time delay mean from Zanner et al. (2009). The BIS index average time delay from this research is 41.41 seconds. The test value from Zanner is 25 seconds, the result value from a One-Sample test is a 16.41 seconds difference with the time delay from our results. The One-Sample test revealed that the p-value is less than 0.005, which means that the time delay is significantly different between the BIS time delay from Zanner (2009) and our results. It is indicated the DoA based on Bayesian student-t distribution is faster in the computation and it is able to reduce time delay.

Table 7-3. One-Sample statistics test for BIS time delay

One-Sample Statistics

	N	Mean	Std. Deviation	Std. Error Mean
Time delay	22	41.41	18.651	3.976

One-Sample Test

	Test Value = 25					
	t	df	p-value	Mean Difference	95% Confidence Interval of the Difference	
					Lower	Upper
Time delay	4.127	21	.000	16.41	8.14	24.68

In order to examine the performance of the Bayesian Student-t distribution, the Blant-Alman graph is presented. Figure 7-11 shows differences between the BIS Index and Bayesian Student-t distribution against their mean and standard deviation. Figure 7-11(a) shows the correlation graph between the BIS Index and Bayesian Student-t. Figure 7-11 provides the Blant-Alman graph showing the mean standard deviation differences between the two methods. The mean standard deviation difference between the two methods is 3.1 with a 95% confident interval. This means that the two method have a similarity in assessing depth of anaesthesia.

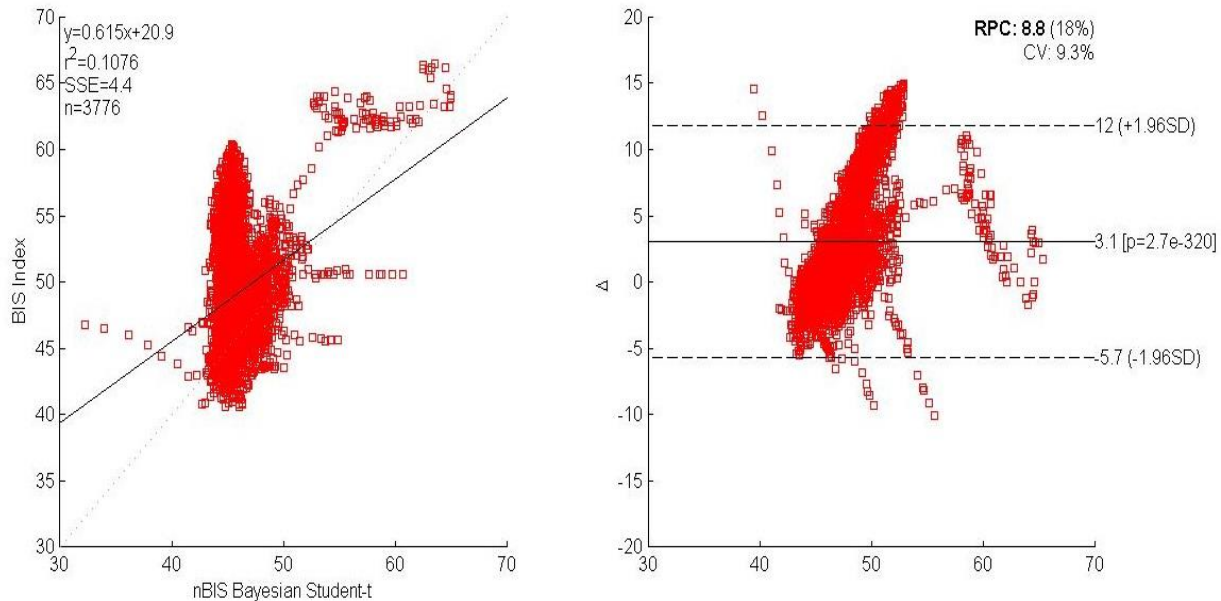


Figure 7-11. Correlation graph and Blant-Alman. (a) Correlation graph between BIS index and Bayesian Student-t. (b) Blant-Alman graph shows the mean standard deviation differences between the two methods

7.4 Summary

This chapter introduced the EEG signal extraction and analysis using the Bayesian Student-t distribution. The experiment in extracting information from the EEG signals revealed that the parameter extracted from the EEG signal using the student-t method has a higher density value than the Gaussian distribution. Then, the parameter is analysed for DoA assessment. The result shows that the Student-t distribution is able to detect the DoA level faster than the BIS index. In addition, the proposed method is a robust in detecting the pattern changes in EEG signals.

The Bayesian Student-t distribution introduced in this chapter is able to improve the computation, and the method can be applied to detect the depth of anaesthesia. The student-t distribution is able to maximise the estimation even though there is

an outlier present in the signal. The result is closely to the BIS value. In addition, the nDoA student is able to reduce the time delay in signal analysis. Therefore, the nDoA based on the student-t distribution can be used as an alternative to monitor DoA.

8 CONCLUSION AND FUTURE WORK

The focus of this research is to improve real time assessment of DoA through EEG signal analysis by developing new methods and algorithms. The challenges in this research are multi-fold. The first challenge is the EEG signal acquisition and conversion, the second is the pre-processing and filtering of EEG signal, the third is the extraction of the EEG signal features and parameters; and the last is the design and evaluation of DoA assessment index. All these challenges listed above have been investigated and addressed in this dissertation.

8.1 Primary work and contributions

Four methods are proposed and investigated to depth of anaesthesia assessment in this dissertation. The first contribution of this research is EEG signal filtering using the Bayesian adaptive LMS filter. This filtering method is applied to EEG signal processing to remove unwanted noise from the measured signals. Chapter 4 discussed the Bayesian adaptive LMS filter and frequency separation technique using the SWT.

The second contribution of this research is to apply the strong analytical signal analysis method based on the Hilbert transform to extract EEG signal features and to assess the DoA in real-time. The method uses the amplitude parameter and instantaneous phase parameter to analyse the EEG signal, as well as to determine the depth anaesthesia.

The third contribution of this research is to apply the Bayesian spike accumulation technique to extract the EEG signal features. The technique sums up the number of spikes appears on each epoch. The accumulation number of spikes is used as a parameter to represent the feature of the EEG signal. The results show that the Bayesian spike accumulation technique is able to extract EEG signal feature efficiently and to be used for DoA assessment.

The fourth contribution of this research is the DoA assessment based on the student-t distribution. In this method, the posterior estimation of the EEG signal is maximised using the Bayesian estimation based on student-t distribution compared to the Gaussian distribution. The proposed method based on student-t distribution is able to estimate the EEG signal and maximise the posterior distribution in DoA assessment. It is also able to detect the patient response and reduce the time delay from computation.

8.2 Outcomes and Conclusions

A novel filtering technique based on the Bayesian adaptive LMS is introduced in this dissertation to filter the EEG signals. The Bayesian adaptive LMS filter is an improved LMS one which is able to define filter weight step size of the adaptive LMS filter. The filter weight step size is computed on every epoch of the EEG signals. By choosing the right filter weight step size, a fast convergence in filter

adaptation can be reached. As a result of the Bayesian adaptive LMS filter, unwanted noise is removed from the EEG signals and clean EEG signal is obtained.

The results of the Bayesian adaptive LMS filtering process shows that the high frequency noise (EMG signal component) and low frequency noise (EOG signal component) have been removed from the EEG signal. Validations of the filtering process have been done using the spectrogram analysis, coherence estimation, cross correlation and the spectral analysis. The spectrogram and spectral analysis indicated that frequency component in the clean signals are correlated with the EEG signal frequency 0.5 – 60 Hz. The results show that the filtering process is able to remove noise and retain the EEG signal information.

After the filtering process, the EEG signal features are extracted and then analysed. The first method for extracting EEG signal features is called the strong analytical signal which is based on Hilbert transform. The method applies the time-frequency analyse techniques to extract the EEG signal feature and to carry out DoA assessment. The instantaneous amplitude and phase from the EEG signal are extracted from the EEG signal using the Hilbert transform. In addition, the amplitude detection technique is also used in the DoA assessment.

The results show that the DoA assessment based on analytical signal has improved the computational time and reduced the time delay. The new DoA assessment method is compared with the commercial BIS DoA monitor which has been used widely in hospitals around the world. The results indicate that the new DoA technique based on the analytical signal perform better than the BIS index in robust and in real-time aspects. In addition, the BIS index and the proposed method have shown a good correlation to each other. The correlation results show that more than 85% of the samples have an r-value of greater than 0.78 which indicates a positive correlation. Furthermore, the results are compared with the anaesthetist's documentation to check the anaesthetic drug response and time delay on the proposed method. The new DoA is less time delay to produce the index, it is

approximately 18 to 190 seconds ahead of the BIS index. The results prove that the new DoA based on strong analytical signal analysis performed well above the BIS index in real-time response.

The Bayesian spike accumulation technique is introduced to further improve the first method and to maximise the EEG features extraction. The Bayesian spike accumulation analyses the signals in time domain. The probability density estimation is based on the Gaussian distribution. The estimated number of spikes decreases as the anaesthetic drug effects on the patients increase.

The Bayesian posterior estimation is computed based on the spike accumulation parameter and the likelihood function of the EEG signals. The result shows that the outcome of the DoA assessment based on the Bayesian spike accumulation features is better than the BIS index. There is a less time delay in computation compared with the BIS index. The time delay of the BIS index is approximately 21 to 103 seconds compared with the Bayesian spike accumulation. The results also show that the Bayesian spike accumulation technique is able to provide the DoA level continuously in poor signal quality. Moreover, the proposed DoA method is not affected by the EMG signals and it is able to respond quickly to the anaesthetic drugs effect. The result of the DoA index based on Bayesian spike accumulation technique is validated with the anaesthetists notes and the BIS index monitor.

The third method introduced for extracting and analysis EEG signal is the Bayesian Student-t distribution. The student-t distribution is more robust compared to the Gaussian technique used in the previous method. The advantage of a student-t distribution is its ability to maximise the posterior estimation even though an outlier is present in the distribution. The experimental results have shown that the posterior estimation of student-t distribution is higher compared to the Gaussian distribution.

The result of the DoA assessment using the student-t distribution has shown a good correlation with the BIS index and it is able to overcome parts of the drawback of

the BIS index. The DoA assessment based on student-t distribution reduces the computation time and responds quicker to stimuli. The average time delay of the BIS is around 41 seconds. The results show the Bayesian student-t distribution is capable to detect the anaesthetic drug effect on the patients faster than the BIS index. The DoA monitoring based on Bayesian student-t distribution is also able to reduce the time delay on the computation.

Compared with the DoA index based on the Bayesian spike accumulation technique, the DoA based on student-t distribution is faster in detecting the changing pattern on the EEG signal. Furthermore, one of the problem in the BIS index monitor is not able to provide the index continuously. This problem can be overcome by using the Bayesian based technique. The BSA and Bayesian student-t distribution are able to provide the index continuously compared with the BIS index. The DoA assessment based on student-t distribution can be used as an alternative for DoA monitoring.

The performance of the three features extraction and DoA assessment technique are depicted in Table 8-1. The computation has been performed using a Quad Core computer with 2.70 GHz (turbo 3.20 GHz), 8 GB RAM, and 64 bit Windows operating system. The time delay is calculated by computing the time difference between BIS and the DoA assessment techniques. The performance of each technique and the time delay difference from the BIS index show that the Bayesian Student-t distribution is more robust compared with the other DoA assessments. Feature extraction and DoA assessment based on Student-t distribution are able to improve the computation time and performed well during surgical conditions. Therefore, the Student-t distribution is the best technique for DoA assessment compared to the strong analytical signal and Bayesian spike accumulation technique.

Table 8-1. Comparisons of DoA assessment methods and performance

Feature extraction and DoA assessment technique	Performance	Time Delay (Sec)
Strong analytical signal	<ul style="list-style-type: none"> • Less computation time • Parameters can be extracted from time domain EEG signal. 	18 – 190
Bayesian spike accumulation	<ul style="list-style-type: none"> • EEG signals are analysed without converting to frequency domain • It is able to compensate the noises in the signals • It is able to provide DoA index even in a poor signal condition • Respond well in real time to anaesthetic drug effect compared with BIS index. 	21 - 103
Bayesian Student-t distribution	<ul style="list-style-type: none"> • Respond well to stimuli during a surgery • The technique is faster in detecting the anaesthetic drug effect • The technique is able to provide an index continuously • It is faster in detecting the changing pattern on the EEG signals 	17 - 79

8.3 Future work

The BSA technique introduced in this research can be further improved especially for detecting the deep anaesthesia levels. Furthermore, future research based on BSA technique can be done by focussing on the effects of the decreasing number

of spike in the EEG signal as the anaesthesia levels changing from awake to deep anaesthesia.

The BSA and Bayesian student-t distribution can be combined for the future research in the DoA monitoring. The experiments from this research can be extend for the future research by finding the drug effects on the patients by using the BSA and the Bayesian student-t distribution technique. This research can be further improved by including more bio-physical parameters. Parameters that could be included in the future research are the mean arterial blood pressure, pharmacokinetics and pharmacodynamics of the drugs, and the percentage of the saturated oxygen in the blood. With the additional parameter, it will improve the DoA monitoring system and will be able to predict patient condition in advance.

Another work that can be done in the future is the application of the DoA technique introduced in this dissertation for a hardware implementation and hospital trial. The DoA assessment techniques introduced in this dissertation can be used alongside anaesthetic monitoring systems in hospitals for further improvement in DoA monitoring.

References

Ahirwal, MK, Kumar, A & Singh, GK 2014, 'Adaptive filtering of EEG/ERP through noise cancellers using an improved PSO algorithm', *Swarm and Evolutionary Computation*, vol. 14, no. 0, pp. 76-91.

Alkire, MT 1998, 'Quantitative EEG Correlations with Brain Glucose Metabolic Rate during Anesthesia in Volunteers', *Anesthesiology*, vol. 89, no. 2, pp. 323-33.

Alkire, MT, Hudetz, AG & Tononi, G 2008, 'Consciousness and Anesthesia', *Science*, vol. 322.

ANZCA 2009, *Safety on Anaesthesia: A review of anaesthesia - related mortality reporting in Australia and New Zealand*, Australian and New Zealand college of anaesthetists (ANZCA), Australia .

Aspect Medical System, I 2009, *BIS VIEW Monitoring System, Service Information Manual*, USA.

Aspect Medical Systems 2009, *BIS Vista Monitoring System*, USA.

Avidan, MS, Zhang, L, Burnside, BA, Finkel, KJ, Searleman, AC, Selvidge, JA, Saager, L, Turner, MS, Rao, S, Bottros, M, Hantler, C, Jacobsohn, E & Evers, AS 2008, 'Anesthesia Awareness and the Bispectral Index', *New England Journal of Medicine*, vol. 358, no. 11, pp. 1097-108.

Bard, JW 2001, 'The BIS Monitor: A review and technology assessment', *American Association of Nurse Anesthetists*, vol. 69, no. 6, pp. 477-83.

- Beecher, HK 1947, 'Anesthesia's Second Power: Probing the Mind', *Science*, vol. 105, no. 2720, pp. 164-6,.
- Bender, R, Schultz, B & Grouven, U 1993, *Classification of EEG signals into general stages of anesthesia in real-time using autoregressive models*, Springer.
- Bennett, C, Voss, LJ, Barnard, JPM & Sleight, JW 2009, 'Practical Use of the Raw Electroencephalogram Waveform During General Anesthesia: The Art and Science', *Anesthesia & Analgesia*, vol. 109, no. 2, pp. 539-50.
- Bischoff, P, Kochs, E & Schulte am Esch, J 1994, "Paradoxical Arousal" During Isoflurane/Nitrous Oxide Anesthesia: Quantitative Topographical EEG Analysis', in J Schulte am Esch & E Kochs (eds), *Central Nervous System Monitoring in Anesthesia and Intensive Care*, Springer Berlin Heidelberg, ch 8, pp. 91-102.
- Bischoff, P, Schmidt, GN & Schulte am Esch, J 2000, 'Assessment of depth of anaesthesia', *Best Practice & Research Clinical Anaesthesiology*, vol. 14, no. 2, pp. 321-34.
- Bischoff, P, Kochs, E, Haferkorn, D & am Esch, JS 1996, 'Intraoperative EEG changes in relation to the surgical procedure during isoflurane-nitrous oxide anesthesia: Hysterectomy versus mastectomy', *Journal of Clinical Anesthesia*, vol. 8, no. 1, pp. 36-43.
- Bishop, CM 2006, *Pattern recognition and machine learning*, Springer, New York, USA.
- Biswas, R, Khamaru, K & Majumdar, KK 2014, 'A Peak Synchronization Measure for Multiple Signals', *Signal Processing, IEEE Transactions on*, vol. 62, no. 17, pp. 4390-8.
- Bowdle, TA 2006, 'Depth of anesthesia monitoring ', *Anesthesiology Clinics*, vol. 24, no. 06, pp. 793-822.
- Brambrink, AM, Evers, AS, Avidan, MS, Farber, NB, Smith, DJ, Martin, LD, Dissen, GA, Creeley, CE & Olney, JW 2012, 'Ketamine-induced neuroapoptosis in the fetal and neonatal rhesus macaque brain', *Anesthesiology*, vol. 116, no. 2, pp. 372-84.

- Brandon Westover, M, Shafi, MM, Ching, S, Chemali, JJ, Purdon, PL, Cash, SS & Brown, EN 2013, 'Real-time segmentation of burst suppression patterns in critical care EEG monitoring', *Journal of Neuroscience Methods*, vol. 219, no. 1, pp. 131-41.
- Braz, LG, Braz, DG, Cruz, DSd, Fernandes, LA, Módolo, NSP & Braz, JRC 2009, 'Mortality in anesthesia: a systematic review', *Clinics*, vol. 64, pp. 999-1006.
- Broek, PLCvd 2003, *Monitoring anesthetic depth: modification, evaluation, and application of the correlation dimension*, [Nijmegen]: Nijmegen University Press.
- Brown, EN, Lydic, R & Schiff, ND 2010, 'General Anesthesia, Sleep, and Coma', *New England Journal of Medicine*, vol. 363, no. 27, pp. 2638-50.
- Bruhn, J, Myles, PS, Sneyd, R & Struys, MMRF 2006, 'Depth of anaesthesia monitoring: what's available, what's validated and what's next?', *British Journal of Anaesthesia*, vol. 97, no. 1, pp. 85-94.
- Castro, A, Almeida, FG, Amorim, P & Nunes, CS 2009, 'A wavelet based method for steady-state detection in anesthesia', Minneapolis, MN, pp. 954-7.
- Christmas, J 2013, 'The effect of missing data on robust Bayesian spectral analysis', in *Machine Learning for Signal Processing (MLSP), 2013 IEEE International Workshop on: proceedings of the Machine Learning for Signal Processing (MLSP), 2013 IEEE International Workshop on* pp. 1-6.
- Christmas, J 2014, 'Bayesian Spectral Analysis with Student-t Noise', *IEEE Transactions on Signal Processing*, vol. 62, no. 11, p. 8.
- Christmas, J & Everson, R 2011, 'Robust Autoregression: Student-t Innovations Using Variational Bayes', *Signal Processing, IEEE Transactions on*, vol. 59, no. 1, pp. 48-57.
- Cooper, GF & Herskovits, E 1992, 'A Bayesian Method for the Induction of Probabilistic Networks from Data', *Machine Learning*, vol. 9, pp. 309-47.

- Dahlhaus, R 2000, 'A likelihood approximation for locally stationary processes', *Annals of Statistics*, vol. 28, no. 6, pp. 1762-94.
- Donoho, DL 1995, 'De-noising by soft-thresholding', *Information Theory, IEEE Transactions on*, vol. 41, no. 3, pp. 613-27, <10.1109/18.382009>.
- Dubois, M, Savege, TM, O'Carroll, TM & Frank, M 1978, 'General anaesthesia and changes on the cerebral function monitor*', *Anaesthesia*, vol. 33, no. 2, pp. 157-64.
- Dutt, A, Joad, AK & Sharma, M 2012, 'Induction for classic laryngeal mask airway insertion: Does low-dose fentanyl work?', *Journal of anaesthesiology, clinical pharmacology*, vol. 28, no. 2, p. 210.
- Ekman, A, Lindholm, ML, Lennmarken, C & Sandin, R 2004, 'Reduction in the incidence of awareness using BIS monitoring', *Acta Anaesthesiologica Scandinavica*, vol. 48, no. 1, pp. 20-6.
- Ellerkmann, RK, Soehle, M, Alves, TM, Liermann, V-M, Wenningmann, I, Roepcke, H, Kreuer, S, Hoefl, A & Bruhn, J 2006, 'Spectral Entropy and Bispectral Index as Measures of the Electroencephalographic Effects of Propofol', *Anesthesia & Analgesia*, vol. 102, no. 5, pp. 1456-62.
- Fienberg, SE 2006, 'When did Bayesian Inference become "Bayesian"?', *Bayesian Analysis*, vol. 1, no. 1, pp. 1-40.
- Fontanet, J, Gabarrón, E, Jospin, M, Vallverdú, M, Gambus, PL & Jensen, EW 2014, 'Comparison of the qNOX and ANI indices of nociception during propofol and remifentanyl anaesthesia', in *8th Conference of the European Study Group on Cardiovascular Oscillations (ESGCO 2014): proceedings of the 8th Conference of the European Study Group on Cardiovascular Oscillations (ESGCO 2014) Trento, Italy*.
- Foo, JYA 2006, 'Comparison of wavelet transformation and adaptive filtering in restoring artefact-induced time-related measurement', *Biomedical Signal Processing and Control*, vol. 1, no. 1, pp. 93-8.
- Franks, NP 2008, 'General anaesthesia: from molecular targets to neuronal pathways of sleep and arousal', *Nat Rev Neurosci*, vol. 9, no. 5, pp. 370-86.

Franks, NP & Zecharia, AY 2011, 'Sleep and general anesthesia', *Canadian Journal of Anesthesia/Journal canadien d'anesthésie*, vol. 58, no. 2, pp. 139-48.

Frey, R 2007-2011, *Bispectral Index*, Advameg Inc.

Freye, E 2005, *Cerebral Monitoring in the OR and ICU*, Springer, Netherlands.

Freye, E & Levy, JV 2005, 'Cerebral monitoring in the operating room and the intensive care unit: An introductory for the clinician and a guide for the novice wanting to open a window to the brain', *Journal of Clinical Monitoring and Computing*, vol. 19, no. 1-2, pp. 1-76.

Gelb, AW, Leslie, K, Stanski, DR & Shafer, SL 2009, *Monitoring the Depth of Anesthesia*, 7, Elsevier, United States of America, viewed December 2010.

Goddard, N & Smith, D 2013, 'Unintended awareness and monitoring of depth of anaesthesia', *Continuing Education in Anaesthesia, Critical Care & Pain*.

Guedel, AE 1920, 'Third stage ether anaesthesia: A sub-classification regarding the significance of the position and movement of the eyeball', *American Journal of Surgery Anesthesia Supplement*, vol. 32, no. 4.

Gul, R, Karis, D, Koksai, GM, Sayilgan, C, Bolayirli, M, Oz, H & Ercan, M 2015, 'Effects of sevoflurane and desflurane on the blood and plasma viscosity', *Medical Science and Discovery*, vol. 2, no. 2, pp. 165-70.

Hall, Jc 1847, 'Extirpation of a large tumour', *The Lancet*, vol. 1.

Harris, EA, Lubarsky, DA & Candiotti, KA 2009, 'Monitored anesthesia care (MAC) sedation: Clinical utility of fospropofol', *Therapeutics and Clinical Risk Management*, vol. 5, no. 1, pp. 949-59.

Heung-II, S & Seong-Whan, L 2013, 'A Novel Bayesian Framework for Discriminative Feature Extraction in Brain-Computer Interfaces', *Pattern Analysis and Machine Intelligence, IEEE Transactions on*, vol. 35, no. 2, pp. 286-99.

Hutchinson, R 1961, 'Awareness during surgery: A study of its incidence', *British Journal of Anaesthesia*, vol. 33, no. 9, pp. 463-9.

Ionescu, D, Margarit, SC, Hadade, AN, Mocan, T, Miron, N & Sessler, D 2013, 'Choice of anesthetic technique on plasma concentrations of interleukins and cell adhesion molecules', *Perioperative Medicine*, vol. 2, no. 1, p. 8.

Ireland, TaoaoGBa 2007, *Recommendation for standards of monitoring during anaesthesia and recovery*, 4th Edition, Portland Place, London.

Ishizawa, Y 2007, 'Mechanisms of anesthetic actions and the brain', *Journal of Anesthesia*, vol. 21, no. 2, pp. 187-99.

Jagadeesan, N, Wolfson, M, Chen, Y, Willingham, M & Avidan, MS 2013, 'Brain monitoring during general anesthesia', *Trends in Anaesthesia and Critical Care*, vol. 3, no. 1, pp. 13-8.

Jensen, EW, Litvan, H, Struys, M & Vazquez, PM 2004, 'Pitfalls and challenges when assessing the depth of hypnosis during general anaesthesia by clinical signs and electronic indices', *Acta Anaesthesiologica Scandinavica*, vol. 48, no. 10, pp. 1260-7.

Jeong, Y-B, Kim, J-S, Jeong, S-M, Park, J-W & Choi, I-C 2006, 'Comparison of the Effects of Sevoflurane and Propofol Anaesthesia on Regional Cerebral Glucose Metabolism in Humans using Positron Emission Tomography', *Journal of International Medical Research*, vol. 34, no. 4, pp. 374-84.

Jianbo, G, Sultan, H, Jing, H & Wen-Wen, T 2010, 'Denoising Nonlinear Time Series by Adaptive Filtering and Wavelet Shrinkage: A Comparison', *Signal Processing Letters, IEEE*, vol. 17, no. 3, pp. 237-40, <10.1109/LSP.2009.2037773>.

Johansen, JW 2006, 'Update on Bispectral Index monitoring', *Best Practice & Research Clinical Anaesthesiology*, vol. 20, no. 1, pp. 81-99.

Jospin, M, Caminal, P, Jensen, EW, Litvan, H, Vallverdu, M, Struys, MMRF, Vereecke, HEM & Kaplan, DT 2007, 'Detrended Fluctuation Analysis of EEG as a

- Measure of Depth of Anesthesia', *Biomedical Engineering, IEEE Transactions on*, vol. 54, no. 5, pp. 840-6.
- Juan, D, Yifang, B, Jinshuo, L, Li, L, Xin, N & Bin, Z 2014, 'Hierarchical Segmentation of Multitemporal RADARSAT-2 SAR Data Using Stationary Wavelet Transform and Algebraic Multigrid Method', *Geoscience and Remote Sensing, IEEE Transactions on*, vol. 52, no. 7, pp. 4353-63.
- Kavitha, PT, Lau, CT & Premkumar, AB 2007, 'Modified ocular artifact removal technique from EEG by adaptive filtering', in *Information, Communications & Signal Processing, 2007 6th International Conference on: proceedings of the Information, Communications & Signal Processing, 2007 6th International Conference on* pp. 1-5.
- Kazama, T, Ikeda, K, Morita, K, Kikura, M, Doi, M, Ikeda, T, Kurita, T & Nakajima, Y 1999, 'Comparison of the Effect-site keO s of Propofol for Blood Pressure and EEG Bispectral Index in Elderly and Younger Patients', *Anesthesiology*, vol. 90, no. 6, pp. 1517-27.
- Kelley, SD 2003, *Monitoring level of consciousness during anesthesia and sedation*, Aspec Medical Systems, Inc, USA.
- Kelley, SD 2012, *Monitoring consciousness*, Second edn.
- Kelly, S 2003, 'Monitoring level of consciousness during anesthesia and sedation. Aspect Medical Systems', *Inc., Newton, MA*.
- Kelz, M, Mashour, G, Abel, T & Maze, M 2009, 'Sleep, Memory, and Consciousness', in RD Miller, et al. (eds), *Miller's Anesthesia, 7th Edition*, Churchill Livingstone, USA, p. 27.
- Kloosterman, F, Layton, SP, Chen, Z & Wilson, MA 2014, *Bayesian decoding using unsorted spikes in the rat hippocampus*, vol. 111.
- Kochs, E, Bischoff, P, Pichlmeier, U & am Esch, JS 1994, 'Surgical Stimulation Induces Changes in Brain Electrical Activity during Isoflurane/Nitrous Oxide Anesthesia: A Topographic Electroencephalographic Analysis', *Anesthesiology*, vol. 80, no. 5, pp. 1026-34.

- Kortelainen, J & Seppänen, T 2013, 'Electroencephalogram-based depth of anaesthesia measurement: Combining opioids with hypnotics', *Trends in Anaesthesia and Critical Care*, vol. 3, no. 5, pp. 270-8.
- Kortelainen, J, Vayrynen, E & Seppanen, T 2011, 'Depth of Anesthesia during multidrug infusion: Separating the effects of Propofol and Remifentanyl using the spectral Features of EEG', *IEEE Transactions on Biomedical Engineering*, vol. 58, no. 5.
- Krieger, A, Panoskaltsis, N, Mantalaris, A, Georgiadis, MC & Pistikopoulos, EN 2014, 'Modeling and Analysis of Individualized Pharmacokinetics and Pharmacodynamics for Volatile Anesthesia', *Biomedical Engineering, IEEE Transactions on*, vol. 61, no. 1, pp. 25-34.
- Krishnaveni, V, Jayaraman, S, Aravind, S, Hariharasudhan, V & Ramadoss, K 2006, 'Automatic Identification and Removal of Ocular Artifacts from EEG using Wavelet Transform', *Measurement Science Review*, vol. 6, no. 4, pp. 45-57.
- Kschischang, FR 2006, 'The Hilbert transform', Electrical and Computer Engineering University Toronto.
- Kuizenga, K, Wierda, JMKH & Kalkman, CJ 2001, 'Biphasic EEG changes in relation to loss of consciousness during induction with thiopental, propofol, etomidate, midazolam or sevoflurane', *British Journal of Anaesthesia*, vol. 86, no. 3, pp. 354-60.
- Kuramoto, T, Oshita, S, Takeshita, H & Ishikawa, T 1979, 'Modification of the Relationship between Cerebral Metabolism, Blood Flow, and Electroencephalogram by Stimulation during Anesthesia in the Dog', *Anesthesiology*, vol. 51, no. 3, pp. 211-7.
- Landes, DP 2002, 'The provision of general anaesthesia in dental practice, an end which had to come?', *British Dental Journal*, vol. 192, no. 3.
- Lapébie, F-X, Kennel, C, Magy, L, Progetti, F, Honnorat, J, Pichon, N, Vignon, P & François, B 2014, 'Potential side effect of propofol and sevoflurane for anesthesia of anti-NMDA-R encephalitis', *BMC Anesthesiology*, vol. 14, no. 1, p. 5.

- Larson, MD 2005, 'History of Anesthetic Practice', in RD Miller (ed.), *Anesthesia*, vol. 7th Edition, ch 1.
- Lenmarken, C, Bildfors, K, Enlund, G, Samuelsson, P & Sandin, R 2002, 'Victims of awareness', *Acta Anaesthesiologica Scandinavica*, vol. 46, pp. 229-31.
- Leung, LS, Luo, T, Ma, J & Herrick, I 2014, 'Brain areas that influence general anesthesia', *Progress in Neurobiology*, vol. 122, no. 0, pp. 24-44.
- Li, Q, Teng, J, Wang, X, Zhang, Y & Quo, J 2003, 'Research of gyro signal denoising with stationary wavelets transform', in *Electrical and Computer Engineering, 2003. IEEE CCECE 2003. Canadian Conference on: proceedings of the Electrical and Computer Engineering, 2003. IEEE CCECE 2003. Canadian Conference on* pp. 1989-92 vol.3.
- Li, T & Li, Y 2014, 'Depth of anaesthesia monitors and the latest algorithms', *Asian Pacific Journal of Tropical Medicine*, vol. 7, no. 6, pp. 429-37.
- Li, X, Li, D, Liang, Z, Voss, LJ & Sleight, JW 2008, 'Analysis of depth of anesthesia with Hilbert-Huang spectral entropy', *Clinical Neurophysiology*, vol. 119, no. 11, pp. 2465-75.
- Liu, Q, Wei, Q, Fan, S-Z, Lu, C-W, Lin, T-Y, Abbod, MF & Shieh, J-S 2012, 'Adaptive computation of multiscale entropy and its application in EEG signals for monitoring depth of anesthesia during surgery', *Entropy*, vol. 14, no. 6, pp. 978-92.
- Liu, W, Thorp, T, Graham, S & Aitkenhead, A 1991, 'Incidence of awareness with recall during general anaesthesia', *Anaesthesia*, vol. 46, no. 6, pp. 435-7.
- Lundy, JS 1940, 'The value of the fundamental science in the establishment of anesthesiology', *Science*, vol. 92, no. 2392, pp. 388-92.
- Madisetti, V 2009, *Digital signal processing fundamentals*, CRC press.

Marchant, N, Sanders, R, Sleigh, J, Vanhauzenhuyse, A, Bruno, M-A, Brichant, JF, Laureys, S & Bonhomme, V 2014, 'How Electroencephalography Serves the Anesthesiologist', *Clinical EEG and Neuroscience*, vol. 45, no. 1, pp. 22-32.

Marjot, R 2009, 'The First Anaesthetics in Bath', in *History of Anaesthesia Society: proceedings of the History of Anaesthesia Society*, DA McKenzie (ed.), Bath.

McKenna, T & Wilton, T 1973, 'Awareness during endotracheal intubation', *Anaesthesia*, vol. 28, no. 6, pp. 599-602.

Migeon, A, Desgranges, F-P, Chassard, D, Blaise, BJ, De Queiroz, M, Stewart, A, Cejka, J-C, Combet, S & Rhondali, O 2013, 'Pupillary reflex dilatation and analgesia nociception index monitoring to assess the effectiveness of regional anesthesia in children anesthetised with sevoflurane', *Pediatric Anesthesia*, vol. 23, no. 12, pp. 1160-5.

Miller, RD 2005, 'History of Anesthetic Practice', in RD Miller (ed.), *Anesthesia*, vol. 7th Edition, ch 1.

Misiti, M, Misiti, Y, Oppenheim, G & Poggi, J-M 2009, *Wavelet Toolbox 4*, The MathWorks, Inc.

Momota, Y, Kaneda, K, Arishiro, K, Kishimoto, N, Kanou, S & Kotani, J 2010, 'Changes in Blood Pressure During Induction of Anesthesia and Oral and Maxillofacial Surgery by Type and Timing of Discontinuation of Antihypertensive Drugs', *Anesthesia progress*, vol. 57, no. 1, pp. 13-7.

Morsi, WG & El-Hawary, ME 2008, 'A New Perspective for the IEEE Standard 1459-2000 Via Stationary Wavelet Transform in the Presence of Nonstationary Power Quality Disturbance', *Power Delivery, IEEE Transactions on*, vol. 23, no. 4, pp. 2356-65.

Musizza, B & Ribaric, S 2010, 'Monitoring the Depth of Anaesthesia', *Sensors Open Access Journal on the science and technology of sensors and biosensors*, vol. 10, pp. 10896-935.

- Muthuswamy, J & Roy, RJ 1999, 'The use of fuzzy integrals and bispectral analysis of the electroencephalogram to predict movement under anesthesia', *Biomedical Engineering, IEEE Transactions on*, vol. 46, no. 3, pp. 291-9.
- Myles, PS 2007, 'Prevention of awareness during anaesthesia', *Best Practice & Research Clinical Anaesthesiology*, vol. 21, no. 3, pp. 345-55.
- Nason, GP & Silverman, BW 1995, 'The Stationary Wavelet Transform and some Statistical Applications', in A Antoniadis & G Oppenheim (eds), *Wavelets and Statistics*, Springer New York, vol. 103, ch 17, pp. 281-99.
- Nguyen-Ky, T, Wen, P & Li, Y 2013, 'Consciousness and Depth of Anesthesia Assessment Based on Bayesian Analysis of EEG Signals', *Biomedical Engineering, IEEE Transactions on*, vol. 60, no. 6, pp. 1488-98.
- Nguyen-Ky, T, Wen, P & Li, Y 2014, 'Monitoring the depth of anaesthesia using Hurst exponent and Bayesian methods', *Signal Processing, IET*, vol. 8, no. 9, pp. 907-17.
- Nguyen-Ky, T, Wen, P, Li, Y & Malan, M 2012, 'Measuring the hypnotic depth of anaesthesia based on the EEG signal using combined wavelet transform, eigenvector and normalisation techniques', *Computers in Biology and Medicine*, vol. 42, no. 6, pp. 680-91.
- Nguyen-Ky, TT, Peng, W, Li, Y & Gray, R 2011, 'Measuring and Reflecting Depth of Anesthesia Using Wavelet and Power Spectral Density', *Information Technology in Biomedicine, IEEE Transactions on*, vol. 15, no. 4, pp. 630-9.
- Nia, HFG & Huosheng, H 2012, 'Applying Bayesian decision theory to peak detection of stochastic signals', in *Computer Science and Electronic Engineering Conference (CEEC), 2012 4th: proceedings of the Computer Science and Electronic Engineering Conference (CEEC), 2012 4th* pp. 117-22.
- Oshima, K 2008, 'Estimation of the Depth of Anaesthesia from Interacting Physiological Oscillators', *École Polytechnique Federale De Lausanne, Swiss*.
- Otto, KA 2008, 'EEG power spectrum analysis for monitoring depth of anaesthesia during experimental surgery', *Laboratory Animals*, vol. 42, no. 1, pp. 45-61.

- Palendeng, M, Wen, P & Li, Y 2014, 'Real-time depth of anaesthesia assessment using strong analytical signal transform technique', *Australasian Physical & Engineering Sciences in Medicine*, vol. 37, no. 4, pp. 723-30.
- Park, T, Eckley, IA & Ombao, HC 2014, 'Estimating Time-Evolving Partial Coherence Between Signals via Multivariate Locally Stationary Wavelet Processes', *Signal Processing, IEEE Transactions on*, vol. 62, no. 20, pp. 5240-50.
- Parker, BM 2006, 'Anesthetics and anesthesia techniques: Impacts on perioperative management and postoperative outcomes', *Cleveland Clinic Journal of Medicine*, vol. 73, no. 1.
- Paule, MG, Li, M, Allen, RR, Liu, F, Zou, X, Hotchkiss, C, Hanig, JP, Patterson, TA, Slikker, W & Wang, C 2011, 'Ketamine Anesthesia during the First Week of Life can Cause Long-Lasting Cognitive Deficits in Rhesus Monkeys', *Neurotoxicology and teratology*, vol. 33, no. 2, pp. 220-30.
- Pauling, L 1961, 'A Molecular Theory of General Anesthesia', *Science*, vol. 34, no. 3471, p. 7.
- Plomley, F 1847, 'Operations upon the eye', *The Lancet*, vol. 1.
- Pollard, RJ, Coyle, JP, Gilbert, RL & Beck, JE 2007, 'Intraoperative awareness in a regional medical system: a review of 3 years' data', *Anesthesiology*, vol. 106, no. 2, pp. 269-74.
- Purdon, PL, Pierce, ET, Mukamel, EA, Prerau, MJ, Walsh, JL, Wong, KFK, Salazar-Gomez, AF, Harrell, PG, Sampson, AL, Cimenser, A, Ching, S, Kopell, NJ, Tavares-Stoeckel, C, Habeeb, K, Merhar, R & Brown, EN 2013, 'Electroencephalogram signatures of loss and recovery of consciousness from propofol', *Proceedings of the National Academy of Sciences*.
- Radtke, FM, Franck, M, Lendner, J, Krüger, S, Wernecke, KD & Spies, CD 2013, 'Monitoring depth of anaesthesia in a randomized trial decreases the rate of postoperative delirium but not postoperative cognitive dysfunction', *British Journal of Anaesthesia*, vol. 110, no. suppl 1, pp. i98-i105.

- Ram, MR, Madhav, KV, Krishna, EH, Komalla, NR & Reddy, KA 2012, 'A Novel Approach for Motion Artifact Reduction in PPG Signals Based on AS-LMS Adaptive Filter', *Instrumentation and Measurement, IEEE Transactions on*, vol. 61, no. 5, pp. 1445-57.
- Rampil, IJ 1998, 'A primer for EEG signal processing in anesthesia', *Anesthesiology*, vol. 89, no. 4, pp. 980-1002.
- Rawlinson, TbG 2014, *Herodotus Books*, viewed 11 March 2015.
- Sandin, RH, Enlund, G, Samuelsson, P & Lennmarken, C 2000, 'Awareness during anaesthesia: a prospective case study', *The Lancet*, vol. 355, no. 9205, pp. 707-11.
- Sanei, S & Chambers, JA 2007, *EEG Signal Processing*, John Wiley & Sons, Ltd, England.
- Schmidt, GN, Bischoff, P, Standl, T, Jensen, K, Voigt, M & Schulte, J 2003, 'Narcotrend(R) and Bispectral Index(R) Monitor Are Superior to Classic Electroencephalographic Parameters for the Assessment of Anesthetic States during Propofol-Remifentanil Anesthesia.pdf>'.
</p></div>

Sebel, PS, Bowdle, TA, Ghoneim, MM, Rampil, IJ, Padilla, RE, Gan, TJ & Domino, KB 2004, 'The Incidence of Awareness During Anesthesia: A Multicenter United States Study', *Anesthesia & Analgesia*, vol. 99, no. 3, pp. 833-9.

Sethares, WA 2007, *Rhythm and transforms*, Springer Science & Business Media.

Shalhaf, R, Behnam, H, Sleight, JW, Steyn-Ross, A & Voss, LJ 2013, 'Monitoring the depth of anesthesia using entropy features and an artificial neural network', *Journal of Neuroscience Methods*, vol. 218, no. 1, pp. 17-24.

Shepherd, J, Jones, J, Frampton, G, Bryant, J, Baxter, L & Cooper, K 2013, 'Clinical effectiveness and cost-effectiveness of depth of anaesthesia monitoring (E-Entropy, Bispectral Index and Narcotrend): a systematic review and economic evaluation', *Health Technology Assessment*, vol. 17, no. 34.

Mario E. Palendeng

146

Sloan, TB & Heyer, EJ 2002, 'Anesthesia for intraoperative neurophysiologic monitoring of the spinal cord', *Journal of Clinical Neurophysiology*, vol. 19, no. 5, p. 14.

Soghomonyan, S, Moran, KR, Sandhu, GS & Bergese, SD 2014, 'Anesthesia and evoked responses in neurosurgery', *Frontiers in Pharmacology*, vol. 5, no. 74.

Soriano, S & Vutskits, L 2015, 'Is There Evidence for Long-Term Neurocognitive Effects of Sedatives?', in KP Mason (ed.), *Pediatric Sedation Outside of the Operating Room*, Springer New York, ch 27, pp. 553-8.

Steyn-Ross, DA 2002, 'Modelling the anaestheto-dynamic phase transition of the cerebral cortex ', The University of Waikato.

Suyi, L & Jun, L 2009, 'The Optimal De-noising Algorithm for ECG Using Stationary Wavelet Transform', in *Computer Science and Information Engineering, 2009 WRI World Congress on: proceedings of the Computer Science and Information Engineering, 2009 WRI World Congress on* pp. 469-73.

Sykacek, P, Rezek, I & Roberts, S 2005, 'Bayes Consistent Classification of EEG Data by Approximate Marginalisation', in M Dirk Husmeier DiplPhys, PhD, , et al. (eds), *Probabilistic Modeling in Bioinformatics and Medical Informatics*, Springer London, vol. Advanced Information and Knowledge Processing pp. 391-417.

System, AM 2009, *Executive Summary - BIS Monitorig*, ASPECT Medical Systems.

Taheri, M, Ahmadi, B, Amirfattahi, R & Mansouri, M 2009, 'Assessment of depth of anesthesia using principal component analysis', *Biomedical Science and Engineering*, vol. 2, pp. 9-15.

Taruttis, A, Rosenthal, A, Kacprowicz, M, Burton, NC & Ntziachristos, V 2014, 'Multiscale Multispectral Optoacoustic Tomography by a Stationary Wavelet Transform Prior to Unmixing', *Medical Imaging, IEEE Transactions on*, vol. 33, no. 5, pp. 1194-202.

Tipping, ME & Lawrence, ND 2005, 'Variational inference for Student-t models: Robust Bayesian interpolation and generalised component analysis', *Neurocomputing*, vol. 69, no. 1-3, pp. 123-41.

Trail, R 2003, 'Anaesthesia: A Modern Concept', in J Keneally & M Jones (eds), *Australasian Anaesthesia 2013*, Bridge Printery Pty Ltd, Melbourne, Australia, p. 9.

Valencia, JF, Melia, USP, Vallverdu, M, Jospin, M, Jensen, EW, Porta, A, Gambus, P & Caminal, P 2014, 'Prediction of response to noxious stimulation during sedation-analgesia by refined multiscale entropy analysis of EEG', in *Cardiovascular Oscillations (ESGCO), 2014 8th Conference of the European Study Group on: proceedings of the Cardiovascular Oscillations (ESGCO), 2014 8th Conference of the European Study Group on* pp. 61-2.

Wang, J, Xiao, Q, Jiang, Y, Guan, S & Gu, S 2009, 'An Adaptive Filter Model Based on Wavelet Transform', in *Intelligent Systems, 2009. GCIS '09. WRI Global Congress on: proceedings of the Intelligent Systems, 2009. GCIS '09. WRI Global Congress on* pp. 136-9, viewed <10.1109/GCIS.2009.342>.

Wei, Q, Liu, Q, Fan, S-Z, Lu, C-W, Lin, T-Y, Abbod, MF & Shieh, J-S 2013, 'Analysis of EEG via multivariate empirical mode decomposition for depth of anesthesia based on sample entropy', *Entropy*, vol. 15, no. 9, pp. 3458-70.

West, JB 2014, 'Humphry Davy, nitrous oxide, the Pneumatic Institution, and the Royal Institution', *American Journal of Physiology - Lung Cellular and Molecular Physiology*, vol. 307, no. 9.

Wikipedia 2015, *Neuron*, viewed April <<https://readtiger.com/wkp/en/Neuron>>.

Wilson, SL, Vaughan, RW & Stephen, CR 1975, 'Awareness, dreams, and hallucinations associated with general anesthesia', *Anesthesia & Analgesia*, vol. 54, no. 5, pp. 609-16.

Xu, L, WU, AS & Yue, Y 2009, 'The incidence of intra-operative awareness during general anesthesia in China: a multi-center observational study', *Acta Anaesthesiologica Scandinavica*, vol. 53, no. 7, pp. 873-82.

Yin, J, Wang, SL & Liu, XB 2014, 'The effects of general anaesthesia on memory in children: a comparison between propofol and sevoflurane', *Anaesthesia*, vol. 69, no. 2, pp. 118-23.

Zanner, R, Pilge, S, Kochs, EF, Kreuzer, M & Schneider, G 2009, 'Time delay of electroencephalogram index calculation: analysis of cerebral state, bispectral, and Narcotrend indices using perioperatively recorded electroencephalographic signals', *Br J Anaesth*, vol. 103, no. 3, pp. 394-9.

Zhiqian, Y, Fuying, T & Jianfeng, W 2005, 'EEG signal processing in anesthesia-using wavelet-based informational tools', in *Engineering in Medicine and Biology Society, 2005. IEEE-EMBS 2005. 27th Annual International Conference of the: proceedings of the Engineering in Medicine and Biology Society, 2005. IEEE-EMBS 2005. 27th Annual International Conference of the* pp. 4127-9.

Zikov, T, Bibian, S, Dumont, GA, Huzmezan, M & Ries, CR 2006, 'Quantifying cortical activity during general anesthesia using wavelet analysis', *Biomedical Engineering, IEEE Transactions on*, vol. 53, no. 4, pp. 617-32.

Zoughi, T, Boostani, R & Deypir, M 2012, 'A wavelet-based estimating depth of anesthesia', *Engineering Applications of Artificial Intelligence*, vol. 25, no. 8, pp. 1710-22.